UNIVERSITY OF TRENTO - Italy

International PhD Program in Biomolecular Sciences
Centre for Integrative Biology
30th Cycle

"Bacterial outer membrane vesicles (OMVs) as a platform for personalized cancer vaccines"

Tutor

Prof. Guido GRANDI

CIBIO, University of Trento

Ph.D. Thesis of

Michele TOMASI

CIBIO, University of Trento

Academic Year 2016-2017

To my mother

Contents

Abstract

Cancer is the second leading cause of death worldwide[1,2]. Tumor cells contain several mutations that can generate neoepitopes, targets of an effective anti-cancer T cell response[3–9]. Increasing evidence demonstrated that cancer vaccines targeting neoepitopes are effective and safe both in preclinical models[10–13] and human patients[14,15]. Bacterial Outer Membrane Vesicles (OMVs) are naturally produced by all Gram-negative bacteria[16,17]. They contain several Microbe-Associated-Molecular Patterns (MAMPs)[18,19], crucial for stimulating innate immunity and promoting adaptive immune responses[20–22]. The ability to engineer OMVs with cancer epitopes[23,24] together with their unique adjuvanticity and safety make them a particularly interesting vaccine platform.

In this study, we have demonstrated that immunization of mice with OMVs activate both innate and adaptive immunity and induce a Th1 immune response, fundamental for an effective cancer vaccine. OMV immunization also caused upregulation of genes involved in MAMPs detection and signal transduction, a central component of the inflammasome and pro-inflammatory cytokines. OMV vaccination induced an upregulation of Th1 key transcription factor and cytokines, while inducing a downregulation of transcription factor and cytokines associated to Th2 response. Moreover, cytokines released by activated macrophages, DCs, T cells and natural killer (NK) cells were induced by OMV vaccination, together with a key chemokine and a protein for immune cell recruitment and adhesion, respectively.

We have successfully engineered OMVs on the surface and in the lumen with OVA$_{257-264}$ CD8 T cell model epitope. These OVA-engineered OMVs induced a high percentage of OVA$_{257-264}$ specific CD8 T cells and protected mice from OVA-expressing tumors. We have shown that OMVs engineered with a tumor specific antigen (TSA) induced a protective response and promoted a significant recruitment of CD4 and CD8 T cells into tumors, while reducing both CD4 regulatory T cells (Tregs) and myeloid-derived suppressor cells (MDSCs). We have also shown in the same mouse model that vaccination with OMVs engineered with two TSAs have a synergistic protective activity in controlling tumor growth. Finally, we have demonstrated that

therapeutic OMV vaccines targeting five different neoepitopes protect mice from tumor growth.

Taken together, our results show that OMVs are a promising platform for effective personalized cancer vaccines.

Introduction

Globally, malignant neoplasms represent the second leading cause of death[1,2]. According to the International Agency for Cancer Research (IARC) in 2012 the global number of new cancer cases and of cancer-related deaths were 14.1 million and 8.2 million, respectively[1]. The same report predicts that in 2030, these numbers will grow to 21.7 million and 13 million. Using epidemiological data from 2012 to 2014, the American Cancer Society (ACS) has calculated that the lifetime probability of developing cancer and dying for cancer in the United States was approximately 1 in 3 and 1 in 5, respectively, for both men and women[25].

Over the last three decades, the 5-year relative survival rate for all cancers has increased by more than 40% in the USA, growing from 49% in 1975-1977 to 69% in 2007-2013[25], while mortality has decreased by 26% from 1991 to 2015[25–27].

In these last years, the great effort in cancer research led to significant advances in many therapeutic disciplines, especially in cancer immunotherapy. Recently, the United States launched the so call "Cancer Moonshot" program, allocating 1.8 billion dollars over seven years to fund the project[28]. The goal is to boost cancer research to improve cancer prevention and early detection, together with the development of new effective cancer treatments while rendering more therapies available to more patients. Among the strategies available to fight cancer, immunotherapy has recently achieved some of the most spectacular results. The following products recently approved by the U.S. Food and Drug Administration (FDA) are worth noting:

- The vaccines against human papilloma virus (HPV) and hepatitis B virus (HBV)[29], which, if universally administered, will eliminate up to 90% of all cervical-[30] and HPV-positive oropharyngeal cancers[31], and 50% of hepatocarcinomas[32,33] respectively.
- Sipuleucel-T in 2010, the first approved therapeutic cancer "vaccine", based on the adoptive transfer of autologous dendritic cells, and used to treat castration resistant prostate cancer patients[34].
- Six checkpoint inhibitors monoclonal antibodies (mAbs) for the treatment of several types of cancers[35]. The therapeutic efficacy of these mAbs is impressive, as demonstrated by the 50% of patients with metastatic melanoma

who showed objective responses when treated with a combination of anti-CTLA-4 and anti-PD-L1 antibodies[36,37].

- Two chimeric antigen receptor (CAR)-T cell therapies:

    1) tisagenlecleucel (Kymriah™) for the treatment of patients up to 25 years of age with B-cell precursor acute lymphoblastic leukemia (ALL)[38,39]. So far, treated patients showed an overall remission rate of 83%[40], with 63% of patients with complete remission[41];

    2) axicabtagene ciloleucel (Yescarta™) for patients with large-B-cell lymphomas [42]. Patient's objective response rate for this treatment is 72%, with a complete remission rate of 51%[43].

Based on these results and on the intense research activity carried out in many laboratories worldwide, immunotherapy is expecting to revolutionize the way cancer patients will be treated.

Immune system and cancer

Background

The role of the immune system in controlling, shaping and eliminating tumors remained controversial until recently. The first evidence of a possible connection between inflammation and cancer goes back to 1880s, when Rudolf Virchow noticed the presence of leukocytes within tumors[44]. In the same years, Anton Chekhov observed and documented the existence of a connection between infection and tumor regression[45]. In the late 1890s, Dr. William B. Coley observed that some cancer patients had remission of their tumor during severe infections. Following this observation, he then intentionally infected with the "Coley's toxin", inactivated toxins from a cocktails of bacteria, over 500 patients, claiming to have induced cancer remission in over 150 people[46]. He demonstrated for the first time that it is possible to affect and/or inhibit cancer growth by stimulating the immune system.

In 1909, Paul Ehrlich suggested that the immune system could recognize and repress cancer development in mammals[47]. In the following years, new discoveries and a deeper understanding of the immune system permitted to Burnet and Thomas to generate the theory of "cancer immunosurveillance". They proposed that the immune

system, and T cells in particular, could protect a host against cancer outgrowth by recognition and elimination of transformed cells early in their development[47,48].

Following the observations that infection was involved in tumor regressions, in 1970s, the live attenuated tuberculosis vaccine Bacillus Calmette–Guérin (BCG) became, and still remains mostly unmodified, the effective treatment for non–muscle invasive bladder cancer[49].

Furthermore, important experiments involving immunocompetent and immunodeficient mouse models demonstrated then the role of both innate and adaptive immunity[50,51] in controlling tumor growth. It was shown that mice lacking an intact immune system develop both carcinogen-induced and spontaneous tumors more rapidly and with greater frequency compared to wild type mice[50–52].

Final evidence for the existence of antitumor immunity came in the 1980s, when interleukin 2 (IL-2) was systemically administered to treat patients with metastatic cancer[53]. An extensive analysis on 270 patients with metastatic melanoma between 1985 and 1993 showed that the efficacy of infusions of high doses of IL-2 was 16%[54]. It was demonstrated that IL-2 induces the growth and proliferation of T cells and NK cells and acts by expanding pre-existing cancer specific effector T cells: therefore IL-2 became the first approved effective cancer immunotherapy for human patients[53].

The immune system

The immune system comprises of innate and adaptive immune responses. The first is the oldest from an evolutionary point of view and confers first line protection against infection by recognizing common features of microorganisms. The innate immune system includes monocytes, macrophages, granulocytes (neutrophils, eosinophils and basophils), mast cells, the complement system, dendritic cells and innate lymphoid cells (ILCs), including natural killer (NK) cells[55,56].

The adaptive immune system is made of B and T lymphocytes, which can recognize different antigens via B and T cell receptors, respectively. These receptors arise from somatic rearrangement of DNA and allow the cell to bind foreign antigens in a specific manner. The two components (adaptive and innate) usually work together to eliminate pathogens[55,56].

When macrophages and DCs recognize MAMPs, they become activated and start releasing cytokines and chemokines, effector molecules that induce a state of inflammation which, within hours, activate and attract more immune cells to the infected tissue. Among these, ILCs and NKs amplify the signals from innate recognition towards adaptive immunity and kill infected cells, respectively[55–57]. Activated antigen presenting cells then migrate to a local draining lymph node to present antigens to T cells. Each T lymphocyte expresses its TCR on the surface together with a cluster of differentiation 3 (CD3) molecule, involved in signal transduction following antigen recognition, and with either a CD4 (CD4 T cells) or CD8 (CD8 T cells or cytotoxic T lymphocytes, CTL) molecule, co-receptors required for antigen binding. T cells recognize antigens bound to a major histocompatibility complex (MHC) molecules. There are two different types of MHC molecules:

- MHC class I, expressed by every nucleated cell, can bind 8-10 amino acid peptides derived from cytoplasmic and viral protein, and present these epitopes to CD8 T cells[55,56];

- MHC class II, expressed only by antigen presenting cells (APCs), a group of cells that specialize in presenting foreign antigens on their surface. MHC II can bind 13-17 amino acid peptides derived from extracellular proteins and present epitopes to CD4 T cells[55,56].

Moreover, through the process of cross-presentation, APCs can also present extracellular peptides on MHC I to CD8 T cells[56,58]. After antigen binding, T lymphocytes proliferate and differentiate into CTLs, which kill target cells, or into helper T cells (Th cells), which activate B cell to secrete antibodies, activate macrophages to destroy engulfed cells and aid CTLs in their killing activity. They can also become regulatory T cells (Tregs), which help to limit possible damage by repressing the activity of other lymphocytes[55–57].

On cell surface, all nucleated cells display both self and non-self antigens on MHC I molecules. The duty of T cells is to detect and to eliminate cells that present foreign peptides, including cancer antigens. During their development, T cells showing high affinity for self-antigens are eliminated in the thymus through the process of central tolerance (negative selection): in this way autoreactive T cells are eliminated and only

non-self targeting T lymphocytes potentially recognizing foreign antigens are allowed to continue their development[55–57].

B lymphocytes can directly bind their cognate antigen via the B cell receptor (BCR), a membrane-bound form of the secreted antibody. After antigen recognition, the B cells proliferate and become plasma cells, effector cells that release antibodies with the same antigen specificity possessed by its progenitor[55–57]. Antibodies exert their protective function in three main ways. They can bind to pathogens or their derived toxins and neutralize them, preventing their access to or interaction with cells. A pathogen can be coated with antibodies, a process called opsonization: macrophages and other phagocytic cells then phagocyte the whole bacteria by recognizing through a specific receptor common features present on all antibodies molecules. Antibodies coating bacteria can also activate the complement system, which lead to the direct lysis or to phagocytosis of the pathogen. Both infected and cancer cells can be recognized by specific antibodies that can engage NK cells, resulting in the elimination of the antibody coated cell through the process of antibody-dependent cell-mediated cytotoxicity (ADCC)[55–57].

Tumor antigens and mechanisms of cancer immunosurveillance

The immune system can eliminate tumor cells by recognizing the differences existing between neoplastic and normal tissues. Tumors develop as a consequence of gene mutations that generate tumor antigens and lead to alterations of cellular morphology and metabolism. These alterations, that give tumors a selective growth advantage over healthy tissues, potentially represent tumors' "Achilles' heel" since our immune system has specifically evolved to recognize the *"non-self"* or aberrant forms of the *"self"*.

Tumor antigens can be divided in three main categories: 1) tumor-associated antigens (TAAs), 2) Cancer germline/cancer testis antigens (CTAs) and 3) Tumor-specific antigens (TSAs)[59,60].

TAAs (Figure 1a) represent proteins encoded in the "wild type" genome and may be either normal differentiation antigens (e.g. rearranged Ig in B cell- and rearranged TCR in T cell-lymphomas) or proteins that are aberrantly expressed, such as over expressed or with different degree of post-translational modifications. Examples of these TAAs are melanosomal proteins like tyrosinase[61], gp100[62], and melanoma antigen

recognized by T cells 1 (MART-1)[63]. These proteins are found overexpressed by malignant melanoma cells but also expressed by normal melanocytes of the skin and the eye[60]. Other TAAs are directly involved in carcinogenesis and are represented by overexpressed normal proteins that possess growth- and survival-promoting functions such as the transcriptional regulator Wilms tumor 1 (WT1)[64] or the epidermal growth factor receptor family member Her2/neu[65].

CTAs (Figure 1a) are genes that are normally expressed in ovary, testis and in trophoblast tissues but found aberrantly expressed also in tumors due to hypo-methylation and gene dysregulation[66]. Examples of these class of antigen are melanoma antigen family A1 (MAGE-A1)[67] and NY-ESO-1[68], the latter being expressed in acute myeloid leukemia, acute lymphoid leukemia, myeloma, breast, lung, esophageal, ovarian, sarcoma, bladder, uterine cancers and melanoma[60]. Although the highly restricted tissue expression made them attractive targets for immunotherapy[69], they are typically expressed only by a subset of tumor cells and are not essential for cancer cell survival[70].

TSAs (Figure 1b) represent antigens not encoded in the normal host genome and that are uniquely expressed by tumor cells. These can be further divided into two classes. One comprises oncogenic viral proteins like EBNA1 and LMP1 and LMP2A from Epstein-Barr virus found in Hodgkin's lymphoma and nasopharyngeal carcinoma[71] or like E6 and E7 proteins from Human Papillomavirus expressed in cervical and head and neck cancers[72]. The other class comprises neoantigens/neoepitopes, abnormal proteins arising from non-synonymous somatic *de novo* point mutations, alterations in the reading frame, DNA insertion and/or deletions and from chromosomal translocations[60]. The majority of tumor relevant mutations consist in single amino acid changes[73] and these create a neoepitope when the mutation generates a peptide that can now be bound to either MHC I (CD8 epitope) or MHC II (CD4 epitope) molecules[74,75]. In some cases, single amino acid mutations can generate neoepitopes recognized by CD4 and a CD8 T cells at the same time or a peptide presented on different MHC class I alleles to different CD8 T cells[14].

Some neoantigens will confer growth advantages to the cell and will be responsible for transformation: these are referred to as "driver" mutations and, for their intrinsic characteristic, will be positively selected in the cancer development.
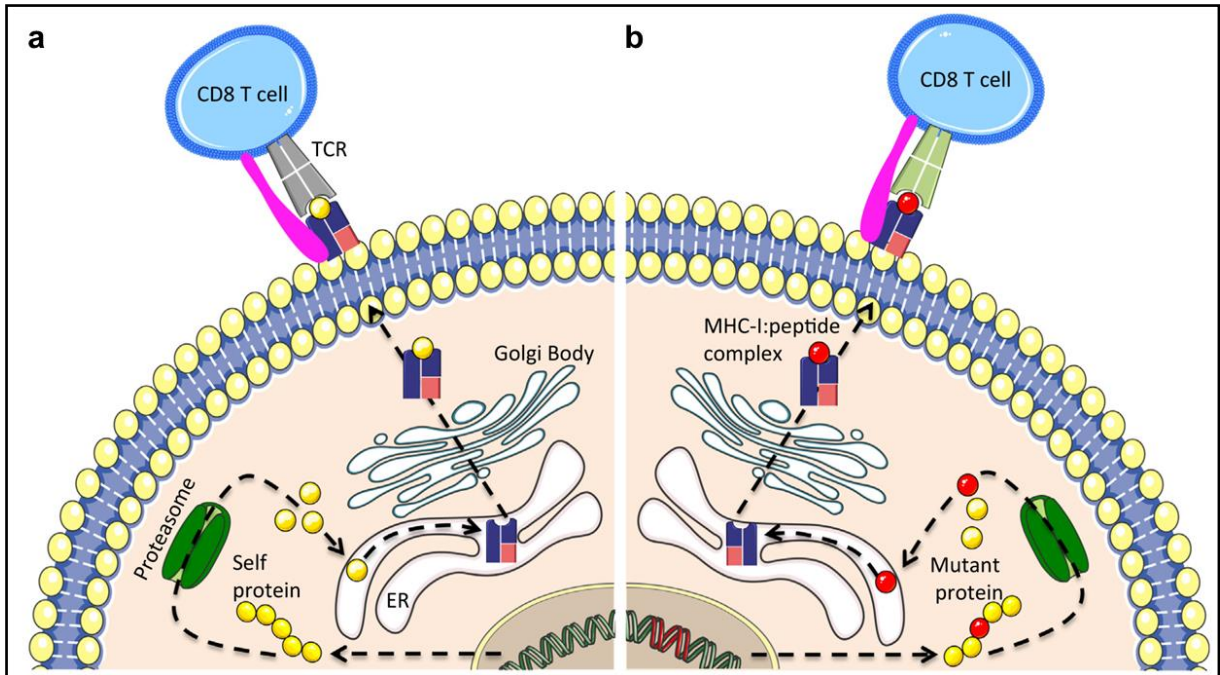
Figure 1 | Tumor antigen presentation by cancer cells. a, *Tumor-associated antigens (TAAs) and cancer germline/cancer testis antigens (CTAs) are proteins encoded in the "wild type" genome and are expressed in several tumors* **b,** *Tumor specific antigens (TSAs) are not encoded in the normal host genome and are unique to a particular tumor. They can be either viral proteins or neoantigens, abnormal proteins arising from non-synonymous, somatic de novo mutations that generate a peptide that can be presented on MHC molecules. Figure modified from Zhang et al., 2017[76].*

On the other hand, "passenger" mutations represent events that do not confer selective growth advantages and are byproduct of genomic instability of the tumor cell[77,78]. There are usually between 1000 and 10000 somatic mutations in adult cancers[79] and the vast majority of neoantigens are passenger mutations that are different in every cancer patient[78].

TAAs, TCAs and TSAs can be processed by APCs, dendritic cells in particular (Figure 2). If this is accompanied with immunogenic signals such as pro-inflammatory cytokines or factors released by dying tumor cells, an anticancer response will be generated (the lack of such signals, one of tumor escape mechanism, lead to peripheral tolerance). APCs then load tumor antigens on MHC I and II molecules and migrate to the lymph nodes where they prime and activate T cells able to recognize the presented cancer antigens. The responding T cell population proliferate, traffic to the tumor site via blood stream and infiltrate the tumor. There, upon recognition of their

cognate antigen bound to MHC I molecules, CTLs eliminate cancer cells[80]. Beyond their well-known activity in enhancing CD8 T cell response and activation of innate antitumor immunity (NK cells), CD4 T cells can also have a direct cytotoxic activity and directly kill tumor cells[81]. The killing of the transforming cell releases additional tumor antigens and immunogenic signals that boost the anti-cancer immune response and can eventually end with tumor elimination.
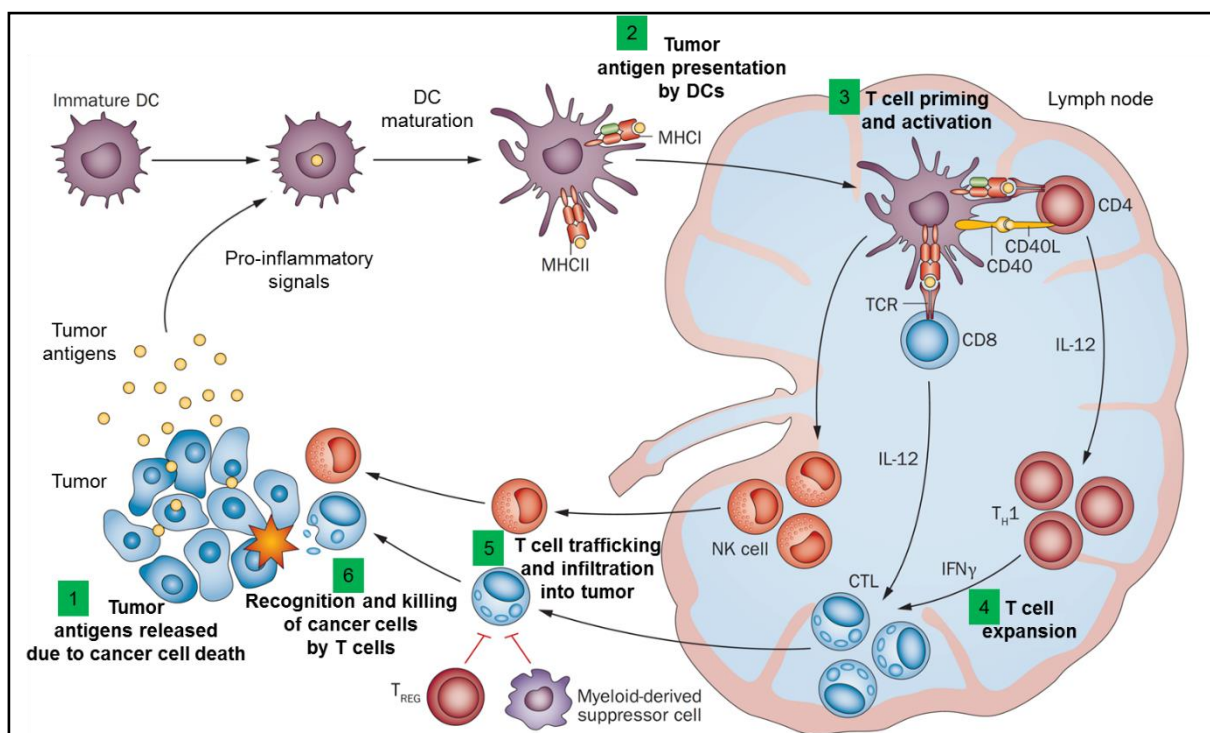
Figure 2 | Tumor immunosurveillance by immune system. Schematic representation of the immunosurveillance process, which lead to tumor elimination by the immune system. Figure modified from Melero et al., 2014[82].

Immunoediting and cancer escape from immunosurveillance

Unfortunately, in cancer patients the immune system fails to completely eliminate developing tumors. According to the "Cancer Immunoediting" concept proposed by Schreiber and collegues[83,84], the immune system has a protective and tumor-promoting role in early and late stages of cancer development, respectively. Immunoediting, in its most complex form, comprises three phases: elimination, equilibrium, and escape (Figure 3).

In the elimination phase, innate and adaptive immunity work together to recognize and eradicate the developing tumor.
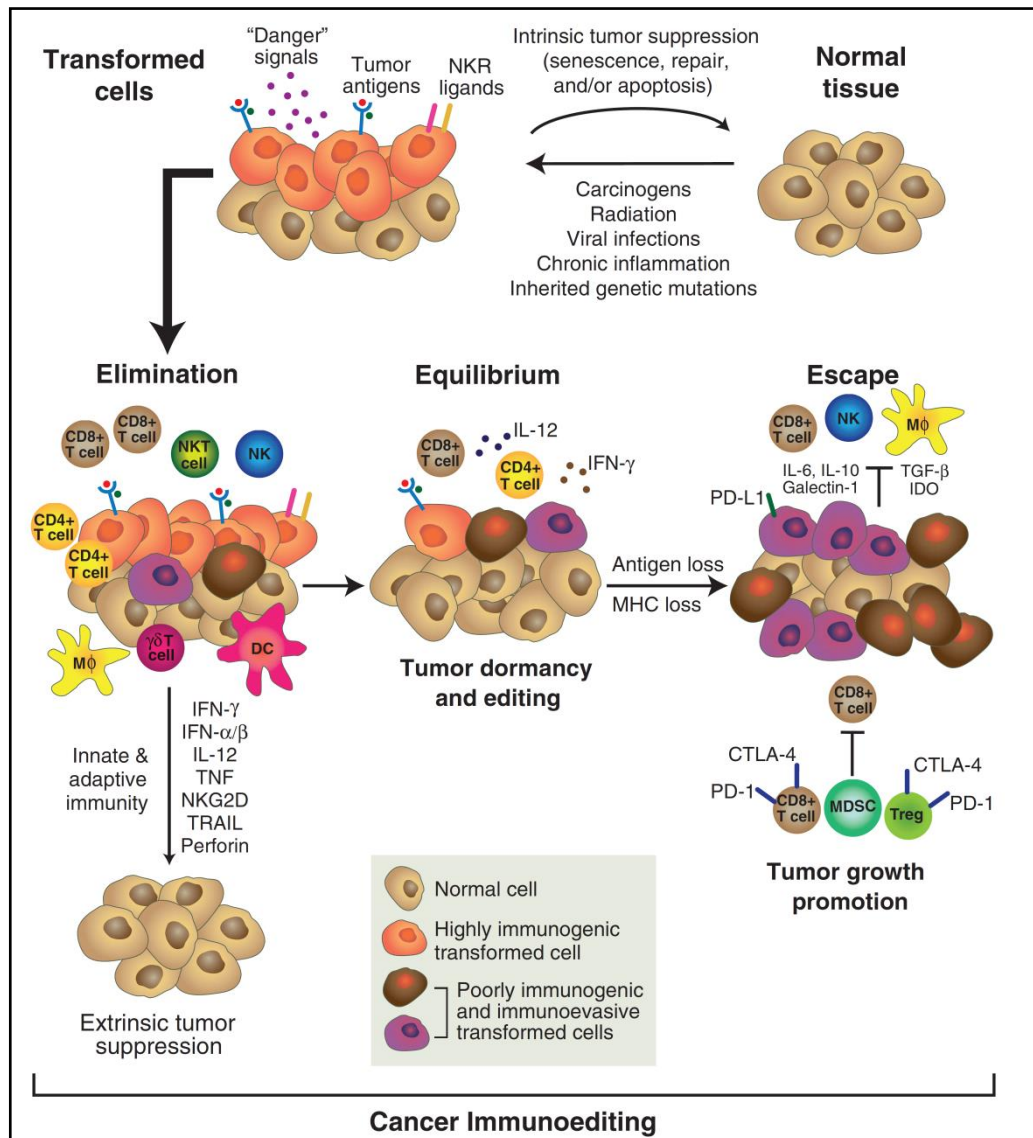
Figure 3 | Cancer immunoediting process. Schematic representation of the three immunoediting phases and the immune mediators involved. Figure taken from Schreiber et al., 2011[84].

If this elimination process is not completely effective and some cancer cells survive, they can enter the equilibrium phase. In this period, the immune system controls tumor outgrowth to keep it in a state of dormancy, which can last for the lifetime of the host[85]. During the equilibrium phase however, there is a constant immune selective pressure on genetically unstable tumor cells. This "editing" force may result in tumor cell variants with reduced immunogenicity, that are no longer recognized by host immune system and that will become clinically apparent cancers, the escape phase.

Tumors can escape immune surveillance in several ways. Cancer cells can lose or downregulate their MHC I molecules[86–88], acquire defects in the antigen processing

machinery[89] or lose their antigenic determinants[90,91]. They can also start expressing ligands for inhibitory proteins such as PDL-1[92,93], secrete immunosuppressive cytokines like IL-10 and TGF-β[94] and factors causing nutrient depletion for immune cells, such as indoleamine 2,3-dioxygenase (IDO)[93]. Moreover, tumors can be infiltrated by suppressive immune cells like CD4 Tregs, M2 macrophages and MDSCs which act together to create an immunosuppressive tumor microenvironment[93,95].

Cancer immunotherapy

Immunotherapy aims at restoring, expanding and at reactivating the original tumor specific immune response, in order to counteract further tumor development with the final goal of eliminating all malignant cells.

There are currently several immunotherapies available[36,96]. These comprise the use of cytokines[97,98], monoclonal antibodies, including antibodies targeting cancer cells[99] and checkpoint inhibitors[36,100], adoptive cell transfer (ACT) of T lymphocytes[101,102] and cancer vaccines[11,13–15,103,104]. Cytokines, checkpoint inhibitors and cancer vaccines are classified as active immunotherapies because they generate their anticancer effect only by reactivating the host immune system and thus generating a long lasting, endogenous immune response. On the other hand, adoptive transfer of T lymphocytes and monoclonal antibodies targeting cancer cells possess intrinsic anticancer activity, are short lived and rely on repeated application of high amount of effector molecules or cells, they represent passive forms of immunotherapy[105,106].

Depending on antigen specificity, we can further divide immunotherapies in specific and non-specific. Cytokines and checkpoint inhibitors induce an antitumor response that has a broad and unknown specificity, and therefore are referred to as non-specific immunotherapies. Conversely, cancer vaccines target specific antigens and are considered active, specific immunotherapies[105,106].

The immunotherapy I will focus on, which is the most relevant for my PhD project, is personalized cancer vaccines.

Cancer vaccines

Vaccination against infectious diseases has been one of the biggest revolution in the medical field. It exploits differences between host and pathogen to mount an immune response that will protect the host from a future infection by the same agent[107,108]. No other medical intervention has saved the number of lives saved by vaccines over the centuries.

Based on its spectacular results and on its mechanisms of action, vaccination is theoretically an ideal strategy to fight cancer and indeed a large number of pre-clinical

and clinical studies involving cancer vaccines have been described over the last two decades.

Contrarily to prophylactic vaccines against infectious diseases, cancer vaccines are administered in a therapeutic modality, when the disease has already escaped immunosurveillance. In fact, antigenic determinant of cancer cells in patients are usually not known before the disease has become clinically apparent. Reeducating the immune system to recognize and eliminate a chronic disease like cancer is a very challenging task, as demonstrated by the modest efficacy of therapeutic vaccines against chronic viral infections such as HPV[109,110] and HBV[111,112].

The goal of cancer vaccination is to achieve a functional and durable immune response and an effective cancer vaccine should comprise:

- Several TSAs to direct the immune response against cancer cells
- One or more immune stimulating molecules (adjuvants)
- A vehicle that allow co-delivery of the previous components to the same APC

The adjuvant component is at least as important as the antigenic part. Adjuvants must stimulate and activate DCs for optimal T cell activation and for a Th1 cellular response. In fact, to be effective, cancer vaccines require the induction of a Th1 polarized immune response, involving IFN-γ releasing CD4 T cells, CD8 T cells and natural killer (NK) T cells acting together in order to eliminate cancer cells[82,113–115]. The lack of these stimuli will result in T cell anergy against antigens present in the vaccine[82]. To be effective, cancer vaccines also have to overcome immune tolerance of tumor cells[116,117]. This is achieved by delivering high quantities of antigen to both MHC class I and II molecules of adjuvant-activated DCs, that consequently will promote both CD8 and CD4 T cell responses[104,117]. In addition to their cytotoxic activity[81], CD4 T cells are needed for optimal and sustained effector CD8 T cell responses and are fundamental to inducing and maintaining CD8 memory[104]. In fact, vaccines should stimulate central memory T cell reactivity, as these cells are more efficient at controlling tumor growth owing to their higher proliferative capacity, persistence and polyfunctionality[118].

The antigenic component is pivotal to direct the response to cancer cells only, avoiding possible off-target effects on non-cancerous self-cells expressing the same proteins present in the vaccine. One of the reasons why cancer vaccines have shown modest therapeutic effect is the unsatisfactory selection of target antigens, which has often been based on shared TAAs. Although being an attractive way to target many patients and many cancers with the same vaccine, it has revealed some important drawbacks. Due to central tolerance, targeting TAAs may result in the complete absence of the T cells specific for that antigen or in T cells that have TCRs with low antigen affinity and functional avidity and therefore not able to properly target and eliminate cancer cells[74,95,119]. Moreover, although being expressed by cancer cells, TAAs are also expressed by healthy tissues and targeting them may result in on-target off-tumor activity, causing disorders ranging from mild to severe and even death[74,120].

In fact, according to an extensive analysis on several clinical trials involving nearly a thousand patients with solid cancers and vaccinated against TAAs, only 3.6% of the immunized patients showed an objective response[118].

Neoepitopes are more attractive immunotherapy targets for several reasons. Neoantigens are not present in the thymus, therefore neoepitope-specific T cells are not subject to central tolerance and the immune system recognize them as non-self[119,121]. This result in high-affinity T cell clones available for immunotherapy that possess functional avidity reaching the avidity strength of anti-viral T cells[119]. Because T cells with TCRs with high affinity for their cognate antigens have greater cytotoxic capacity, longer persistence in the tumor environment and decreased susceptibility to immune suppression[120], these T cells may be of pivotal relevance to tumor control. Moreover, for their intrinsic definition, neoantigens are expressed only by cancer cells and therefore immune therapies targeting such antigens are less likely to induce autoimmunity[76,120,121] and hence are theoretically safer.

One of the first publications describing the relevance of neoantigens in cancer immunotherapy reported the case of a melanoma patient whose spontaneous anti-cancer immune response generated T cells against both TAAs and against

neoantigens formed by somatic point mutation in five different genes. The most important result was that the T cell response against neoantigens prevailed over the response against TAAs[3]. Further evidence for the importance of neoepitopes as central tumor-rejection antigens comes from animal studies and clinical trials involving immune checkpoint inhibitors. These antibodies target inhibitory proteins expressed by activated T cells, namely CTLA-4, with a major role in dampening T cell priming and activation, and PD-1, that blocks T cell effector functions within the tissues[36,60,117]. CTLA-4 has temporally delayed expression compared to CD28 molecule[100], but it has higher affinity to CD80/86 compared to the activating counterpart CD28[60]. PD-1 is upregulated following antigen stimulation and continuous or chronic TCR activation maintain his expression at high levels[122]. Its ligand, PD-L1, is constitutively expressed by both immune cells like T cells, B cells, NK cells and DCs, and by non-immune cells like epithelial cells and vascular endothelial cells. Its expression can be upregulated by many other types of cells in the presence of a strong inflammatory signal such as IFN-γ[92,123] and some tumors can constitutively express PD-L1 as a mechanism of immune evasion[124]. Therefore, although in different ways, both CTLA-4 and PD-L1 dampen or totally stop tumor elimination by the immune system. The blockade of either of these inhibitory pathways with specific antibodies removes the inhibitory signals and amplifies preexisting, or triggers new, antitumor immune responses[36,60,100]. In particular, blockade of CTLA-4 eliminates Tregs and promotes T cell priming[12,36,60], while blockade of PD-1 promotes T cell activation and effector functions[12,36,100,125].

Although the therapeutic efficacy of checkpoint inhibitor antibodies is impressive, only a fraction of patients respond to the therapy. Several studies aiming to investigate the reasons for such partial response have revealed the importance of mutation frequencies in tumors. It has been demonstrated that the higher the mutation load in a tumor, the higher the sensitivity to checkpoint inhibitors and the better the clinical response[121]. A higher number of mutations in a tumor means a higher number of neoepitopes as possible target of immune cells.

In patients with metastatic melanoma, a cancer characterized by a high number of mutations due to exposure to UV-light, the degree of clinical benefits correlated with the mutational load of patients. Patients with higher number of exomic mutations experienced a significantly higher long-term benefit compared to patients with lower

mutational tumors after treatment with ipilimumab, an anti CTLA-4 antibody. Moreover, activated CD8 T cells specific for tumor neoepitopes were present after checkpoint blockade treatment[4].

Even more striking evidence for the central role of neoepitopes as tumor rejection antigens, comes from the analysis of the correlation of the response to checkpoint inhibitors and the mutational loads within the same tumor type.

A study analyzing patients with non-small-cell lung carcinoma (NSCLC) treated with pembrolizumab, an antibody targeting PD-1, showed that current or former smokers
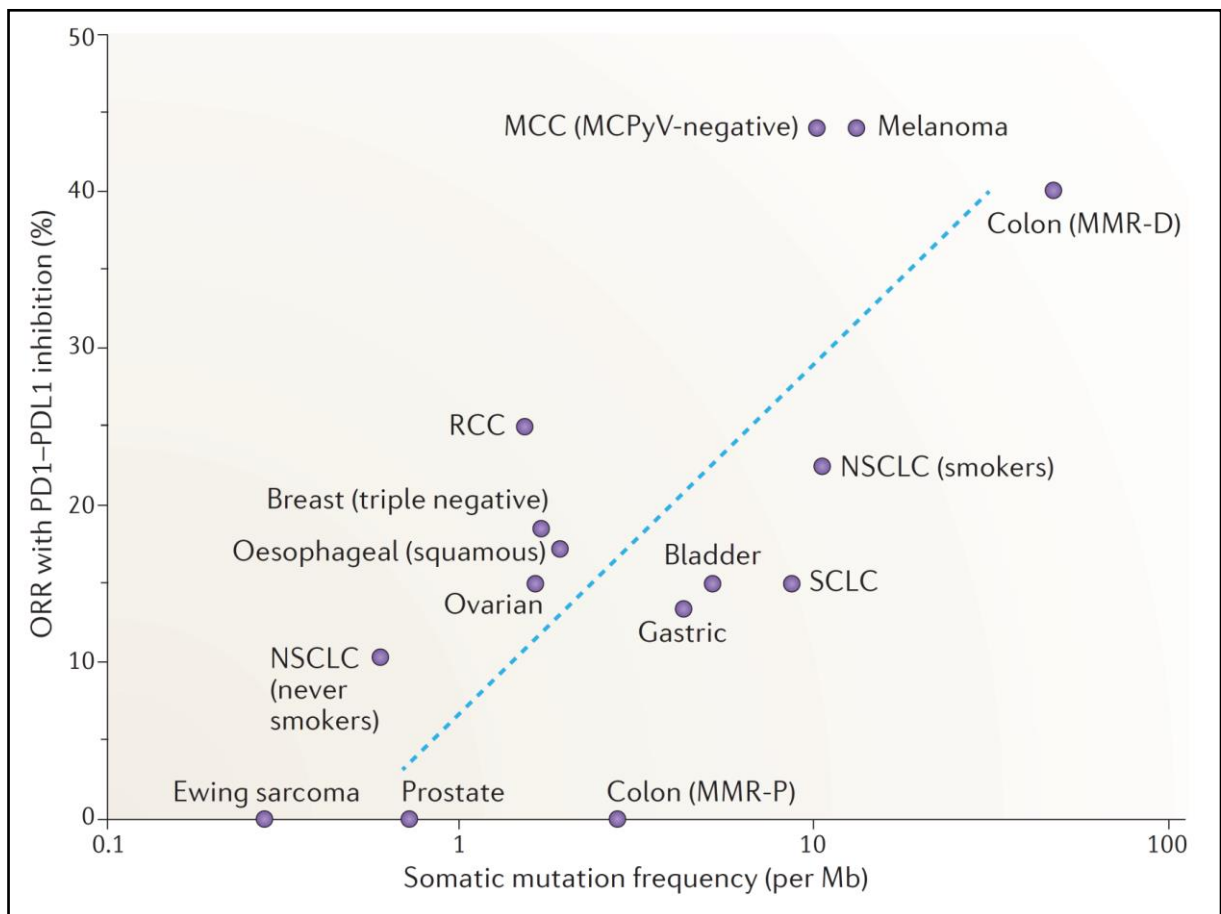
Figure 4 | The clinical efficacy of PD-1 or PD-L1 blockade correlates with the frequency of somatic mutations present in the tumor. *This graph shows the correlation of PD-1 or PD-L1 inhibitors efficacy calculated as objective response rate (ORR) with the tumor somatic mutation frequency. Melanoma, characterized by a high mutational load, which means high number of neoepitopes, showed high ORR to PD-1 or PD-L1 inhibitors. The importance of mutations, and therefore of neoepitopes, as tumor rejection antigens is even more appreciable comparing ORR and somatic mutation frequency within the same tumor type, e.g. non-small-cell lung carcinoma (NSCLC) in current or previous smoker patients versus NSCLC in patients who had never smoked cigarettes and mismatch repair deficient (MMR-D) versus mismatch repair proficient (MMR-P) colon cancer patients. MCC (MCPyV negative), Merkel cell polyomavirus negative Merkel cell carcinoma, RCC, renal cell carcinoma; SCLC, small-cell lung cancer. Figure taken from Yarchoan et al., 2017[121].*

(tobacco smoke is a mutation inducing agent) had a response rate of 22.5%, as compared with 10.3% among patients who had never smoked cigarettes[126] (Figure 4). Moreover, PD-1 blockade induced neoepitope specific CD8 T cells that paralleled tumor regression[5].

Similar results have been reported in colorectal cancers patients treated with pembrolizumab. Patients with DNA mismatch repair deficient tumors, characterized by high mutation burden, had an objective response rate and progression-free survival rate of 40% and 78%, respectively. By contrast, patients with mismatch repair proficient colorectal cancers had a much less favorable response, 0% and 11% respectively[127] (Figure 4). In the same study, patients with non-colorectal cancers that were also DNA mismatch repair deficient showed responses similar to those observed in patients with mismatch deficient colorectal cancers, confirming the importance of neoepitopes in immune related cancer growth control. Very recently, it was also demonstrated that by targeting the DNA repair process it is possible to trigger neoepitopes generation and to inhibit tumor outgrowth in preclinical animal models[128].

Since 2011, the FDA has approved six checkpoint inhibitor antibodies[35] as a consequence of their efficacy in the treatment of several human cancers. They represent one of the most remarkable achievements in cancer therapy over the last decades.

Furthermore, combining CTLA-4 and PD-1 blockade showed synergistic effects both in preclinical studies[129,130] and clinical trials[37,131], due to the simultaneous elimination of Tregs and release of neoepitope specific T cell effector functions.

The importance of neoepitopes in controlling cancer outgrowth also emerged in patients treated with adoptive T cell transfer therapy. In this approach, tumor infiltrating lymphocytes (TILs) are expanded and activated in vitro and then reinfused back into the patient after lymphodepletion[132]. This last step is very important for the success of the treatment and contribute to efficient tumor regression and persistence of oligoclonal repopulation of the host with transferred antitumor lymphocytes[133]. In fact, lymphodepletion eliminates Tregs and other immunosuppressive cells as well as all lymphocytes which compete with the transferred tumor-reactive T cells for the homeostatic cytokines IL-7 and IL-15[134].

An important research in 2005[6] reported the analysis of T cell antigen reactivity and the *in-vivo* persistence of T cells in a melanoma patient, who experienced a complete regression of all metastatic lesions following adoptive transfer of autologous tumor-reactive TILs previously expanded. The analysis revealed several T cell clones specific for two neoepitopes generated by point mutations in melanoma cells. These neoepitope specific T cells were still present after one month from the adoptive transfer and were present at higher level in the tumor site compared to peripheral blood[6]. Another study identified seven different melanoma specific neoepitopes recognized by *in vitro* expanded TILs in three different patients who had shown objective responses to ACT therapy[7]. It was shown that adoptive transfer of neoepitope specific T cells could mediate tumor regression also in non-melanoma epithelial cancers, characterized by a low number of mutations. In one patient with epithelial cancer, TILs revealed the presence of CD4 Th1 cells recognizing a neoepitope expressed by the tumor. Adoptive transfer of TILs containing more than 95% of cancer neoepitope specific CD4 Th1 cells mediated tumor regression[8]. Further analyses of TILs in patients with epithelial cancers revealed the presence of CD4 and/or CD8 T cells targeting one to three neoepitopes expressed by the patient's own tumor in 9 out of 10 cases[9]. Moreover, none of the neoepitopes were shared between the patients. This evidence further supports a personalized approach for effective cancer treatment.

Personalized cancer vaccines

Based on the strong evidence of the pivotal role of neoepitopes in eliciting potent anti-cancer immune responses, "personalized cancer vaccines" formulated with neoepitopes are being developed and are emerging as a promising therapeutic approach.
Recently, next generation sequencing completely transformed the way we detect neoepitopes, making patient-specific neoepitopes mapping feasible both from cost and time perspectives. In this approach, summarized in Figure 5, tumor cells and normal tissue from a patient are subjected to whole exome and RNA sequencing to identify all patient specific, non-synonymous somatic mutations, constituting the patient specific "mutanome". RNA sequencing is an important step that allows the identification of

mutations in genes that are transcriptionally active. Confirmed mutations are analyzed *in silico* for MHC class I and class II binding and skimmed through several filters like antigen processing or whether the mutant epitope has a stronger predicted binding affinity compared to the corresponding wild type peptide. An important parameter is the abundance of the epitope, which is estimated indirectly by quantitating RNA expression levels.
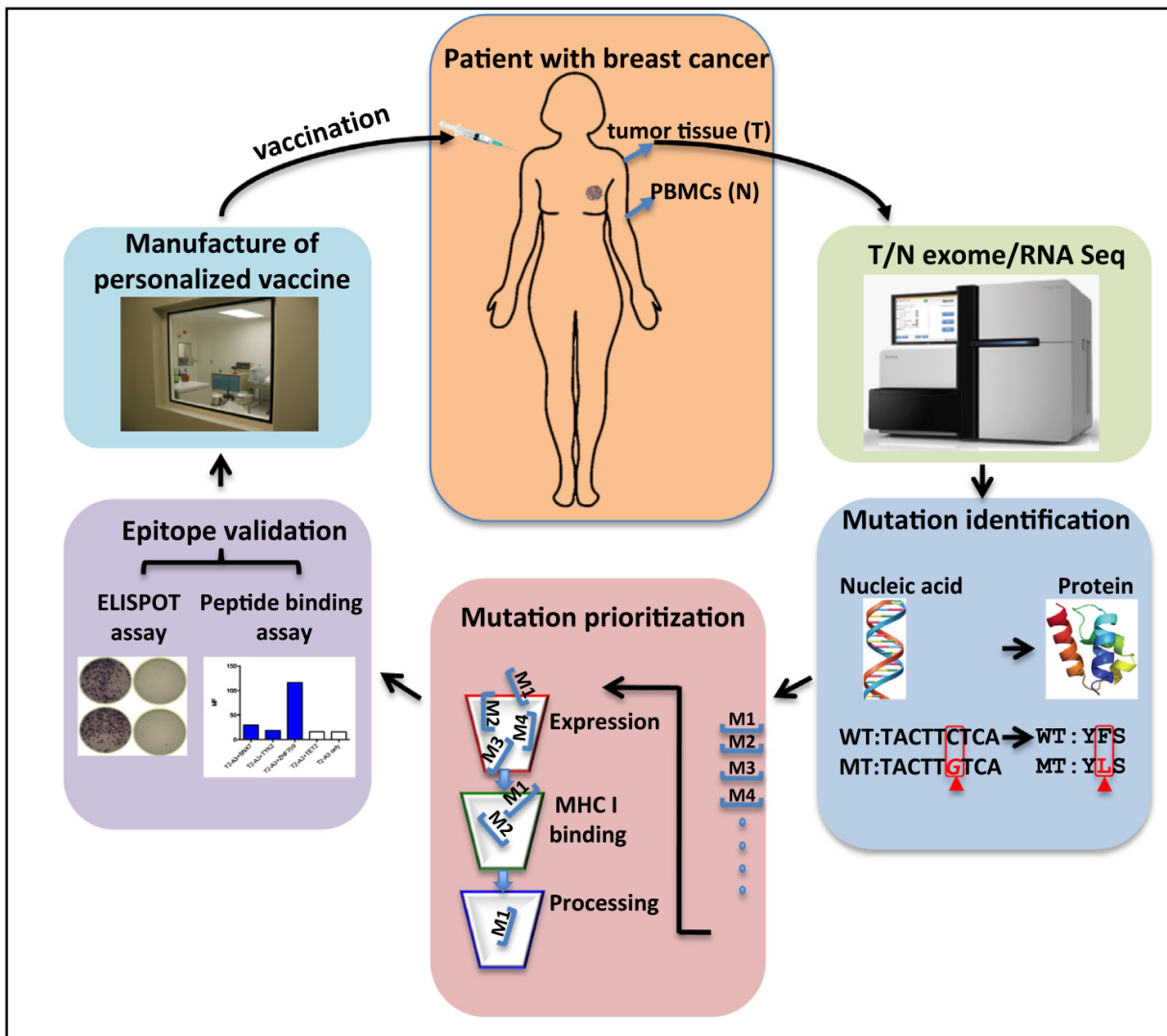
Figure 5 | Workflow for the generation of personalized vaccine formulations targeting neoantigens. *This figure summarizes the key steps for the generation of personalized cancer vaccine formulations targeting patient specific neoepitopes. PBMCs, peripheral blood mononuclear cells. Figure taken from Zhang et al., 2017*[76].

The list of candidate neoepitopes can be synthetized and validated by identifying mutant neoepitope-specific T cells in fresh patient TILs through functional assays (such as ELISPOT assays, peptide binding assay and/or intracellular cytokine staining) and/or MHC-multimer screenings. Recently, new bioinformatics approaches allow the

prediction and validation *in silico* of patient specific cancer neoantigens[11,14], thus avoiding the time consuming *in vitro* validation. Validated neoepitope can be synthetized under good manufacturing practice (GMP) conditions and used to either expand neoepitope-specific TILs for ACT or to formulate personalized cancer vaccines[60,76,135,136].

In one study, using the genomics and bioinformatics approaches described above, researchers identified neoepitopes that worked as T-cell rejection antigens following PD-1 and/or CTLA-4 blockade therapy in tumor bearing mice. More importantly, when these neoepitopes were incorporated as synthetic long peptides in therapeutic vaccines they were as effective as checkpoint blockade immunotherapy in inducing tumor rejection[12]. So it has been revealed that, beyond being important targets in checkpoint blockade therapy, tumor-specific neoepitopes can also be used to develop personalized cancer-specific vaccines[12].

In another research, whole-exome and RNA sequencing was used in combination with mass spectrometry to identify neoepitope that were filtered and prioritized to predict the most immunogenic ones. The resulting peptides were validate *in vivo*, obtaining three neoepitope that induced a neoepitope specific T cell population when used to immunize MHC I matched mice. More importantly, these neoepitopes were also able to protect mice from tumor growth both in a prophylactic and in a therapeutic schedule[13].

Using an approach they previously developed[10], the same research group demonstrated in three different tumor models that the majority of cancer specific mutations is immunogenic and recognized by CD4 T cells. Moreover, RNA-based therapeutic vaccination with these CD4 neoepitopes conferred strong antitumor activity[11]. Another important result of the previous study is that they generated a method for the selection of identified mutation as RNA vaccine candidates that rely exclusively on bioinformatics prioritization based on their expression levels and MHC class II binding affinity. They also demonstrated that the approach is suitable for prediction of neoepitopes in human cancers.

In fact, in a following publication the same group applied the approach to the first in human personalized mutanome vaccine against melanoma[14]. They identified non

synonymous tumor specific mutations in thirteen patients with stage III and IV melanoma. They selected ten of those mutations (five for one patient) according to predicted high MHC class II binding affinity together with high expression of the neoepitopes as RNA levels and according to high MHC class I binding affinity and created a RNA-vaccine unique for each patient. Sixty percent of the predicted neoepitopes were immunogenic in patients and the responses were mediated mostly by CD4 T cells and by a mix of CD4 and CD8 T cells. All patients showed significantly reduced metastatic events after vaccination, with the result of a sustained progression-free survival. One patient showing fast disease progression after vaccination, experienced a complete response after combination therapy with PD-1 blockade[14]. In another clinical trial, six melanoma patients were vaccinated with a mix of adjuvants and several long peptides encoding up to 20 personal neoepitopes predicted on their MHC class I binding affinity[15]. Vaccination induced both CD4 and CD8 neoepitope specific T cells and despite their prediction method, surprisingly vaccination induced T cells were mostly CD4 T cells as observed in the previous study. All patients that started vaccination with stage IIIB/C melanoma remained without disease recurrence for more than two years. Two patients that started treatment with stage IV melanoma and showed lung metastasis had recurrent disease after vaccination. However, both achieved complete tumor regression after PD-1 blockade therapy[15].

Together, these two human studies proved the safety, feasibility and clinical efficacy of personalized, patient specific, multi neoepitope directed cancer vaccination. Moreover, in both cases patients with recurrent diseases became tumor free after pembrolizumab therapy[14,15], suggesting a synergistic effect of vaccination and checkpoint inhibitors therapies.

All the data obtained from the studies reported above provide compelling evidence that patient specific, neoepitope targeting vaccines are an effective cancer immunotherapy. Moreover, to overcome tumor escape derived from immunoediting-driven neoantigen-loss[137], the most effective strategy appears to be personalized cancer vaccination targeting several trunk driver mutations, combined with checkpoint blockade therapy to obtain full therapeutic efficacy.

Bacterial outer membrane vesicles (OMVs)

OMVs are non-replicating structures of 20-250 nm naturally released by all gram-negative bacteria from the budding out of the outer membrane[16,17]. Reflecting their origin, they contain mostly lipopolysaccharide (LPS), glycerophospholipids and outer membrane and periplasmic proteins[138], together with DNA, RNA and peptidoglycan[139]. OMVs have several functions, including inter and intra species cell-to-cell cross-talk, biofilm formation, genetic transformation, defense against host immune responses, and toxin and virulence factor delivery to host cells[138,140]. OMVs are an emerging attractive vaccine platform because of several characteristics. OMVs possess a built-in adjuvanticity, carrying many MAMPs, such us LPS, lipoproteins, peptidoglycan, and flagellin[18,19]. By binding to pathogen recognition receptors on immune cells, these molecules play a key role in stimulating innate immunity and promoting adaptive immune responses[20–22]. In fact OMVs activate macrophages and induce maturation of DCs and their consequent production of pro-inflammatory cytokines[139]. Several works have demonstrated that OMVs elicit a Th1-skewed immune response[141–143], which is needed to eliminate both intracellular pathogens and cancer cells[82,113–115].

OMV protein content can be easily and promptly manipulated by altering the OMV-producing strain with molecular and synthetic biology techniques. OMVs can be engineered with selected antigens, either heterologous protein both in the lumen and on the surface[144,145]. Recently, our group showed that different bacterial antigens could be delivered to the lumen of *E. coli* vesicles by fusing their coding sequences to a leader peptide for secretion[142]. Furthermore, we showed that heterologous lipoproteins could be incorporated into the OMV membrane[23] and that through such polypeptides it is possible to deliver heterologous antigens as fusion protein to the OMV surface[23,24]. More importantly, it has been demonstrated by our and other groups, that OMVs induce both B and T cell responses specific for the delivered antigens [24,141,142,146–148].

Finally, OMV vaccines are safe and effective. In fact, an OMV-based vaccine has been approved to prevent *Neisseria meningitidis* serogroup B infections in humans[149,150].

OMVs production can be promptly scaled-up from laboratory to industrial levels. Using mutant strains showing hyper-vesiculating phenotype[146,151], OMVs can be rapidly and easily purified from bacterial culture supernatant with detergent-free methods[23,142,151,152]. Once the supernatant is separated from the biomass of these

mutant strains, the purification of the vesicles can be carried out using tangential flow filtration with production yield higher than 100 mg of vesicles (protein content) per liter of culture[153] under GMP conditions.

Due to these characteristics, OMVs appear to be an ideal tool for the creation of a vaccine platform suitable for personalized medicine. Once patient's specific neoepitopes are selected through *in silico* approaches, these can be expressed in OMVs and the resulting engineered vesicles can be rapidly purified in high amounts under GMP conditions.

Aim of the thesis

Our laboratory is interested in the exploitation of OMVs as a vaccine platform. Therefore, the aim of my thesis is to set the groundwork for the use of engineered OMVs in personalized cancer vaccines. The main goals of my experimental work can be summarized as follows:

1. Analysis of immune genes induced by OMV vaccination with the objective of elucidating the mechanisms of activation of innate and adaptive immunity

2. Decoration of OMVs with a CD8 T cell epitope in order to follow the T cell population induced by OMV vaccination and the capacity of OMV vaccination to protect mice from tumor challenge

3. Analysis of antigen specific CD8 T cell response and protection from tumor challenge induced by OMV vaccination

4. Demonstration of the general applicability of an OMV-based vaccine platform in personalized cancer vaccines by demonstrating the ease and efficiency with which OMVs can be decorated with foreign epitopes and the capacity of engineered OMVs to control tumor growth using different mouse models

5. Setting up a protocol for OMV engineering that is compatible with the timing of the personalized cancer vaccine approach.

Results

Immune gene expression analysis in mice immunized with OMVs

First, we wanted to investigate how OMVs affect immune gene expression. We immunized mice subcutaneously with 20 μg of OMVs from *E. coli* BL21(DE3)*ΔompA* strain, our OMV-overproducing strain, and after 36 hours, we collected draining lymph nodes and extracted the total RNA. The schedule of tissue collection after immunization was chosen according to the time DCs, macrophages and monocytes require to migrate to lymph nodes and interact with T cells[154].

After retrotranscription, qPCR was performed to compare gene expression levels in term of RNA amount in mice immunized with either OMVs or PBS, the OMV resuspension buffer, as a control. We analyzed 84 genes involved in host innate and adaptive immune responses to bacterial infection using the Qiagen RT² Profiler™ PCR Array Mouse Innate & Adaptive Immune Responses. This array, among all genes, includes several cytokines, T cell activation and Th1 immune response markers.

It is important to note that by collecting whole lymph nodes, we are taking and analyzing a mixed cell population consisting of immune cells, such as DCs, monocytes, macrophages, T, B and NK cells, as well as other cell types like epithelial, endothelial and stromal cells (fibroblasts and pericytes). This is very useful to have a wide picture of the ongoing immune response, which is naturally carried out by several different cell types, and provides an average expression level of a specific gene. On the other hand, this type of analysis might underestimate or completely ignore gene changes occurring in a small cell population only, which are eventually diluted in the mixed-cell samples analyzed.

Figure 6, which reports the Log10 of the normalized gene expression levels in mice injected with either OMVs or PBS, provides a snapshot on how many, and to what extent, genes are up- and down regulated in draining lymph nodes upon OMV administration. Genes whose expression varies less than twofold fall within the two dotted lines, while genes that are upregulated and downregulated more than two fold

are plotted as red dots and green dots, respectively, above and below the dotted lines. In total 19 genes were upregulated by OMVs while 5 were down-regulated.
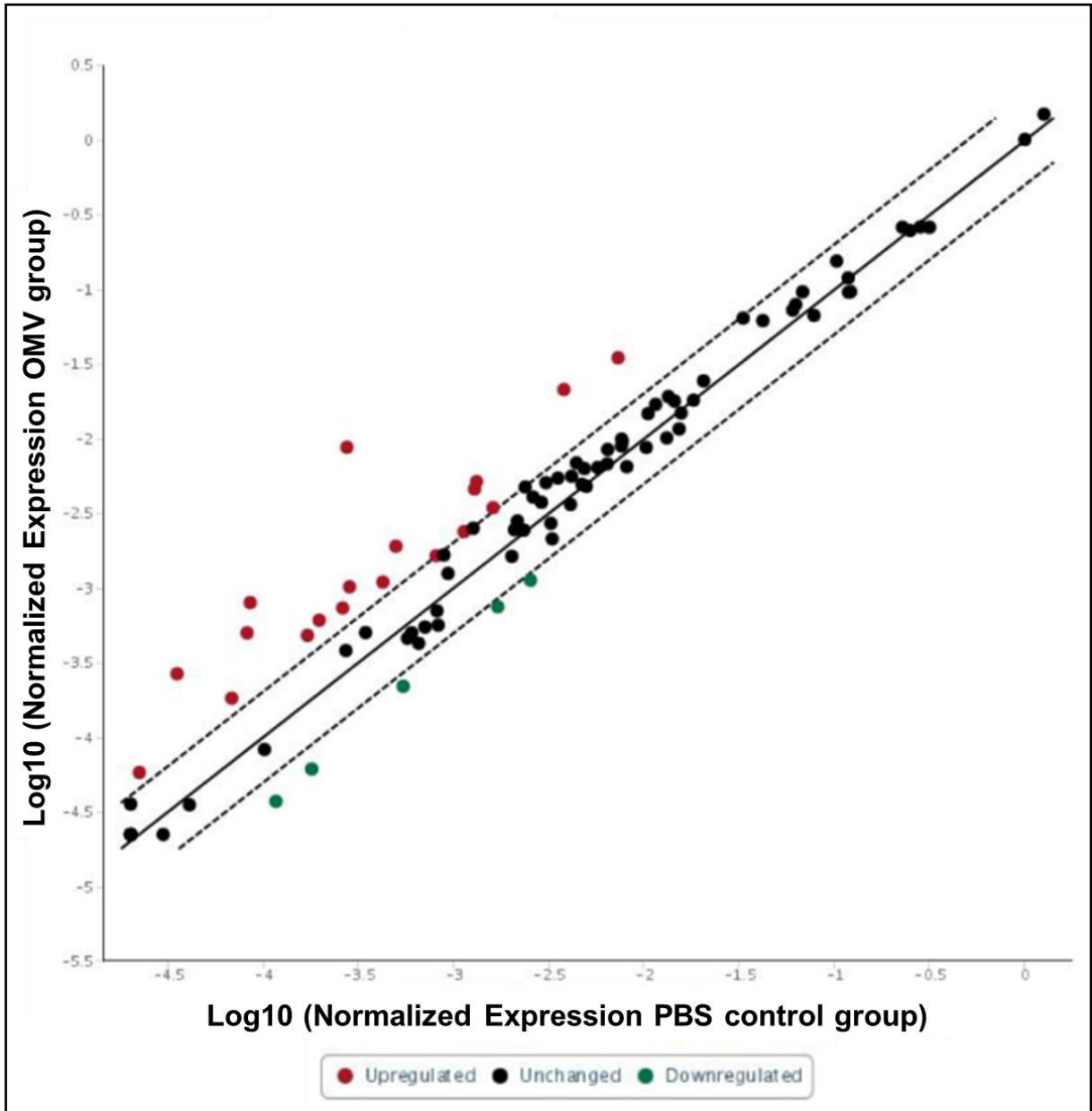
Figure 6 | Snapshot of the extent of immune gene changes induced by OMV vaccination. *This graph shows the log10 of the normalized expression level of each gene in OMV treated versus PBS control group. In this plot, genes with similar expression level in the two groups fall between the two dashed lines. Genes upregulated or downregulated more than two times stand out above and below, respectively, the dashed lines. To help a quick visualization, upregulated and downregulated genes are plotted in red and green, respectively.*

Table 1 reports the list of upregulated and downregulated interesting genes, grouped on the basis of their role in immune responses.

Gene	Fold regulation		Gene	Fold regulation
Pro-inflammatory cytokines			*Th1 response*	
IL-1α	4.0		IFN-γ	3.4
IL-1β	58.6		IL-18	1.7
IL-6	8.3		Stat1	1.6
TNF-α	2.0		T-bet (Tbx21)	2.4
MAMPs detection and signaling			*Th2 response*	
CD14	5.0		GATA3	-1.8
NOD2	2.8		IL-4	-3.6
MyD88	2.5		IL-5	-3.5
Ticam (Trif)	2.6		IL-13	-7.0
IRF7	4.1			
Other genes			*Chemoattraction and adhesion*	
GM-CSF	4.3		Itgam	3.8
NLRP3	7.9		Cxcl10	4.8

Table 1 | Immune gene affected by OMV immunization in mice. *Gene expression level was analyzed by qPCR on cDNA retrotranscribed from RNA extracted from draining lymph nodes of mice immunized with either OMVs or PBS. Fold change was calculated by dividing the normalized expression of a gene in OMV treated sample by the normalized expression level of the same gene in the PBS control group. Gene expression level was provided as fold regulation, which is equal to the fold change for up-regulated genes, while it is the negative inverse of the fold change for down-regulated genes.*

The first interesting observation was the upregulation of genes involved in MAMP signaling, important to activate innate immunity upon microbe detection. They include CD14, NOD2 and NLRP3. CD14 is involved in LPS sensing and was upregulated fivefold in the OMVs treated group compared to PBS control group (Figure 7b and Figure 7e). This is in line with the fact that LPS represents the most abundant and relevant MAMPs in OMVs, being found at a concentration of more than 100 mg/mg of OMV proteins. There was a remarkable activation of the inflammasome machinery (NLRP3 was upregulated by 7.9 times, Figure 7e), which is induced by TLRs and NOD signaling and activated by cellular stress, extracellular ATP, disruption of lysosomes and intracellular LPS. Finally, NOD2, which responds to intracellular concentration of peptidoglycan-deriving muramyl dipeptide, was upregulated by 2.8 times (Figure 7b). This supports the notion that OMVs are endocytosed by phagocytic cells and are

subsequently partially released from the vesicular compartment into the cytoplasm thorough mechanisms not yet fully elucidated.

A second group of genes was that involved in signal transduction upon engagement of MAMP receptors and some cytokine receptors (IL-1 and IL-18 receptors). They include MyD88 and Ticam1, which were found upregulated by 2.5 and 2.6 fold, respectively (Figure 7b). In addition IRF7, which is also activated by TLR9 and is responsible for Type I interferons production, was upregulated 4.1 times (Figure 7b), suggesting a role of CpG dsDNA which has been reported to be present in OMVs.

A third important group of genes which was upregulated encodes pro-inflammatory cytokines, released by activated APCs. They promote vasodilatation and are important for the infiltration and activation of both innate and adaptive immune cells at the site of infection. They included IL-1α, IL-1β, IL-6, upregulated by 4, 58.6 and 8.3 times respectively. TNF-α showed a 2 fold increase, while GM-CSF a 4.3 upregulation (Figure 7a and Figure 7e). The expression of these cytokines is in line with the observed activation of MAMP receptors.

OMV vaccination induced the activation of NLRP3 inflammasome, responsible for the release of biologically active IL-1 β and IL-18 (Figure 7a and Figure 7c). NLRP3, induced after TLRs and NOD signaling, was found strongly upregulated by 7.9 times and the pro inflammatory IL-18 was upregulated by 1.7 times (Figure 7e).

Investigating genes involved Th1/Th2 differentiation, which are induced by the innate mediators analyzed above, data shows a strong induction of a type 1 response (Figure 7c). We found the key Th1 marker IFN-γ upregulated by 3.4 times and, as already pointed out, the cytokine IL-18 upregulated by 1.7 times. IFN-γ signaling through IFN-γ receptor, via transcription factor Stat1, induces transcription of the master regulator of Th1 differentiation, T-bet (Tbx21). We found both these two key components upregulated upon OMV immunization: Stat1 was upregulated by 1.6 times and T-bet was upregulated by 2.4 times.

In line with the notion that Th1- and Th2-type of immune responses are mutually exclusive and OMVs induced a Th1-skewed response, Gata3 transcription factor, that

drives Th2 differentiation, was downregulated by 1.8 times. This translated in downregulation of IL-4, IL-5 and IL-13 by 3.6-, 3.3- and 7 fold, respectively (Figure 7d). All these are Th2 cytokines controlled by Gata3.

We also found GM-CSF, a cytokine induced in activated macrophages and DCs as well as in activated NK and T cells, upregulated by 4.3 times (Figure 7e). Cxcl-10, a chemokine involved in T cell, NK cell and DC recruitment after IFN-γ signaling, showed a 4.8-fold upregulation and Itgam, molecule responsible for leukocytes adhesion and extravasation, had a 3.8-fold increase after OMV injection (Figure 7e).

Taken together, these results show that OMV vaccination is extremely efficient in stimulating innate immunity and a Th1-skewed response.

a Pro-inflammatory cytokines

b MAMPs detetcion and signaling

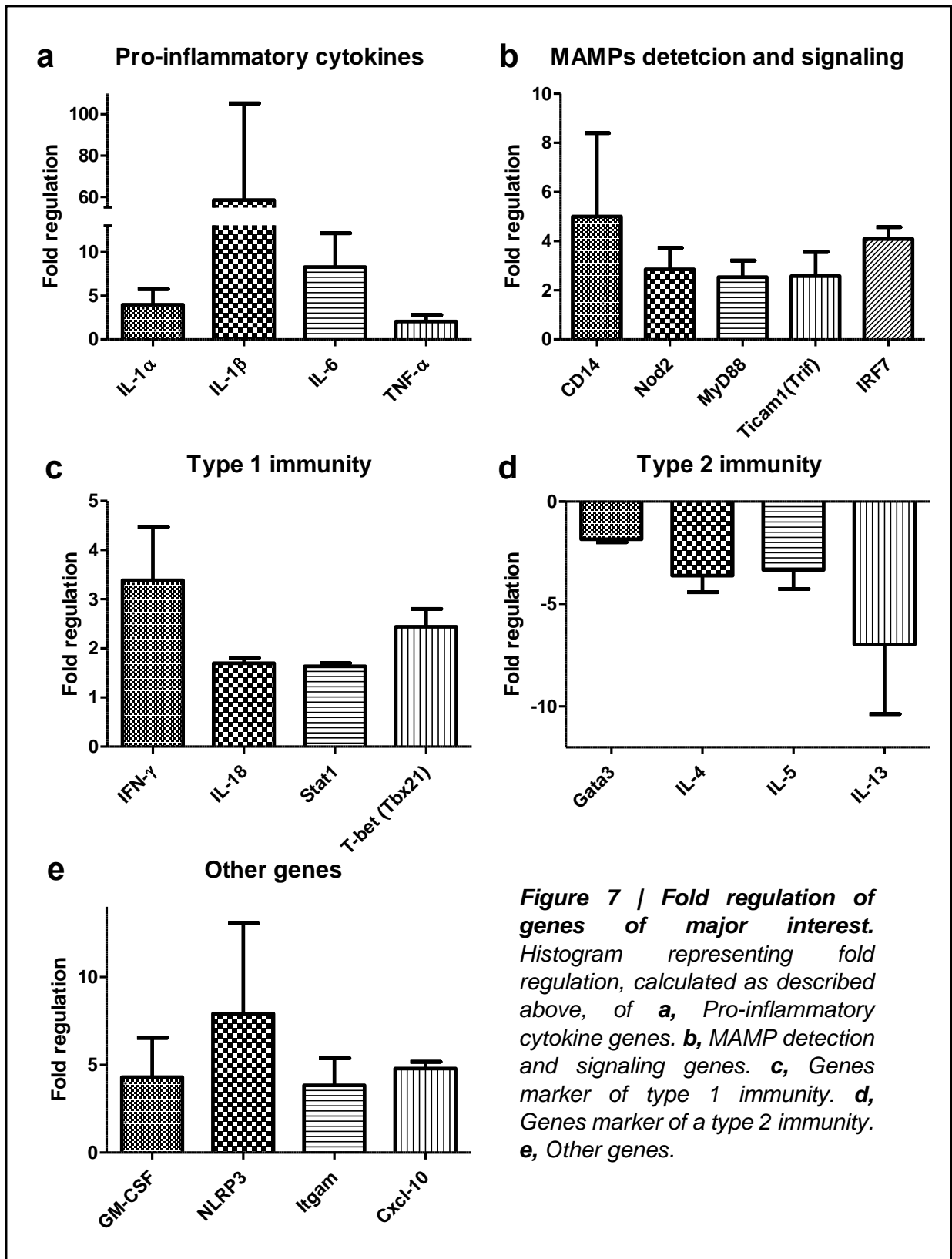**c** Type 1 immunity

d Type 2 immunity

e Other genes

Figure 7 | Fold regulation of genes of major interest. Histogram representing fold regulation, calculated as described above, of *a,* Pro-inflammatory cytokine genes. *b,* MAMP detection and signaling genes. *c,* Genes marker of type 1 immunity. *d,* Genes marker of a type 2 immunity. *e,* Other genes.

OMV engineering with OVA$_{257-264}$ as a model epitope

OVA$_{257-264}$ as CD8 T cell model epitope

One of the goal of my research was to investigate whether vaccination with OMVs engineered with specific CD4 and/or CD8 T cell epitopes could elicit epitope-specific cell-mediated immune responses and whether such responses could be protective against tumors expressing such epitopes. Moreover, we wanted to investigate whether differences in antigen compartmentalization in OMVs, i.e. lumen vs. surface, could affect the quality and quantity of epitope-specific T cell responses.

To this purpose, as model epitope we selected the OVA$_{257-264}$ peptide from chicken ovalbumin, a CD8 epitope known to be immunogenic in H-2 Kb mice (C57BL/6 mice). We chose OVA$_{257-264}$ for three main reasons. First, the epitope has been extensively used in many mouse studies and therefore there is a large body of published data to use as reference. Second, OVA$_{257-264}$ specific dextramers are available, an extremely useful tool to follow OVA$_{257-264}$-specific T cells in a quantitative manner. Third, a B16F10 murine melanoma cell line stably transfected with chicken OVA is available, which can be used to test whether the levels of OVA$_{257-264}$-specific T cells induced by immunization could be strong enough to protect syngeneic C57BL/6 mice from the challenge with such engineered cell line.

OMV engineering with OVA$_{257-264}$ epitope

To obtain OVA$_{257-264}$ epitope expression in OMVs, we fused it to specific carrier proteins, selected in our laboratory for their efficient delivery of foreign antigens in OMVs. In particular, the *E. coli* maltose binding protein (MBP) was used to obtain OVA$_{257-264}$ expression in the lumen of OMVs, while for a surface exposition, OVA$_{257-264}$ was fused to the PSP protein (no details of PSP can be given for confidentiality reasons). MBP is naturally present in the periplasm of *E. coli*[155]. During the vesiculation process, the protein is encapsulated in the lumen of OMVs[19] and therefore heterologous polypeptides fused to MBP are delivered inside the OMVs. By contrast, PSP is a lipoprotein which reaches the *E. coli* outer membrane. Polypeptides fused to

the C-terminus of PSP are transported to the outer membrane and therefore are compartmentalized in the OMV membrane during vesiculation.

The cloning of OVA$_{257-264}$ antigen was made with the following criteria:

1) To increase antigen concentration in OMVs, three copies were fused in tandem to the carrier protein;

2) To facilitate its processing and presentation on MHC class I, OVA$_{257-264}$ was fused to the carrier proteins flanked by its natural flanking sequences[156]. Furthermore, each copy of OVA$_{257-264}$ with flanking sequences was separated from each other by a glycine-glycine flexible spacer[156];

From now on, the three copies of the OVA$_{257-264}$ with flanking sequences and separated by glycine-glycine spacer will be referred to as OVA (for amino acid sequence of OVA see Material and Methods section, Table 3 and Figure 18 in the Appendix section).

The mini-gene encoding OVA was chemically synthesized and fused to the 3'-end of either PSP or MBP using Polymerase Incomplete Primer Extension (PIPE) method[157], obtaining pET-PSP-OVA and pET-MBP-OVA plasmids, respectively. Plasmids encoding the fusion proteins were used to transform the *E. coli* OMV-overproducing strain BL21(DE3)*ΔompA* and OMVs were purified (see Figure 18 in the Appendix section for details). Briefly, BL21(DE3)*ΔompA* pET-PSP-OVA and BL21(DE3)*ΔompA* pET-MBP-OVA strains were grown at 30°C to OD$_{600}$=0.5 and the expression of the recombinant proteins was induced by addition of 0.1 mM of isopropil-ß-D-1-thiogalactopyranoside (IPTG) for four hours. Cells were pelleted and supernatant filtered with a 100 KDa membrane. After 2 hours of ultracentrifugation, OMVs were resuspended with sterile-filtered PBS. Finally, to assess the presence of the fusion proteins, 20 μg of OMVs (protein content) purified from BL21(DE3)*ΔompA* pET-PSP-OVA (PSP-OVA OMVs), from BL21(DE3)*ΔompA* pET-MBP-OVA (MBP-OVA OMVs) and from BL21(DE3)*ΔompA* transformed with the pET empty vector ("Empty" OMVs) as a control, were separated by SDS-PAGE using Any kD™ Criterion™ TGX Stain-Free™ Protein Gel. Proteins were revealed by Coomassie staining. Figure 8a shows a typical pattern of the total protein contents of OMVs. The recombinant proteins accumulated with high efficiency in OMVs, as indicated by the bands marked with a

star. The presence of $OVA_{257-264}$ epitope fused to the carrier proteins was confirmed by Western Blot analysis. 20 μg of PSP-OVA OMVs, of MBP-OVA OMVs and of "Empty" OMVs as a control were separated as above. Proteins were transferred onto nitrocellulose membranes and bands corresponding to $OVA_{257-264}$ epitope were revealed using α-OVA polyclonal antibodies. As shown by the bands in Figure 8b, $OVA_{257-264}$ epitope is efficiently incorporated in both PSP- and MBP-OMVs.
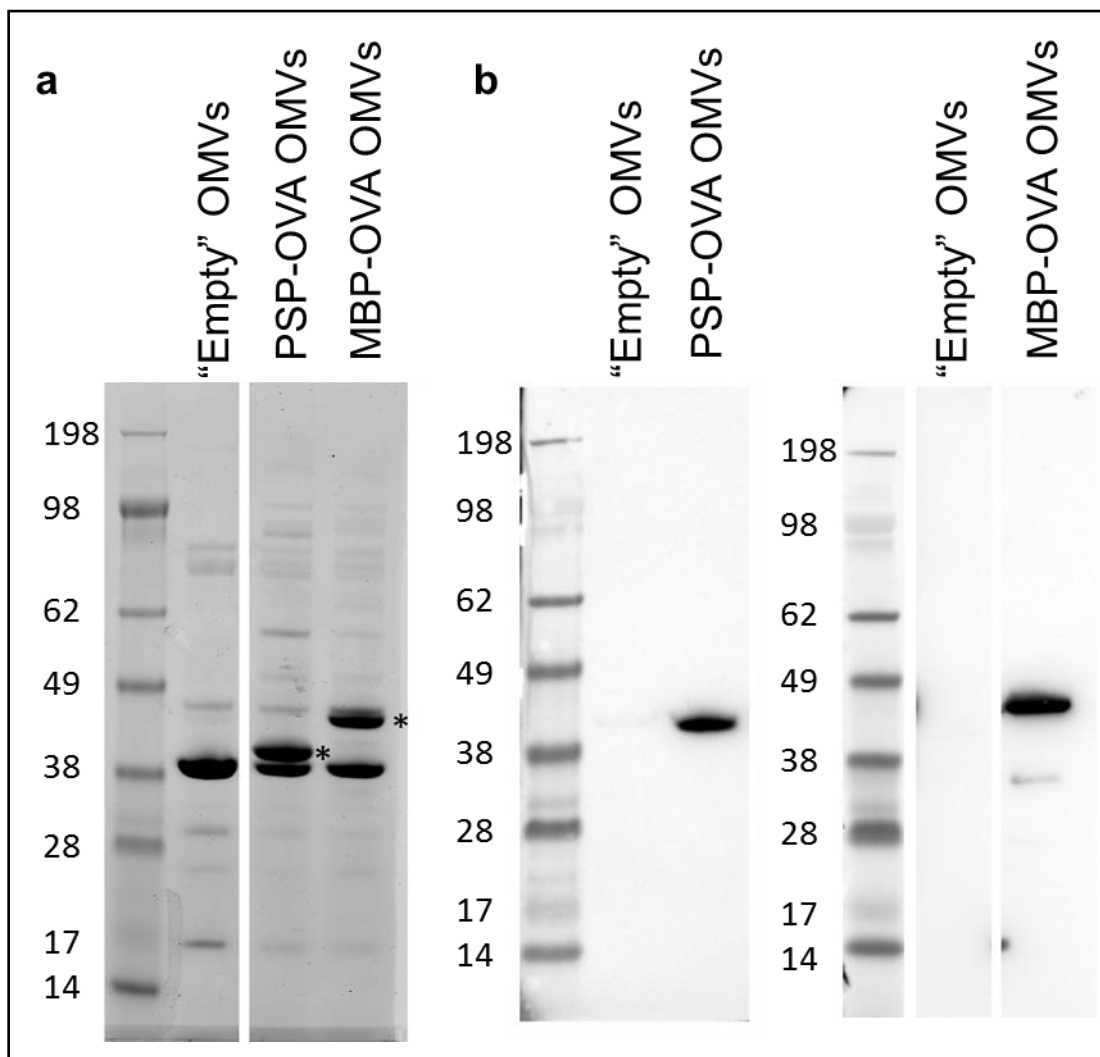
Figure 8 | $OVA_{257-264}$ is efficiently expressed in OMVs. a, SDS-PAGE analysis of 20 μg of OMVs purified from BL21(DE3)ΔompA pET-PSP-OVA (PSP-OVA OMVs) and from BL21(DE3)ΔompA pET-MBP-OVA (MBP-OVA OMVs) strains. As a control were used OMVs purified from BL21(DE3)ΔompA strain transformed with pET empty vector ("Empty" OMVs). PSP-OVA and MBP-OVA proteins are indicated by a star. **b,** Western blot analysis of 20 μg of PSP-OVA, MBP-OVA OMVs and "Empty" OMVs as a control. $OVA_{257-264}$ epitope was detected using α-OVA polyclonal antibodies.

Analysis of antigen compartmentalization in bacterial cells and OMVs

To fully characterize OVA-engineered vesicles and to assess the correct antigen localization in OMVs, we performed Triton X-114 assay on OMVs and flow cytometry analysis on whole cells.

When OMVs are solubilized with Triton X-114 detergent and exposed at temperatures above its cloud point (23°C), two phases are generated: an aqueous phase, containing polar and hydrophilic molecules, and a detergent-enriched, lipophilic phase, containing hydrophobic molecules, including lipoprotein[158]. Because of their difference in hydrophilicity/hydrophobicity, the periplasmic MBP fusion protein and the lipidated PSP fusion protein should be enriched in the aqueous and in the detergent phases, respectively.

100 μg of PSP- and MBP-OMVs were therefore solubilized with 1% Triton X-114 solution and after temperature shift, the proteins present in the two phases were precipitated by chloroform-methanol and resuspended in Laemmli buffer. The proteins present in the two phases and in total OMVs (20 μg) were separated by SDS-PAGE using NuPAGE™ 4-12% Bis-Tris Protein Gels and analyzed by Western Blot using α-OVA antibodies. As shown in Figure 9, PSP-OVA localize in the hydrophobic phase (9a) while MBP-OVA localize in the aqueous phase (9b). These data confirm that PSP-OVA is associated to the lipid membrane bilayer of OMVs, while MBP resides in their lumen.

To assess PSP-OVA and MBP-OVA localization in bacteria, BL21(DE3)*ΔompA(*pET-PSP-OVA) and BL21(DE3)*ΔompA(*pET-MBP-OVA) strains were grown at 30°C to OD$_{600}$=0.5 and the expression of the recombinant proteins was induced by addition of 0.1 mM of IPTG for four hours. Cells were collected, incubated with the α-OVA antibodies and subsequently with secondary Alexa Fluor®488 anti-rabbit total IgGs antibodies. Finally, cells were fixed with 2% formaldehyde and analyzed by flow cytometry. The data shown in Figure 9c indicated that PSP-OVA fusion was surface exposed as deducible from the marked increase in the population of cells positive for α-OVA antibodies. By contrast, the staining of bacteria only with secondary Alexa Fluor®488 anti-rabbit antibodies showed no increase in fluorescence signal,

confirming specificity of the signal. The staining of bacteria expressing MBP-OVA showed no increase in fluorescence signal, confirming the periplasmic localization of the fused protein (Figure 9d).
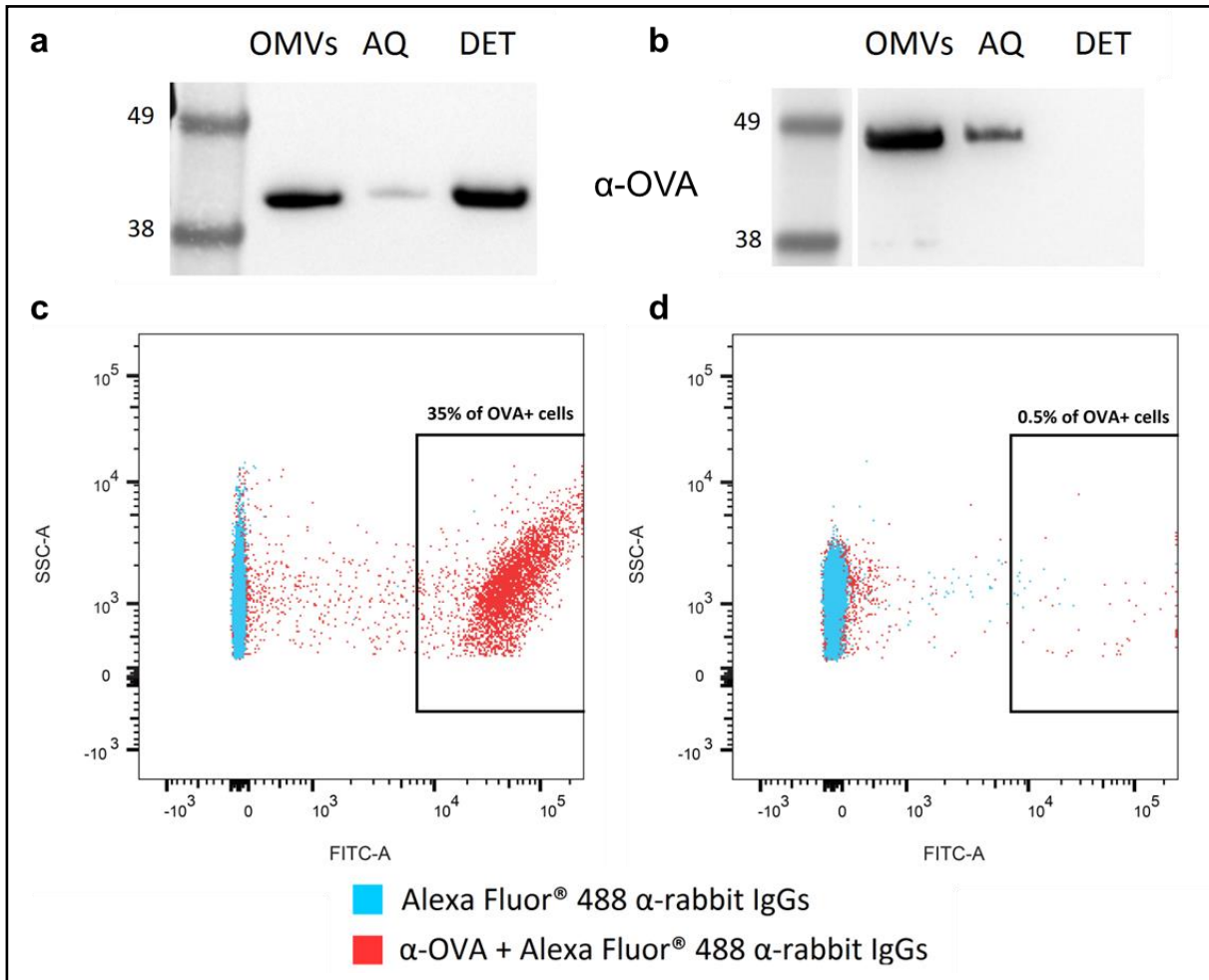
Figure 9 | OVA$_{257-264}$ epitope is exposed on the surface of PSP-OVA OMVs. a, b, *Triton X-114 assay: 100 µg of PSP-OVA OMVs (**a**) and MBP-OVA OMVs (**b**) were solubilized with 1% Triton X-114, obtaining an aqueous phase enriched in hydrophilic proteins and a detergent phase enriched in membrane-associated proteins. After chloroform-methanol precipitation, proteins from both phases, together with proteins from total OMVs (20 µg) were separated by SDS-PAGE and transferred on a nitrocellulose membrane for a Western blot analysis. The presence of the OVA$_{257-264}$ epitope in either aqueous or detergent phase was detected using α-OVA antibodies.* ***c, d,*** *Flow cytometry analysis. Bacterial cells from BL21(DE3)ΔompA pET-PSP-OVA (**c**) and BL21(DE3)ΔompA pET-MBP-OVA (**d**) strains were stained with rabbit α-OVA antibodies. Signal was detected using Alexa Fluor® 488 α-rabbit IgGs antibodies. As a control, cell were stained with Alexa Fluor® 488 α-rabbit IgGs antibodies only.*

Analysis of epitope specific T cell response induced by epitope-decorated OMVs

We have demonstrated that OMV vaccination can activate innate immunity and induce type 1 immunity (Figure 7) and that we can express antigen both in the lumen and on the surface of OMVs (Figure 8 and Figure 9). Next, we analyzed if engineered OMVs induced an epitope-specific CD8 T cell response. To this aim, we immunized C57BL/6 mice with 20 μg of PSP-OVA OMVs and MBP-OVA OMVs. Mice immunized with "Empty" OMVs were used as a control. Mice were vaccinated 2 times on day 0 and day 7 and blood was analyzed for the presence of $OVA_{257-264}$-specific CD8 T cells on day 12 or 13 (schedule in Figure 11a).

One way to detect and quantify antigen specific T cells is to exploit the natural interaction between MHCI-peptide complexes and TCRs in flow cytometry. Since a single TCR possesses low affinity for a MHCI-peptide complex, multimers, which carry multiple copies of MHCI-peptide complexes, have been developed. These molecules bind several TCRs with the same antigen specificity, allowing a more stable interaction between these compounds and the lymphocyte.
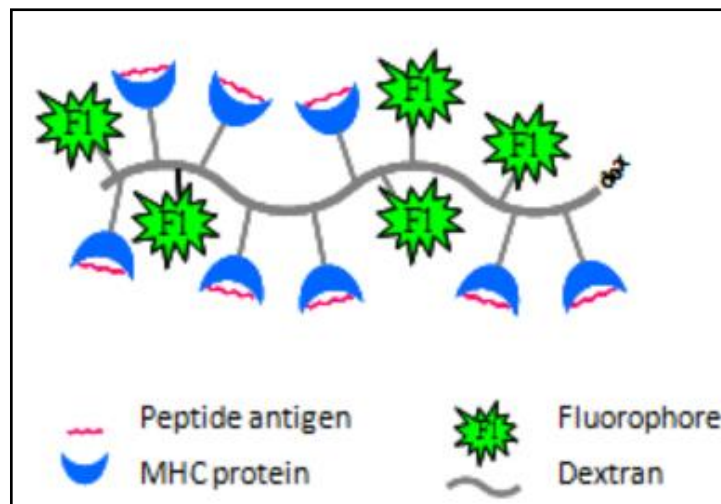

Figure 10 | Dextramer molecule. *Representation of a dextramer molecule, made of a dextran backbone which bears MHCI-peptide complexes and fluorochrome molecules. This structure allows the recognition of T cells carrying TCRs with either high or low affinity for MHCI-peptide complexes and gives high stability to the dextramer molecule. Figure taken from www.immudex.com*[159]

In particular, dextramers are MHC multimers made of MHCI-peptide complexes linked to a dextran backbone carrying several fluorochrome molecules[159,160] (Figure 10). The use of dextramers allows the identification of antigen-specific T cells independently from their ability to secrete cytokines and can therefore detect also antigen specific T cells that do not secrete IFN-γ, such as in less differentiated cells.

Furthermore, for their intrinsic nature, by physically binding to lymphocytes dextramers give a direct evidence of the presence of antigen specific CD8 T cells, as opposed to intracellular cytokines staining (ICS), which is an indirect measurement.

For a better detection of antigen specific CD8 T lymphocytes, a strategy to exclude unwanted cell populations and reduce the background noise was adopted, with minor modifications as previously described[161,162]. To reduce nonspecific binding of dead cells (7-AAD positive), monocytes (CD11b positive) and B lymphocytes (CD19 positive), a "dump channel" was created. α-CD11b and α-CD19 antibodies were labelled with the same fluorochrome, which had the same fluorescence of the 7-AAD: in this way, all three were acquired in the same fluorescent channel and excluded from the following analyses. Even though the staining was performed after Fc receptor blocking with α-CD16/CD32 antibodies, the exclusion of these cells is very important because all of them can bind in a nonspecific manner to antibodies and dextramer molecules, affecting the final evaluation of $OVA_{257-264}$ specific CD8 T cells. Moreover, since red blood cells compose the vast majority of peripheral blood cells, they were lysed and eliminated.

After the exclusion of all the above-mentioned cells, T lymphocytes were selected for CD3 expression. $OVA_{257-264}$ specific CD8 T cells were detected as the population positive to Dextramer and CD8 signals at the same time, gating on the CD3 positive population.

In order to detect the residual level of nonspecific staining and background noise, a negative control dextramer, which carries an irrelevant peptide, was used with the same gating strategy. Finally, dextramer positive, i.e. the $OVA_{257-264}$ specific CD8 T cell population, was calculated as percentage of the whole CD8 T cells.

As shown in Table 2, both PSP-OVA and MBP-OVA OMVs induced $OVA_{257-264}$-specific CD8 T cells at an average percentage of 1.8 and 0.7%, respectively. An average frequency of OVA-specific T cell response of 3.7% was obtained immunizing mice with 20 μg of "Empty" OMVs adsorbed to 100 μg of synthetic OVA peptide (ads-OVA OMVs). "Empty" OMVs alone did not induce any $OVA_{257-264}$ specific CD8 T cells.

Mouse	% of $OVA_{257-264}$ specific CD8 T cells in mice immunized with		
	PSP-OVA OMVs	MBP-OVA OMVs	$OVA_{257-264}$ adsorbed to "Empty" OMVs
1	0.5	1.4	2.4
2	1.4	0.3	5.7
3	5.9	0.2	4.1
4	0.3	0.4	1.0
5	0.6	0.3	6.5
6	2.2	0.1	1.9
7	0.1	0.3	1.4
8	2.1	2.6	3.8
9	1.6	0.9	2.0
10	3.0	0.7	7.8
Average	**1.8**	**0.7**	**3.7**

Table 2 | Percentage of $OVA_{257-264}$ specific CD8 T cells induced by OMV vaccination in C57BL/6 mice. Percentage of OVA specific CD8 T cells was calculated as fraction of the CD8 and dextramer positive events on the total of CD8 positive events. Data accumulated from 2 independent experiments of 5 mice/group each (n=10).

Figure 11 shows a representative dextramer analysis of epitope-specific CD8 T cells induced by PSP-OVA (11b), MBP-OVA (11c), ads-OVA (11d) and "Empty" (11e) OMV vaccination.

Considering that the OVA epitope represents less than 10% of each fusion protein and that mice received 20 μg of OMVs, approximately 0.2-0.4 μg of OVA peptide/dose were administered. This amount is approximately 200-fold lower than the amount of synthetic OVA peptide adsorbed to OMVs (100 μg peptide/20 μg OMVs). Therefore, when the antigen is physically associated to OMVs as in engineered OMVs, the elicitation of $OVA_{257-264}$ specific T cells is much more efficient.

This is in line with the notion that co-delivering of antigen and adjuvant is a prerequisite for an optimal cell-mediated immunity.

In conclusion, both PSP-OVA OMVs and MBP-OVA OMVs elicited high OVA$_{257-264}$ specific T cells, PSP-OMVs being probably superior to the other fusion. Whether this difference is due to the effect of epitope compartmentalization within the vesicles or rather to a different expression level of the fusion proteins remains to be investigated.

Noteworthy, the high mean fluorescence of OVA$_{257-264}$ specific T cells induced by both PSP-OVA and MBP-OVA OMVs indicates that T cells possess high avidity for cognate MHC class I-peptide complexes. This result is very important, because only T cells with high affinity for their target are useful for and will possibly give some chances to therapeutic cancer vaccination.
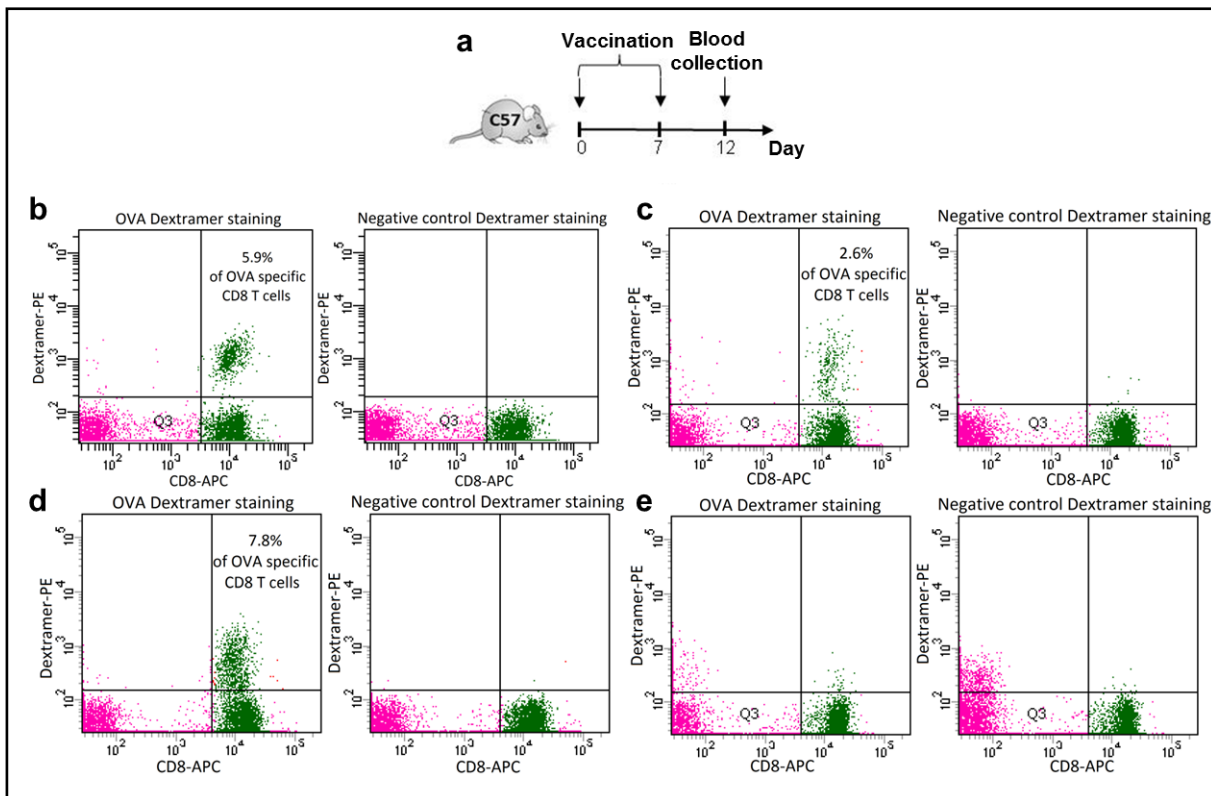
Figure 11 | OVA engineered OMVs induce OVA$_{257-264}$ specific CD8 T cells in C57BL/6 mice. a, *C57BL/6 mice were subcutaneously immunized two times on day 0 and day 7 and blood was collected on day 12. The analysis of OVA$_{257-264}$ specific CD8 T cells was performed with OVA$_{257-264}$ specific dextramers on whole blood after red blood cell lysis. As a control, a staining with a negative control dextramer, which bear an irrelevant peptide, was included in each analysis. **b-d,** Representative dextramer analysis performed on blood from a mouse immunized with **b,** PSP-OVA OMVs, **c** with MBP-OVA OMVs, **d,** with "Empty" OMVs adsorbed with 100 OMVs µg of OVA$_{257-264}$ synthetic peptide and **e,** with "Empty" OMVs as a control.*

OMV-based vaccine efficacy in cancer mouse models

OVA-OMV vaccines protect mice from B16-OVA tumors

With the previous experiments, we demonstrated that OVA-OMVs induce OVA specific T cells. We next asked the question whether such response could protect mice from OVA-expressing tumors. The cell line used in this experiment was the B16-OVA, a derivative of the murine melanoma B16F10 cell line transfected with a plasmid encoding secreted chicken ovalbumin. Before initiating the challenge experiments, ovalbumin expression in the culture supernatant of B16-OVA was assessed by ELISA, while the presence of the $OVA_{257-264}$ epitope within the OVA protein sequence was confirmed by sequencing the PCR product obtained by amplifying the ovalbumin cDNA from B16-OVA total RNA.

Once the presence and expression of the OVA antigen in B16-OVA was confirmed, we subcutaneously injected 2.85×10^5 cells in C57BL/6 mice (five mice/group) and the day after each mouse received 20 μg of PSP-OVA-OMVs, the engineered vesicles which gave a T cell response higher than MBP-OMVs (see previous section). Immunization was repeated every three days for a total of five injections (see immunization schedule in Figure 12a and details in Materials and Methods section). Mice immunized with "Empty" OMVs were used as a control and experiments were repeated twice on groups of 5 mice.

Tumor growth was followed over a period of 18 days from the challenge, measuring tumor size with a caliper. As shown in Figure 12b, immunization with PSP-OVA-OMVs strongly inhibited tumor growth and the average tumor size after 18 days from challenge was 290 mm^3 as opposed to an average of 2054 mm^3 in control mice (P=0.0001).
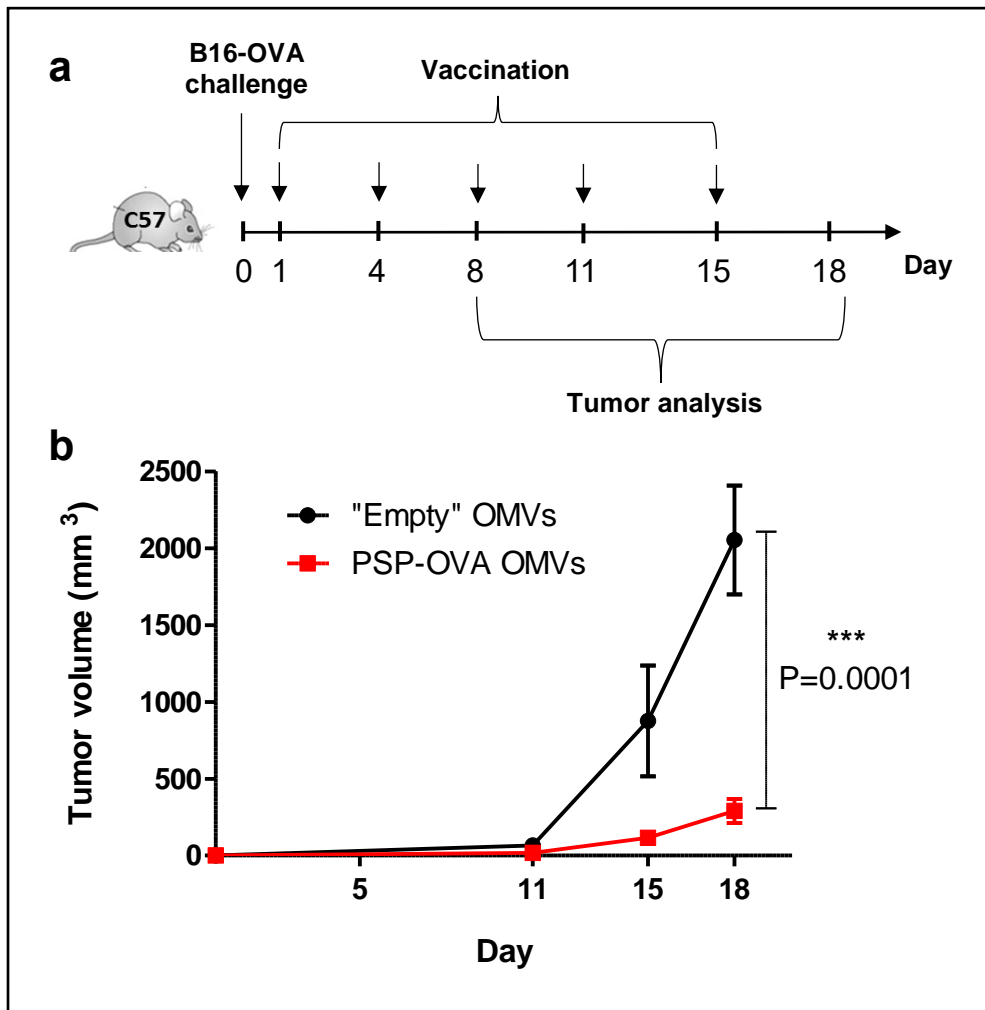
Figure 12 | PSP-OVA OMV vaccine protect mice from B16-OVA tumors. a, *C57BL/6 mice were challenged with B16-OVA cells on day 0 and subcutaneously immunized on day 1, 4, 8, 11 and 15 with either PSP-OVA OMVs or "Empty" OMVs. Tumor growth was followed starting from day 8.* **b,** *Tumor growth (mean ± s.e.m.) in C57BL/6 mice (n=10) immunized with PSP-OVA OMVs or "Empty" OMVs as a control. Data accumulated from 2 independent experiments of 5 mice/group each. Statistical analysis was performed using unpaired, two-tailed Student's t-test.*

Synergistic protective activity of OMVs engineered with two antigens

The data shown in the previous section indicate that OMVs engineered with a TSA can protect mice from tumors expressing the epitope with which OMVs were engineered. In the clinical setting, anticancer vaccines based on single epitopes may not be highly effective in establishing long-term, disease-free survival due to the immunoediting process, that selects tumor cells resistant to single-target therapies. Therefore, vaccine formulations that combine more than one antigen are expected to be a prerequisite to bring cancer vaccines to the clinic.

Therefore, we next asked the question whether OMVs engineered with two cancer epitopes had a superior protective activity of OMVs engineered with either of the two antigens.

The epitopes selected for these experiments were the B cell epitope EGFRvIII and the CD4 epitope M30, two epitopes expressed in B16F10-EGFRvIII cell line (see Material and methods section for details).

EGFRvIII is a ligand-independent, constitutively active mutated form of the human epidermal growth factor receptor (EGFR) generated by an in-frame deletion and found in many malignant brain tumors (up to 60% of primary glioblastoma multiforme is EGFRvIII positive) and other cancers such as breast, ovarian and prostate cancer[163]. The in-frame deletion creates a peptide sequence which is not found in normal cells and therefore constitutes an ideal target for immunotherapy[163,164]. Indeed, a peptide vaccine based on such epitope have been tested in PhaseII/PhaseIII trials in glioblastoma patients[165,166].

A derivative of B16F10 cell line is available that constitutively expresses EGFRvIII and therefore such cell line can be exploited to test the efficacy of EGFRvIII-OMV vaccines in the syngeneic B57BL/6 mice.

M30 CD4 epitope has been recently described in B16-F10 melanoma cells[11]. The epitope derived from a mutation, not present in C57BL/6 mice, occurring in the *kif18b* gene, one component of a protein complex involved in microtubule depolimerization[167]. RNA-based vaccine expressing M30 neoepitope have been shown to protect C57BL/6 mice from the challenge of B16F10 tumor[11].

Since B16F10-EGFRvIII cell line also carries the M30 mutation, such cell line can be used to test whether OMVs decorated with EGFRvIII and M30 epitopes could elicit a

synergistic protective response against B16F10-EGFRvIII tumor growth in C57BL/6 mice.

In this particular experiment, OMVs were engineered using fHbp as carrier protein. fHbp is a *Neisseria meningitidis* lipoprotein that we previously shown to reach the surface of *E. coli* and to be capable of chaperoning foreign polypeptides when fused to its C-terminus[23].

We first tested whether OMVs decorated with the Nm-fHbp-vIII fusion protein carrying three copies of EGFRvIII peptide at its C-terminus could induce α-EGFRvIII antibodies and whether such α-EGFRvIII immune response could protect mice from B16F10-EGFRvIII challenge. Briefly, a synthetic DNA encoding three copies of EGFRvIII peptide was fused to the 3' end of the fHbp gene, generating the plasmid pET-Nm-fHbp-vIII. We then transformed the plasmid in *E. coli* BL21(DE3)*ΔompA* strain and purified Nm-fHbp-vIII OMVs.

We then immunized mice (n=16) for a total of three times every fourteen days with 20 μg of Nm-fHbp-vIII OMVs or with 20 μg of "Empty" OMVs as a control (Figure 13a). Seven days after the third immunization, sera were collected as indicated in material and methods section and the induction of α-EGFRvIII antibodies was confirmed by ELISA (Figure 13b). Briefly, Nunc Immobilizer Amino plates were coated with EGFRvIII peptide, sera dilutions from each group added and α-EGFRvIII IgGs were revealed using alkaline phosphatase-conjugated goat α-mouse total IgG. As shown in Figure 13b, Nm-fHbp-vIII OMVs but not "Empty" OMVs induced high titers of α-EGFRvIII antibodies in C57BL/6 mice. To determine the Th1 or Th2 polarization of the response induced by Nm-fHbp-vIII OMV vaccination, we investigated IgG isotype composition. ELISA was performed as described above and IgG1 and IgG2a were detected using phosphatase-conjugated goat α-mouse IgG1 and IgG2a, respectively. As shown in Figure 13b, a large amount of α-EGFRvIII antibodies belonged to IgG2a class, as a result of the Th1 immune response[168] induced by OMV vaccination.

On day 35, 0.5x10^5 B16F10-EGFRvIII cells were subcutaneously injected in each mouse and tumor growth followed for thirty days. Immunization with Nm-fHbp-vIII OMVs markedly reduced tumor growth in a statistically significant manner compared to control mice, immunized with "Empty" OMVs (Figure 13c, P<0.001). While all but one control mice developed large tumors 30 days after the challenge, with an average

tumor volume of 850 mm^3, mice immunized with Nm-fHbp-vIII OMVs developed tumors with average volumes of approximately 400 mm^3. Remarkably, eight mice were completely protected from tumor growth (Figure 13c).

On day 65, 30 days after B16F10-EGFRvIII cell challenge (Figure 13a), we analyzed the tumor-infiltrating cell population both in Nm-fHbp-vIII OMV immunized and control mice. Two tumors per group were randomly collected and mechanically and enzymatically disaggregated, obtaining a single cell suspension. The percentage of CD4 T cells, CD8 T cells, Tregs, and MDSCs populations was evaluated by flow cytometry using specific antibodies.

Leukocyte population was detected using α-CD45 antibody. Of this population, helper T and cytotoxic TILs were selected as positive for CD4 and CD8 molecules, respectively. Tregs were identified as FoxP3 positive CD4 cells while MDSCs were recognized as leukocytes positive for CD11b and Gr1 markers. CD4, CD8 and CD11b/Gr1 double positive cell populations were calculated as a percentage of the total leukocyte population. Tregs were calculated as percentage of FoxP3 positive cells of the CD4 population.

In line with the Th1 profile of the immune response, Nm-fHbp-vIII OMV immunization induced a statistically significant increase of CD4 and CD8 T cells associated with a simultaneous reduction of both CD4 Treg and MDSC cells at tumor site (Figure 13d).
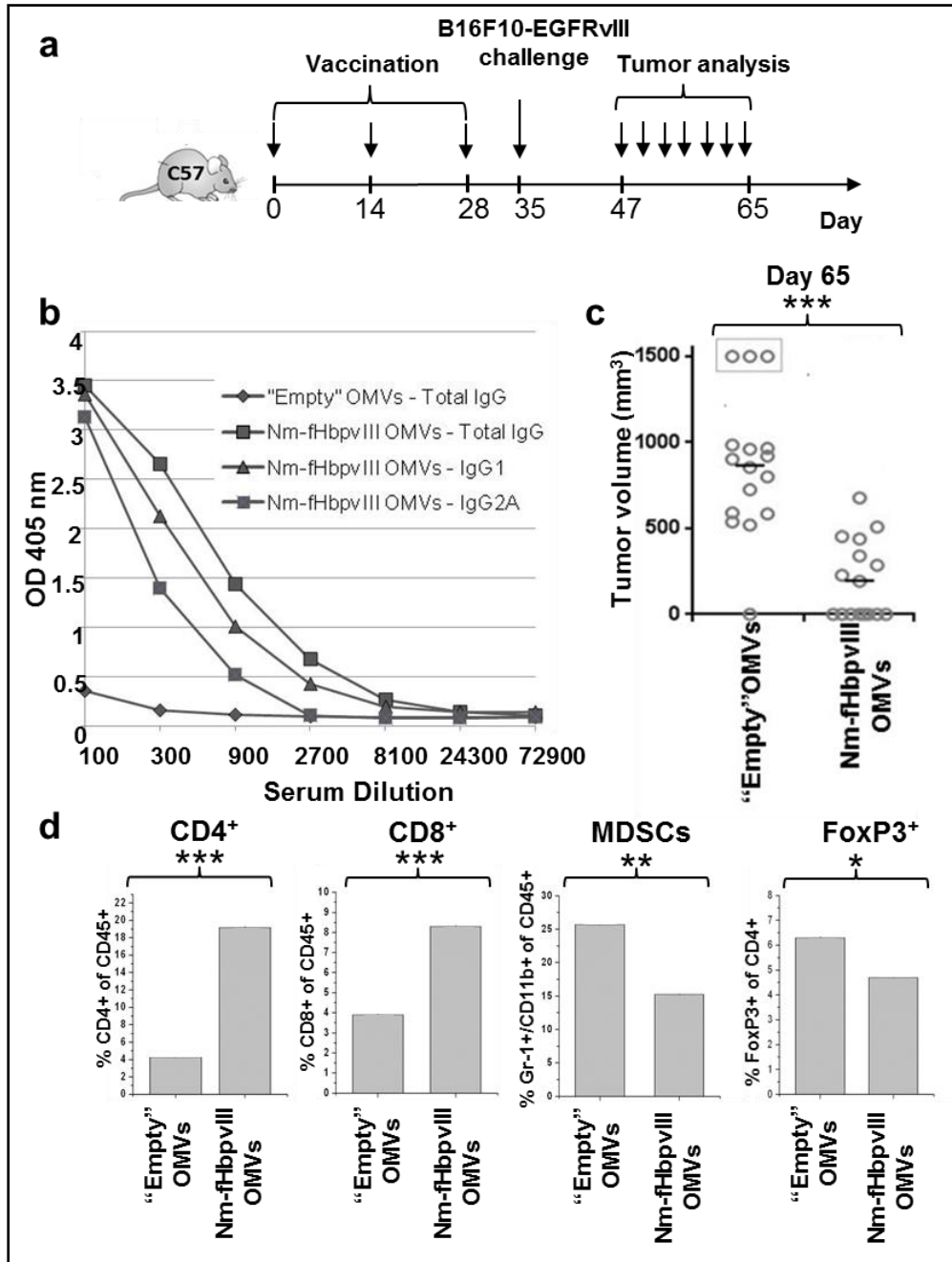
Figure 13 | Nm-fHbp-vIII OMVs vaccination generates α-EGFRvIII antibodies, protects mice from B16F10-EGFRvIII tumors and induces an increase in CD4 and CD8 T cells and decrease in Treg and MDSCs infiltrated in B16F10-EGFRvIII tumors. a, C57BL/6 mice (n=16) were intraperitoneally immunized three times with either Nm-fHbp-vIII OMVs or "Empty" OMVs on day 0, 14 and 28. Seven days after the last immunization, mice were challenged with B16F10-EGFRvIII cells and tumor growth was followed. At the end of the experiment (day 65), 2 tumors per group were collected and analyzed. *b,* α-EGFRvIII antibody titers in C57BL/6 mice immunized with "Empty" OMVs and with Nm-fHbpvIII OMVs. Sera from mice immunized as reported in *a,* were pooled and total IgG, IgG1 and IgG2a were measured by ELISA. *c,* Tumor volume at day 65 in mice immunized either Nm-fHbp-vIII OMVs or "Empty" OMVs. *d,* Histograms with percentages of tumor infiltrated cells calculated by flow cytometry analysis. *P < 0.05; **P < 0.01; ***P < 0.001. Statistical analysis was performed using unpaired, two-tailed Student's t-test.

52

Once demonstrated that Nm-fHbp-vIII OMVs induced a robust protection in C57BL/6 mice challenged with B16F10-EGFRvIII cell line, we investigated if we could increase their protective activity by engineering them with a second antigen (M30 neoepitope). We therefore made a fusion protein consisting of fHbp fused to three copies of the M30 neoepitope followed by three copies of the vIII peptide (See Material and methods section for details). This construct was transformed in *E. coli* BL21(DE3)*ΔompA* strain and Nm-fHbp-M30vIII OMVs were purified.

To investigate if these vesicles were able to induce M30 specific CD4 T cells, we intraperitoneally immunized C57BL/6 mice with 20 μg of Nm-fHbp-M30vIII OMVs on day 0 and on day 7, and spleens from each mouse were collected on day 12 (Figure 14a). Mice immunized with 20 μg of "Empty" OMVs adsorbed with 100 μg of M30 peptide or immunized with 20 μg of "Empty" OMVs were used as a positive and negative controls.

Single cell suspension was obtained from each spleen and splenocytes were incubated with 2 mg/ml of M30 peptide. If immunization induced M30 specific T cells, antigen recognition by splenocytes would determine their activation and following release of IFN-γ. Therefore, by monitoring IFN-γ release after in vitro stimulation with the cognate antigen it is possible to follow antigen specific T cell generation. As negative control, cells were stimulated with 2 mg/ml of an unrelated peptide (not present in the vaccine formulation): this stimulation should result in no or minimal, non-specific IFN-γ release.

As shown in Figure 14b, Nm-fHbp-M30vIII OMVs did induce M30-specific CD4 T cells, as demonstrated by the release of IFN-γ by splenocytes from mice immunized with Nm-fHbp-M30vIII OMVs and stimulated with M30 peptide. This M30 specific population was induced also, at the same magnitude, in mice immunized with "Empty" OMVs adsorbed with M30 peptide. The frequencies of IFN-γ positive T cells in both cases were greater than the percentages obtained with non-specific stimulation generated by an unrelated peptide, which was probably caused by impurities present in the synthetic polypeptide.

To investigate the protective activity, C57BL/6 mice (n=6) were immunized every fourteen days for a total of three times (Figure 13a) with 20 μg of Nm-fHbp-M30vIII OMVs. Seven days after the last immunization, 0.5×10^5 B16-EGFRVIII cells were

subcutaneously injected in each mouse and tumor growth followed for thirty days. Vaccination with Nm-fHbp-M30vIII OMVs completely protected mice from tumor growth (P<0.001, Figure 14c).

All together, these experiment strongly demonstrate that when the TSA vIII and the neoepitope M30 are co-delivered, they have a synergistic activity in protecting mice from tumors expressing both antigens.
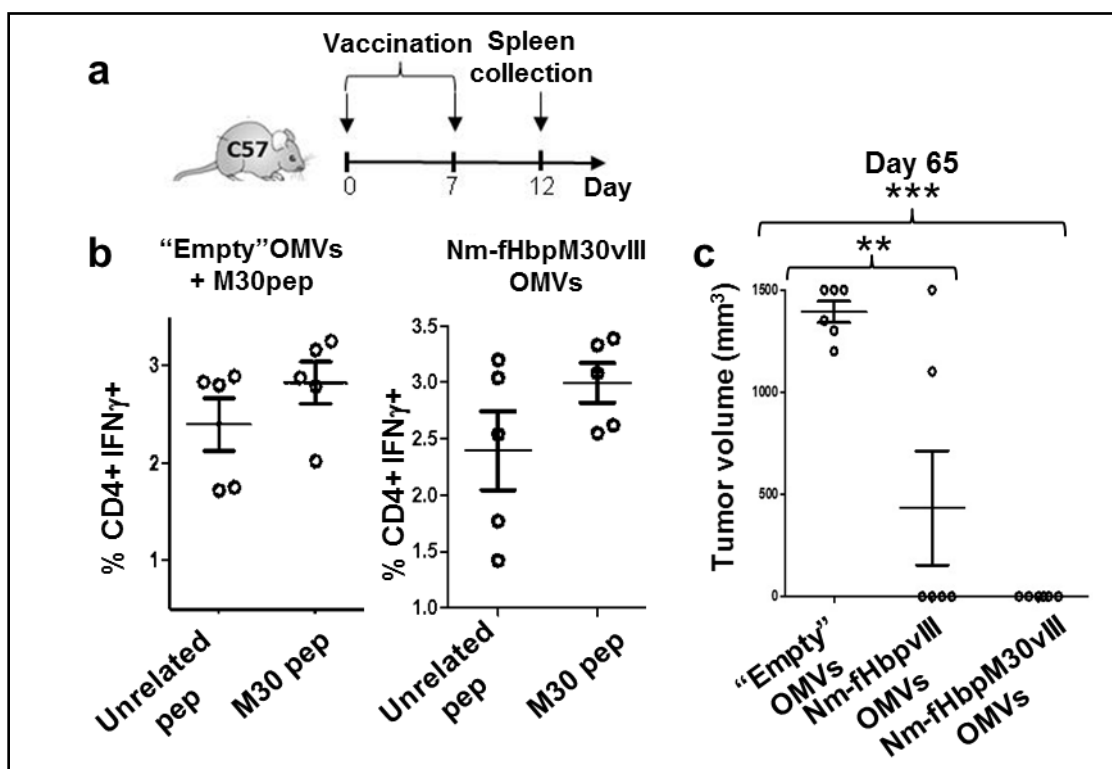
Figure 14 | Synergistic protective activity of OMVs engineered with two antigens. a, C57BL/6 mice (n=5) were intraperitoneally immunized two times on day 0 and day 7 with either Nm-fHbp-M30vIII OMVs, "Empty" OMVs adsorbed with 100 µg of M30 synthetic peptide or "Empty" OMVs as a control and spleens were collected on day 12. b, Splenocytes from mice treated with the different OMV vaccines were in vitro stimulated with M30 peptide or with an unrelated peptide mix as a control. The release of IFN-γ by CD4 T cells able to recognize the M30 was determined by flow cytometry. Analysis of "Empty" OMV immunized mice not shown. c, C57BL/6 mice (n=6) were immunized with either Nm-fHbp-vIII OMVs, with Nm-fHbp-M30vIII OMVs or with "Empty" OMVs as a control following the schedule described in Figure 13a. The graph represents tumor volume (mean ± s.e.m) on day 30 after B16F10-EGFRvIII challenge in the differently treated mice. **P < 0.01; ***P < 0.001. Statistical analysis was performed using unpaired, two-tailed Student's t-test.

OMV platform in personalized immunotherapy

The effectiveness of personalized cancer vaccines relies on the use of multiple neoepitopes selected among those generated by specific mutations present in each individual patient. Usually, 5 to 20 epitopes are considered, in order to minimize tumor immune escape driven by cancer immunoediting. For instance, in the two recent publications describing the positive results in melanoma patients, ten[14] and up to twenty[15] epitopes were included in the final formulations, respectively. A second fundamental requirement of any personalized medicine approach is the time necessary to formulate the vaccines once neoepitopes have been selected. A period not exceeding three months is considered acceptable to allow the patient to be promptly vaccinated after the tumor is resected and sequenced. Therefore, for the OMV platform to be compatible with personalized medicine, it has to be tested both for its capacity to include multiple neoepitopes, for the time needed to engineer the OMV-producing strain, to purify the vesicles and prepare the final formulation.

Based on the above, we decided to challenge the OMV system by testing its applicability with five neoepitopes present in CT26 murine cell line and previously described to induce protective T cell responses in BALB/c mice[11].

Before engineering the vesicles with the five selected epitopes M03, M20, M26, M27 and M68, we first verified their immunogenicity and protective activity by using synthetic peptides absorbed to "Empty" OMVs.

To test immunogenicity, 20 μg of purified OMVs were mixed with 20 μg of each of the five synthetic peptides (ads-pentatope OMVs) and mice were intraperitoneally immunized on day 0 and day 7 (Figure 15a). On day 12, we performed ICS on splenocytes *in vitro* stimulated with 0.4 mg/ml of each of the five peptides (the five peptides as a group are referred to as pentatope). 3 out of 5 mice immunized with ads-pentatope OMVs generated CD4 and CD8 pentatope-specific T cells, as demonstrated by IFN-γ released by splenocytes when stimulated with pentatope peptide mix (Figure 15b). To demonstrate that the release of IFN-γ was pentatope-specific, the same splenocytes were stimulated with an unrelated peptide mix. This time, no T cell activation was detected. As a further control, we performed the same analysis on splenocytes collected from mice immunized with "Empty" OMVs. As shown in Figure 15b, in this group only a marginal and negligible CD8 T cell activation could be detected
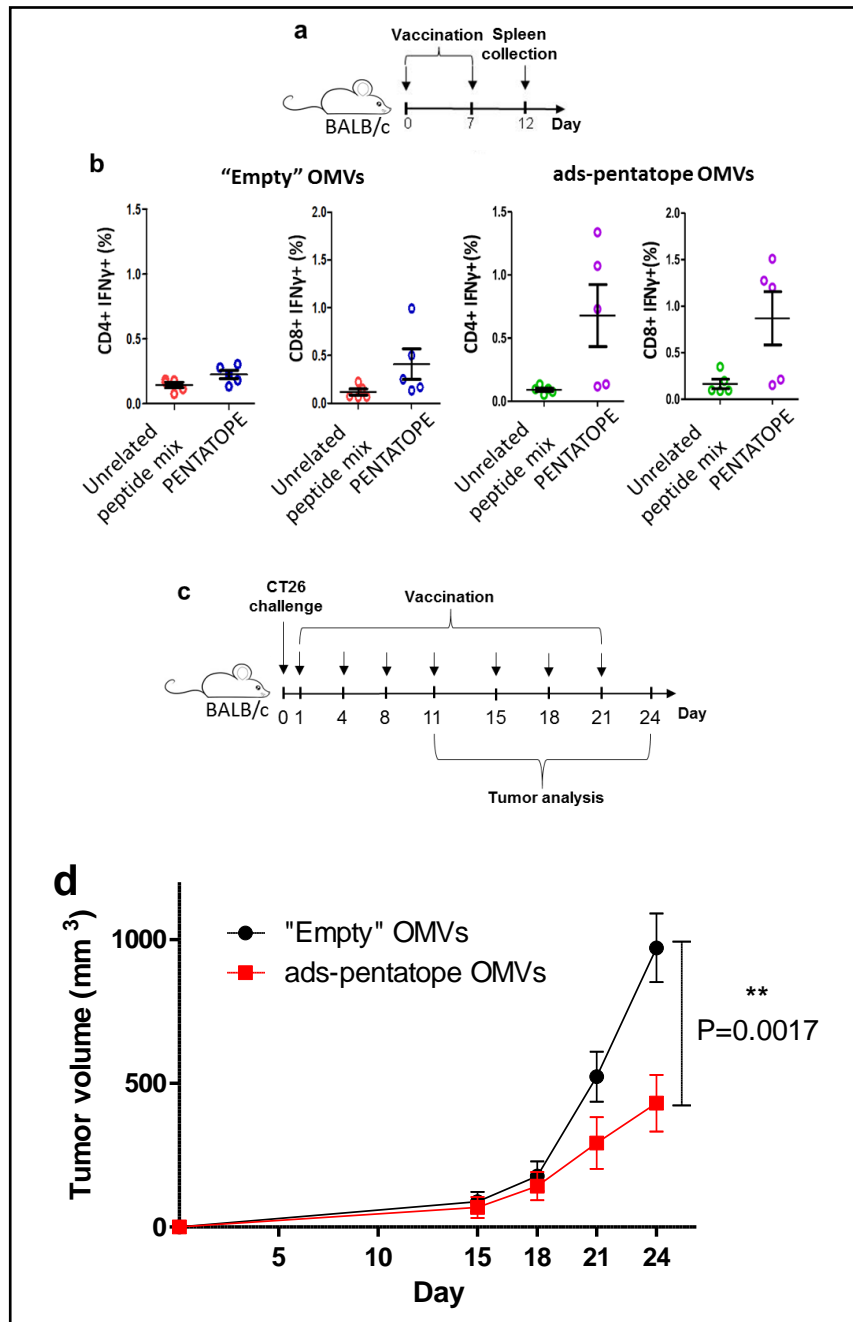
Figure 15 | ads-pentatope OMV vaccine induces pentatope specific T cells and protects mice from CT26 tumors. a, *BALB/c mice (n=5) were intraperitoneally immunized two times on day 0 and day 7 with either ads-pentatope OMVs or "Empty" OMVs and spleens were collected on day 12.* **b,** *Splenocytes from ads-pentatope OMV or "Empty" OMV immunized mice were in vitro stimulated with the five peptides of the pentatope or with an unrelated peptide mix as a control. The release of IFN-γ by CD4 and CD8 T cells able to recognize the pentatope was analyzed by flow cytometry.* **c,** *BALB/c mice were challenged with CT26 cells on day 0 and immunized on day 1, 4, 8, 11, 15, 18 and 21 with either ads-pentatope OMVs or "Empty" OMVs. Tumor growth was followed starting on day 11.* **d,** *Tumor growth (mean ± s.e.m.) in BALB/c mice (n=14) immunized with ads-pentatope-OMVs or "Empty" OMVs as a control. Data accumulated from 2 independent experiments of 6 mice/group and 8 mice/group, respectively. Statistical analysis was performed using unpaired, two-tailed Student's t-test.*

when splenocytes were stimulated with pentatope peptides, whereas no pentatope-specific CD4 T cells was generated by "Empty" OMVs vaccination.

Once demonstrated the immunogenicity of ads-pentatope OMVs, we assessed the capacity of pentatope-specific T cell population to protect mice from CT26 challenge. We subcutaneously injected 1.5×10^5 CT26 cells in BALB/c mice and one day after challenge the animals were immunized intraperitoneally with 20 μg of ads-pentatope OMVs and the therapeutic immunization was repeated every three days for a total of seven injections (Figure 15c). Tumor growth was followed by measuring tumor size periodically with a caliper.

As shown in Figure 15d, 24 days after tumor cell injection, mice vaccinated with ads-pentatope OMVs had an average tumor volume of 431 mm^3 while mice immunized with "Empty" OMVs as a control showed an average tumor volume of 972 mm^3. This data demonstrate that ads-pentatope OMVs strongly inhibited CT26 tumor growth in BALB/c mice (P=0.0017).

Having demonstrated the capacity of the pentatope to elicit protective immune responses, we moved to OMV engineering, setting up a protocol that could be compatible with personalized vaccination. In particular, the strategy we tested was to produce five vesicles, each carrying one copy of an epitope and to prepare the final formulation by mixing equal amounts of each of the five engineered OMVs.

Figure 16 schematizes the experimental protocol reporting the time necessary to complete each step. In essence, the plasmid encoding PSP (pET-PSP) was modified by inserting a cloning site carrying BamHI/XhoI restriction sites immediately up-stream the PSP stop codon (no details can be given for confidentiality reasons). Meanwhile, single stranded oligonucleotides, each coding for the forward and reverse strand of each one of the five neoepitopes, were chemically synthesized. Once annealed, these oligonucleotides were designed to create overhangs corresponding to BamHI and XhoI sequences at the 5' and 3', respectively, of the created minigene (see Materials and Methods section and Table 5 for details). Moreover, a stop codon was added at the end of the sequence coding each one of the neoepitopes. After annealing of forward and reverse synthetic oligonucleotides, the double stranded DNA fragments with BamHI and XhoI overhangs were ligated to pET-PSP linearized with BamHI and XhoI

and the mixture was used to transform BL21(DE3)Δ*ompA* strain. From selected recombinant clones, the correctness of the PSP-neoepitope fusions was sequence verified and the clones were finally used to purify OMVs as described above.
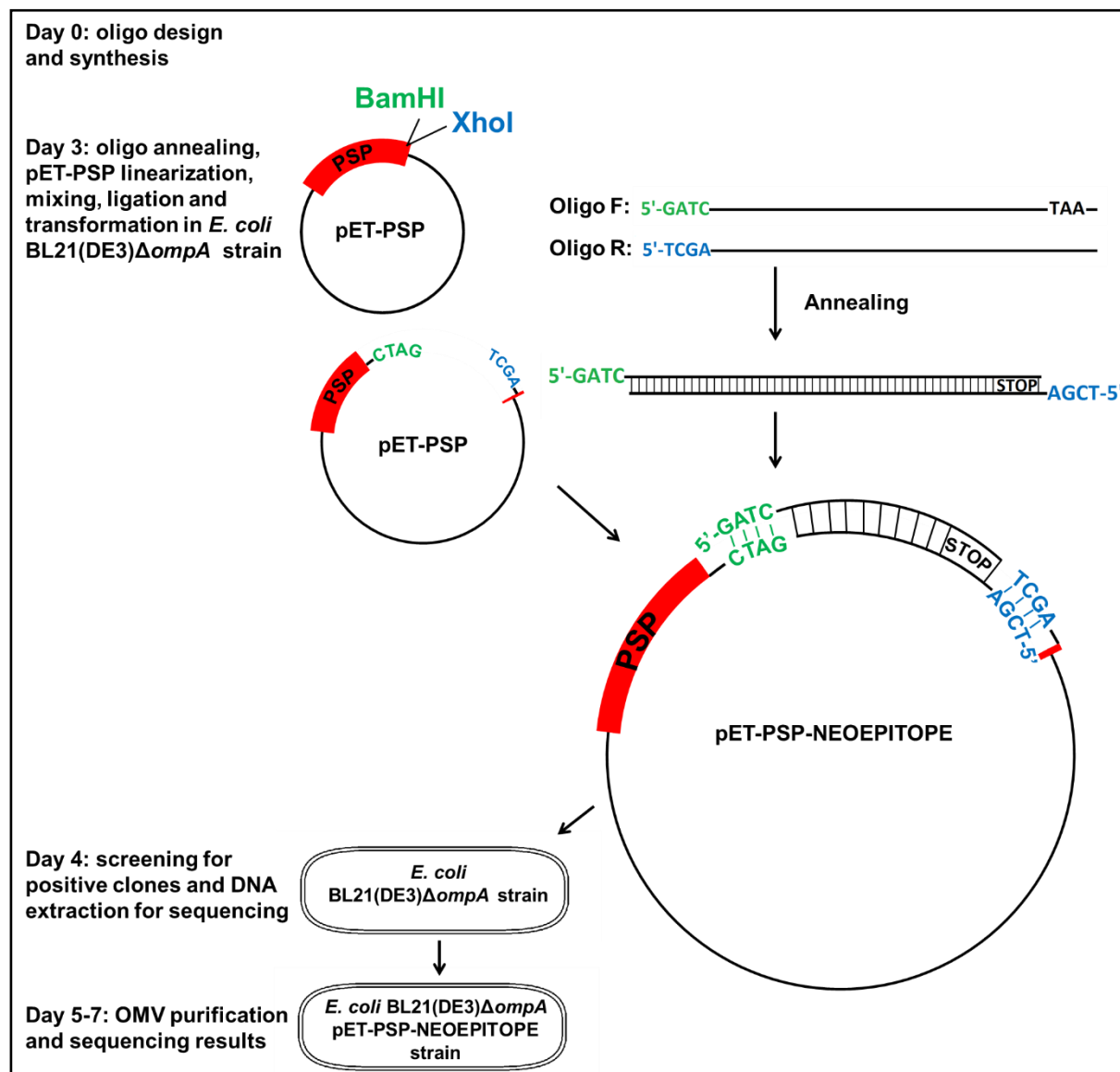
Figure 16 | Protocol for the use of OMV as a personalized cancer vaccine platform. *Schematic representation of the steps and timing involved in the engineering of OMVs with specific cancer neoepitopes using the protocol set up for the use of OMVs as personalized cancer vaccine platform.*

20 μg of each one of the five OMVs expressing one of the selected antigens (PSP-M03, PSP-M20, PSP-M26, PSP-M27 and PSP-M68 OMVs) were separated by SDS-PAGE using Any kD™ Criterion™ TGX Stain-Free™ Protein Gel. As a control, "Empty" OMVs were included and proteins were revealed by Coomassie staining. As shown in Figure 17, the fusion proteins represented a major component of total OMV proteins.

In terms of timing, the whole process required less than seven working days by the time oligonucleotides were designed and synthesized.

In conclusion, the OMV platform appears to be perfectly suitable for personalized cancer vaccines.
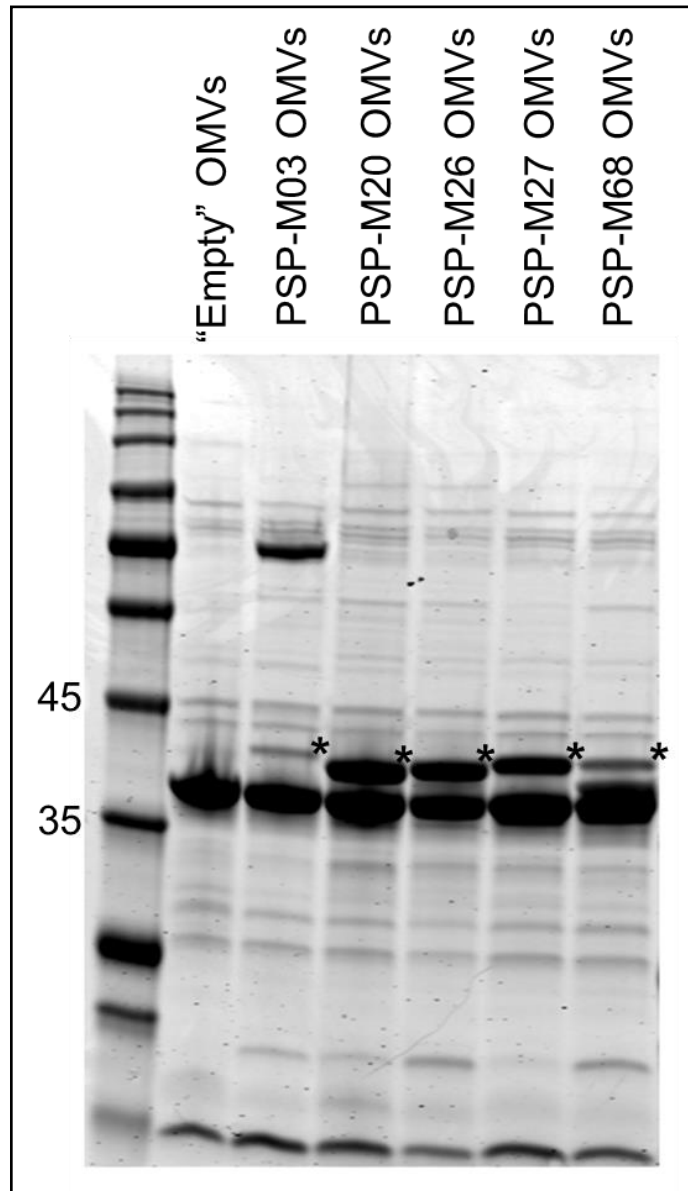
Figure 17 | OMVs are efficiently engineered with CT26 neoepitopes. *SDS-PAGE analysis of 20 µg of OMVs purified from BL21(DE3)ΔompA pET-PSP-M03 (PSP-M03 OMVs), BL21(DE3)ΔompA pET-PSP-M20 (PSP-M20 OMVs), BL21(DE3)ΔompA pET-PSP-M26 (PSP-M26 OMVs), BL21(DE3)ΔompA pET-PSP-M27 (PSP-M27 OMVs) and BL21(DE3)ΔompA pET-PSP-68 (PSP-M68 OMVs). OMVs purified from BL21(DE3)ΔompA strain transformed with the empty pET vector ("Empty" OMVs) were used as a control. Recombinant fusion proteins are indicated by a star.*

Discussion

The final goal of this work was to demonstrate that OMVs can be exploited in personalized cancer vaccines. We believe that the data presented fully support OMVs future use in cancer immunotherapy.

The first important message of our work emerges from the analysis of gene transcription profile in draining lymph nodes after OMVs injection. One of the expected advantages of OMVs over other adjuvant/delivery systems is that they carry several MAMPs[18,19] targeting different cellular receptors involved in activation of immune responses. Since it is known that combinations of more than one adjuvant can work synergistically thus amplifying the stimulation of innate immunity[169], OMVs are theoretically an ideal vaccine platform. Our transcription profile analysis fully confirmed our expectations (Figure 7).

In line with the abundancy of LPS and lipoproteins in OMVs[18,19,139], genes involved in the TLR4 and TLR2 pathways (CD14, MyD88, Ticam1) appeared up-regulated[170,171]. Furthermore, the presence of DNA and peptidoglycan in OMVs[18,19,139] is also consistent with the observed up-regulation of IRF7[172] and NOD2[173], respectively.

The simultaneous stimulation of several pattern recognition receptors (PRRs) by OMVs described above, explains the upregulation of the pro-inflammatory cytokines TNF-α, IL-1β, IL-6 that we identified with the analysis. This cytokine profile is associated with M1 macrophages, which promotes Th1 T cell differentiation and tumor cell elimination[174].

The strong activation (7.9 fold) of NLRP3 is particularly important. Such activation can be due to the stimulation of TLR4 and NOD2, which in turn activate the transcription of NLRP3[175–179]. Since NOD2- and TLR4-induced NLRP3 inflammasome needs further stimuli to become activated[175–177], one of the triggering signals can come from caspase-11, which is activated by cytoplasmic LPS[175,176]. This is consistent with a recent work demonstrating that OMVs after being phagocytosed are release in to the cytoplasm and activate caspase-11[180].

Moreover, according to data from our[24] and other laboratories[141,181] showing that OMVs elicit cell-mediated immunity, our transcription profile analysis demonstrated that OMV

strongly induce a type 1 immune response together with a concomitant inhibition of type 2 differentiation. The cytokines IL-12, IL-18 and IFN-γ are crucial for the development of Th1 cells[182], together with Stat-1 and the master regulator of Th1 differentiation, T-bet (Tbx21)[115,182,183]. All these genes are upregulated in lymph nodes after OMV vaccination. Moreover, also GM-CSF is usually upregulated in activated macrophages and DCs, but it is also released by activated NK and T cells and can be considered as T cell activation indicator. Although in our array IL-12 gene is not included, by looking at its downstream pathways we have an indirect evidence of its role in OMV immunization. IL-12 is produced by activated DCs and macrophages following signaling through TLRs and stimulates cell-mediated immunity by inducing Th1 cell development[174]. IL-12 induces NK cells to release IFN-γ, which activates macrophages and enhances their bactericidal activity in early phases of innate response to infection[184]. It also synergizes with pro-inflammatory cytokines like IL-18 in stimulating IFN-γ production, as well as the cytotoxicity of NK and CD8 T cells[174,185]. Furthermore, IL-12 produced by activated macrophages and DCs, TCR signaling following MHC II-antigen binding together with IFN-γ released by activated NK drive the Th1 differentiation of naive Th0 CD4 T cells. In these cells, IL-12 induces activation of STAT4, which results in IFN-γ production, while IFN-γ signaling induces STAT1 to activate the crucial transcription factor T-bet[184,185]. Moreover, T-bet represses differentiation into Th2 cell by inhibiting the key IL-4 gene and affecting the function of GATA3[182]. In fact, Th2 differentiation can be initiated by IL-4: this cytokine induces GATA3 transcription factor, master regulator of Th2 differentiation and responsible for the transcription of IL-4, IL-5 and IL-13[182,185,186].

The fact that we have found upregulated key players of Th1 differentiation (IL-18, IFN-γ, STAT1 and T-bet) and downregulated pivotal components of a Th2 differentiation (IL-4, GATA3, IL-5 and IL-13) is a solid and compelling evidence not only for a strong activation of adaptive immunity by innate response, but also unequivocally support the suitability of OMVs in personalized cancer vaccines.

Finally, OMV vaccination induced both adhesion molecule and chemokines. In fact, we found Itgam, molecule responsible for leukocytes adhesion and extravasation[187], upregulated in lymph nodes of OMV-immunized mice.

Remarkable is the upregulation of the chemokine CXCL-10, which is induced in response to IFN-γ by leukocytes and monocytes, but also secreted by epithelial cells, endothelial cells and fibroblasts[188]. It is important to attract monocytes, activated Th1 CD4 T cells, effector CD8 T cells, NK and NK T cells[189]. Therefore, CXCL10 is a crucial chemokine for an effective anticancer response, and the fact that OMVs foster its upregulation provide further evidence for the applicability of OMVs as a platform for personalized cancer vaccine.

The second relevant result of this work is that immunization with OMVs engineered with T cell epitopes induce a potent epitope specific T cell response.

We decorated OMVs with the CD8 model epitope $OVA_{257-264}$. By fusing three copies of the epitope to two different carrier proteins (PSP and MBP) we successfully delivered high amount of the fusion protein to the surface and the lumen of the OMV, respectively (Figure 8 and Figure 9). Both PSP-OVA and MBP-OVA OMVs induced OVA-specific CD8 T cell population: however, the percentage of OVA-positive CD8 T cells measured in the blood was higher after PSP-OVA OMVs immunization compared to the luminal counterpart (Figure 11 and Table2). Rather than to antigen amount, differenced in OVA specific CD8 T cell induced, if confirmed, can be attributed to the mechanism of cross-presentation, responsible for the OVA peptide loading on MHCI, that appear to be more efficient when the epitope is exposed on the OMV surface.

The elicitation of OVA specific CD8+ T cells correlated with a robust protection in mice challenged with B16-OVA cell line. Compared to control mice, a 90% reduction (P=0.0001) in tumor growth was observed in mice challenged with B16-OVA cells and therapeutically vaccinated with PSP-OVA OMVs (Figure 12b). This indicated that the OVA specific CD8 T cells induced by PSP-OVA OMV vaccination have cytotoxic and effector function.

Personalized cancer vaccines should contain multiple epitopes in order to overcome tumor immune escape driven by cancer immunoediting. We therefore tested the protective activity of a combination of two epitopes, the B cell epitope EGFRvIII[163,164] and the CD4 T cell epitope M30[10,11], both expressed in the murine B16F10-EGFRvIII

cell line. We first demonstrated that mice immunized with EGFRvIII-OMVs induced a strong protection against B16F10-EGFRvIII challenge in C57BL/6 mice (Figure 13c). Interestingly, protection not only correlated with the elicitation of α-EGFRvIII antibodies (Figure 13b) but also with tumor infiltration of CD4 and CD8 T cells and concomitant reduction of MDSCs and Tregs (Figure 13d). Although we do not have a direct evidence, according to the reported cell mediated cytotoxicity induced by α-EGFRvIII antibodies[164], we can speculate that infiltrated CD4 and CD8 T cells are specific for mutation-derived neoepitopes present of B16F10-EGFRvIII cells. In fact, the neoepitopes released by tumor cells after vIII-antibody mediated NK cytotoxicity or complement activation might be taken up by antigen presenting cells, which then elicit a neoepitope specific T cell immune response. Moreover, α-EGFRvIII antibody coated tumor cells might be directly phagocytosed by APCs[190] and therefore neoepitopes presented on both MHC class I and class II molecules to T cells. B16-F10 are a malignant melanoma cell line characterized by a high mutational load and therefore a high frequency of cancer-specific neoepitopes[10,11]. This should promote the elicitation of a large population of neoepitope-specific T cells, whose importance has been widely demonstrated in both preclinical[11–13] and clinical studies[4–9,14,15,126].

Once we demonstrated the protective activity of EGFRvIII-OMVs, after challenge with B16F10-EGRFvIII cells, we immunized C57BL/6 mice with OMVs engineered with both EGFRvIII and M30. Our data demonstrated that the two epitopes worked synergistically, providing a full protection against the challenge with the cancer cell line (Figure 14c).

The efficacy of combination of more than one epitope was further confirmed using five neoepitopes expressed in CT26 cell line[11]. OMVs, when formulated with these five cancer neoepitopes and therapeutically injected in BALB/c mice challenged with CT26 cells, induced neoepitope specific T cells (Figure 15b) and a strong inhibition of tumor growth compared to control mice (P=0.0017, Figure 15d).

The last message of this work is the demonstration that the OMV platform is fully compatible with personalized medicine. In the clinical setting is mandatory that, once the patient-specific neoepitopes are identified by exome/RNA sequencing of tumor

biopsies, the final vaccine formulation including selected neoepitopes is ready to be injected into the patient in less than three months[14].

For this reason, we set up a protocol to efficiently and promptly engineer OMVs with several antigens. We demonstrated that our cancer vaccine platform could be efficiently used to build a personalized cancer vaccine in extremely short time (Figure 16 and Figure 17). In fact, we have demonstrated that it is feasible to create vaccines containing neoepitopes deriving from *de novo* mutations in cancer cells in less than seven working days.

Altogether, we have provided compelling evidence for a future use of OMVs as an effective personalized cancer vaccine platform.

Future perspectives

We have demonstrated that OMVs activate both innate and adaptive immunity and that vesicles induce a Th1-skewed immune response. Furthermore, we have demonstrated in mouse models that single- and double-antigen engineered OMVs induce epitope specific immune responses, which protect mice from growth of tumors expressing such antigens. Moreover, we set up a protocol to efficiently engineer OMVs with cancer neoantigens, which is suitable for a personalized cancer vaccine approach.

There are still a few unanswered questions we would like to address in the near future. First, our studies on protective activity of engineered OMVs have been restricted to the analysis of primary, subcutaneously implanted, tumors. Since metastases are the main cause of death in humans, it will be important to see whether OMV immunization can also prevent their formation. Considering that the tumor cell lines we used can also be used for metastases models, we can use them to answer this question.

Second, as pointed out several times in this document, an effective cancer vaccine should include several (five to twenty) different patient-specific neoepitopes. This opens the question on how to engineer OMVs in order to accommodate all required epitopes. One possibility is to fuse strings of different epitopes to the carrier protein. We are already testing this approach and we already know that strings of up to five to ten epitopes can be efficiently expressed in OMVs. We are currently investigating, using a variety of different epitopes, what the maximum number of antigens is, that can be expressed in OMVs with this approach. Alternatively, OMVs can be engineered with single (or few) epitopes and subsequently combinations of different engineered OMVs can be mixed to create the final vaccine formulation. Considering the ease with which OMVs can be produced, this second option should be also compatible with clinical applications for personalized cancer therapies. In line with this, we will test if OMVs engineered with the CT26 neoantigens are able to protect mice from tumor growth.

Finally, to be applicable in the clinic, the process for OMV production must be robust and reproducible. Therefore, a number of analytical assays have to be set-up to analyze the yield of OMVs in fermentation, the quantity of OMVs purified from culture supernatant, the quality of OMVs in terms of protein content, and presence of possible

contaminants deriving from the fermentation process. To solve this question, our group is also working on implementing different analytical methods, including mass spectrometry, spectroscopic and electrophoretic analysis which will be used to quality control every different batch of engineered OMVs.

All these experiments will provide us comprehensive information on the OMV platform suitability and efficacy in personalized cancer vaccine immunotherapy.

Materials and methods

Chemicals, cell lines and animals

LB broth medium and ampicillin were purchased from Sigma-Aldrich.

Bacterial stock preparations for each strain were stored at -80°C in 20% dimethyl sulfoxide (DMSO). Cells were tested for mycoplasma before animal injection.

Roswell Park Memorial Institute (RPMI) medium and Fetal Bovine Serum (FBS) were purchased from Gibco, Life Technologies. Penicillin/streptomycin/L-glutamine (PSG) was purchased from Thermo Fisher Scientific. Geneticin™ G418 was purchased from Gibco, Thermo Fisher Scientific.

Mouse melanoma B16F10 and CT26 mouse colon carcinoma cell lines, were kindly given by the Department of Biomedical and Clinic Sciences of the University of Florence.

B16F10-EGFRvIII cell line, a melanoma cell line stably expressing human EGFRvIII was kindly provided by Prof. J. H. Sampson from the Department of Neurosurgery of the Duke University Medical Center in North Carolina (U.S.).

B16-OVA cell line, a B16F10 cell line transfected with a plasmid carrying a complete copy of chicken ovalbumin (OVA) mRNA and the Geneticin (G418) resistance gene, was kindly provided by Cristian Capasso and prof. Vincenzo Cerullo from the Laboratory of Immunovirotherapy, Drug Research Program, Faculty of Pharmacy, University of Helsinki.

C57BL/6 and BALB/c female 4-6 week old mice were purchased from Charles River Laboratories and kept and treated in accordance with the Italian policies on animal research at CIBIO, University of Trento, Italy.

Bacterial strains and culture conditions

Plasmid assembly using the polymerase incomplete primer extension (PIPE) method[157] was carried out in *E. coli* HK-100 strain. OMVs were purified from *E. coli* BL21(DE3)Δ*ompA* strain as previously described[23,24,191]. *E. coli* was routinely grown in LB broth medium (Sigma-Aldrich) at 30°C and/or 37°C and 180 rpm. When required, Ampicillin (Amp) was added to a final concentration of 100 µg/ml. Stock preparations of strains in LB and 20% glycerol were stored at -80°C. Each bacterial manipulation

was started from an o/n culture inoculum of a frozen stock or of a single colony from LB plate.

B16F10, B16F10-EGFRvIII and CT26 cell lines were cultured in RPMI supplemented with 10% FBS and PSG, and grown at 37°C in 5% CO_2.

B16-OVA cell line was cultured in RPMI supplemented with 10% FBS, PSG and 5 mg/ml Geneticin™ (Gibco, Life Technologies) and grown at 37°C in 5% CO_2.

Amino acid sequences of the epitopes

All peptides were purchased from GenScript.

Peptide	Sequence
OVA$_{257-264}$	SIINFEKL
OVA	QLESIINFEKLTEGGQLESIINFEKLTEGGQLESIINFEKLTE
EGFRvIII	LEEKKGNYVVTDH
3xEGFRvIII	GSLEEKKGNYVVTDHGSLEEKKGNYVVTDHGSLEEKKGNYVVTDH
M30	PSKPSFQEFVDWENVSPELNSTDQPFL
M03	DKPLRRNNSYTSYIMAICGMPLDSFRA
M20	PLLPFYPPDEALEIGLELNSSALPPTE
M26	VILPQAPSGPSYATYLQPAQAQMLTPP
M27	EHIHRAGGLFVADAIQVGFGRIGKHFW
M68	VTSIPSVSNALNWKEFSFIQSTLGYVA

Table 3 | Epitopes. *Amino acid sequences and name of each epitope used in this work.*

Analysis of immune gene expression in mice immunized with OMVs

C57BL/6 (n=3) mice were subcutaneously immunized with 20 μg of OMVs purified from *E. coli* BL21(DE3)Δ*ompA* strain or PBS (OMVs resuspension buffer) as a control. After 36 hours, draining lymph nodes were collected and total RNA extracted using RNeasy Mini Kit (Qiagen) as per manufacturer's instruction. cDNA was retrotranscribed using RT^2 First Strand Kit (Qiagen) following manufacturer's instruction. Gene expression levels were assessed by qPCR using RT² Profiler™ PCR Array Mouse Innate & Adaptive Immune Responses (Qiagen) following manufacturer's instruction using

BioRad CFX384 instrument. qPCR data analysis was performed using the web portal available on the Qiagen website (http://www.qiagen.com/geneglobe, www.qiagen.com/it/shop/genes-and-pathways/data-analysis-center-overview-page/) to create the scatter plot in Figure 6. qPCR data analysis for each gene was performed using the cycle threshold (C_T) method. Briefly, ΔC_T was normalized subtracting to the C_T of each gene in a group the average of the three C_T values (3 mice/group) of β2-microglobulin reference housekeeping gene ($\Delta C_T = C_T$(gene in OMV/PBS group)-C_T(average of the three mice of C_T values of β2-microglobulin in OMV/PBS group). $\Delta\Delta C_T$ was obtained by subtracting the average of ΔC_T in the PBS group to the ΔC_T in the OMV immunized group for each gene ($\Delta\Delta C_T = \Delta C_T$(OMVs group)- ΔC_T(PBS group)). Fold Change is then calculated using the $2^{\wedge}(-\Delta\Delta C_T)$ formula. Gene expression level is then calculated as fold regulation, which is equal to the fold change for up-regulated genes, while it is the negative inverse of the fold change for down-regulated genes. Histogram of fold regulation were created using GraphPad Prism 5.03.

pET-PSP-OVA and pET-MBP-OVA generation

Plasmid assembly was made by the polymerase incomplete primer extension (PIPE) method[157].

Full sequence of both Maltose binding protein (MBP) and PSP (no details of PSP can be given for confidentiality reasons) were previously cloned in our laboratory in the pET21b+ plasmid.

The synthetic gene encoding for 3 copies of OVA$_{257-264}$ epitope with its flanking sequences separated by a glycine-glycine flexible spacer was purchased from GeneArt® Gene Synthesis (LifeTechnologies). Full sequence of the construct is 5'-CAGCTGGAAAGCATTATTAACTTTGAAAAACTGACCGAAGGTGGTCAGCTGGAA AGCATTATTAACTTTGAAAAACTGACCGAAGGTGGTCAGCTGGAAAGCATCATC AACTTCGAAAAACTGACCGAA-3'.

The peptide coded by this construct will be referred to simply as OVA (sequence: QLESIINFEKLTEGGQLESIINFEKLTEGGQLESIINFEKLTE).

To clone OVA to pET-PSP and obtain the fusion protein PSP-OVA:

pET-PSP was linearized using Nohisflag and PSP-Rev primers, OVA construct was amplified with OVAPSP-F and OVAPSP-R primers (Table 3). Finally, PCR products

were mixed together and used to transform *E. coli* HK100 competent cells, obtaining pET-PSP-OVA.

To clone OVA to pET-MBP and obtain the fusion protein MBP-OVA, pET-MBP was linearized using Nohisflag and MBP-Rev primers, OVA construct was amplified with OVAMBP-F and OVAMBP-R primers (Table 3). Finally, PCR products were mixed together and used to transform *E. coli* HK100 competent cells, obtaining pET-MBP-OVA.

Oligo name	Sequence
OVAPSP-F	5'-TAATTAAAGCTGCAAAACAGCTGGAAAGCATTATTAACTTTGAAAAAC-3'
OVAPSP-R	5'-TGGTGATGGTGATGTTATTCGGTCAGTTTTTCGAAGTTGATGATGCTTTC-3'
PSP-Rev	5'-TTTTGCAGCTTTAATTAATTTTTCTTTTAAATCTTTACGC-3'
OVAMBP-F	5'-ACTCGTATCACCAAGCAGCTGGAAAGCATTATTAACTTTG-3'
OVAMBP-R	5'-GTGATGGTGATGTTATTCGGTCAGTTTTTCGAAGTTGATG-3'
MBP-Rev	5'-CTTGGTGATACGAGTCTGCGC-3'
Nohisflag	5'-TAACATCACCATCACCATCACGATTACAAAGA-3'

Table 4 | Primers. *List of all primers used to OVA$_{257-264}$ to pET-PSP and pET-MBP.*

pET-Nm-fHbp-vIII plasmid expressing Nm-fHbp fused to three copies of EGFRvIII peptide separated by a Glycine-Serine spacer, was generated as previously described[23].

pET-Nm-fHbp-M30-vIII plasmid carrying Nm-fHbp gene fused to three copies of M30 peptide and three copies of EGFRvIII peptide, each copy intercalated by a Glycine-Serine spacer, was generated as previously described[24].

OMV purification and SDS-PAGE

Plasmids containing the genes of interest were used to transform *E. coli* BL21(DE3)Δ*ompA* strain. Recombinant clones were grown at 30°C and 180 rpm in LB medium (starting OD$_{600}$ = 0.05) and, when the cultures reached an OD$_{600}$ value of 0.5, protein expression was induced by addition of 0.1 mM IPTG (Sigma-Aldrich). After 4 hours, culture supernatants were separated from living bacterial cells by a centrifugation step at 6,000 x g for 15 minutes followed by a filtration through a 0.22

µm pore size filter (Millipore). Supernatants were then subjected to high-speed centrifugation (200,000 x g for 2 hours) and pellets containing the OMVs were finally re-suspended in sterile 1X PBS. OMVs amounts were estimated by measuring protein concentration using DC protein assay (Bio-Rad) or NanoDrop (Thermo Fisher Scientific). 20 μg (protein content) were resuspended in sodium dodecyl sulfate-polyacrylamide gel electrophoresis (SDS-PAGE) Laemmli buffer and heated at 100°C for 10'. Proteins were separated using NuPAGE™ 4-12% Bis-Tris Protein Gels (Thermo Fisher Scientific) in MES (2-morpholin-4-ylethanesulfonic acid) buffer (Thermo Fisher Scientific) or using Any kD™ Criterion™ TGX Stain-Free™ Protein Gel (BioRad) in TrisGlicyne buffer (BioRad).Finally proteins were revealed by Coomassie Blue staining.

Western Blot

Purified OMVs (20 µg of protein content) were suspended in Laemmli buffer and were then separated using NuPAGE™ 4-12% Bis-Tris Protein Gels (Thermo Fisher Scientific) in MES buffer (Thermo Fisher Scientific) or using Any kD™ Criterion™ TGX Stain-Free™ Protein Gel (BioRad) in TrisGlicyne buffer (BioRad). Proteins separated by SDS-PAGE were subsequently transferred onto nitrocellulose membrane (iBlot™ Transfer Stack, nitrocellulose, Thermo Fisher Scientific) with iBlot® Dry Blotting System (Thermo Fisher Scientific). The membranes were blocked at room temperature (RT) for 30' by agitation in blocking solution (10% skimmed milk and 0.05% Tween 20 dissolved in PBS (PBST)). Rabbit polyclonal α-OVA antibodies (pAbs) were incubated for 1 hour at RT or o/n at 4°C. The pAbs were custom made by Genscript and were used at 0.8 µg/ml concentration in 1% skimmed milk-PBST. After three washing steps of 5' in PBST, the membranes were incubated in 1:2,000 dilution of peroxidase-conjugated anti-rabbit total IgGs (Dako) for 1 hour in 1% skimmed milk-PBST, and after 2 washing steps of 5' in PBST and 1 wash of 5' in PBS, antibody binding was detected by using the Novex™ ECL Chemiluminescent Substrate Reagent Kit (Thermo Fisher Scientific) at ChemiDOC (BioRAS) instrument.

Triton X-114 assay

Protein phase partitioning with Triton X-114 (Sigma-Aldrich) was assessed with minor modification from previous work[158]. 100 μg of OMVs were diluted in 450 μl of PBS, then ice cold 10% TritonX-114 was added to 1% final concentration and the OMV-containing solution was incubated at 4 °C for 1 h under shaking. The solution was then heated at 37 °C for 10' and the aqueous phase was separated from the detergent by centrifugation at 13,000 x g for 10'. Proteins in both phases were then precipitated by standard chloroform/methanol procedure, separated by SDS-PAGE electrophoresis and the protein of interest visualized by Western blot using α-OVA antibodies.

Flow cytometry on bacteria

E. coli BL21(DE3)Δ*ompA* strain transformed with pET-PSP-OVA and *E. coli* BL21(DE3)Δ*ompA* strain transformed with pET-MBP-OVA were grown at 30°C and 180 rpm in LB medium (starting OD_{600} = 0.05) and, when the cultures reached an OD_{600} value of 0.5, protein expression was induced by addition of 0.1 mM IPTG (Sigma-Aldrich). After induction, a volume corresponding to OD=1 was collected from each culture and centrifuge at 14,000 rpm 10'. Pellet was resuspended in 1ml PBS/BSA 1% and further diluted 1:50 in PBS/BSA 1%. 50 μl/well were put in 96 well plate. 50 μl of 2x solution of rabbit α-OVA antibodies (final concentration is 8 µg/ml) in PBS/BSA 1%were added in selected wells and cell incubated for 1h at 4°C. Cells were then washed 2 times with 100-200 μl/well of PBS/BSA 1% and centrifuged centrifuge for 10' at 3500 rpm and 4°C. 100 µl/well of Alexa Fluor®488 α-rabbit IgGs (Thermo Fisher Scientific) diluted 1:200 (final concentration is 10 μg/ml) in PBS/BSA1% were added in selected wells and incubated for 1h at 4°C in the dark. Cells were then washed 2 times with 100-200 μl/well of PBS/BSA 1% and centrifuged centrifuge for 10' at 3,500 rpm and 4°C. Cells were fixed with 100 μl PBS/Formaldehyde 2% for 15' at room temperature. Cells were then washed 2 times with 100-200 μl/well of PBS and centrifuged centrifuge for 10' at 3,500 rpm and 4°C. Cells were finally resuspended cells in 200 μl of PBS and stored at 4 °C in the dark or acquired to the Flow cytometry. Data were analyzed using FlowJo v10.1.

Animal studies

Mice were monitored twice per day to evaluate early signs of pain and distress, such as respiration rate, posture, and loss of weight (more than 20%) according to humane endpoints. Animals showing such conditions were anesthetized and subsequently sacrificed in accordance with experimental protocols, which were reviewed and approved by the Animal Ethical Committee of The University of Trento and the Italian Ministry of Health.

Mice immunization

For T cell generation, C57BL/6 or BALB/c mice were subcutaneously or intraperitoneally injected with either 20 μg of engineered OMVs, with 20 μg of "Empty" OMVs adsorbed to a total of 100 μg of a single or a mix of synthetic peptides or with 20 μg of "Empty" OMVs. Immunization were performed on day 0 and on day 7. On day 12-13, either blood or spleens were collected and analyzed.

Tumor challenge experiments

2.85×10^5 B16-OVA cells were subcutaneously injected in C57BL/6 mice on day 0. Mice were then immunized on day 1, 4, 8, 11 and 15 with either 20 μg of PSP-OMVs or 20 μg of "Empty" OMVs. Tumor growth was followed from day 8 on every 3 days.

C57BL/6 mice were immunized intraperitoneally on day 0, 14 and 28 with either 20 μg of Nm-fHbpvIII OMVs, Nm-fHbp-M30-vIII OMVs or "Empty" OMVs. On day 35, blood was collected by submandibular bleeding to measure α-EGFRvIII antibodies. On the same day, 0.5×10^5 B16F10-EGFRvIII cells were subcutaneously injected in mice and tumor growth was followed every 3 days from day 47 to the end of the experiment (day 65).

1.5×10^5 CT26 cells were subcutaneously injected in BALB/c mice on day 0. Mice were then immunized on day 1, 4, 8, 11, 15 and 21 with either 20 μg of ads-pentatope-OMVs (20 μg of "Empty" OMVs adsorbed to 20 μg/peptide of M03, M20, M26, M27 and M68) or 20 μg of "Empty" OMVs. Tumor growth was followed from day 11 on every 3 days.

Tumor measurements

Tumor volume was measured unblinded with a caliper and calculated using the formula $(AxB^2)/2$ where A was the largest and B the smallest diameter of the tumor. Statistical analysis (unpaired, two-tailed Student's t-test) and graphs were processed using GraphPad Prism 5.03 software.

T cell detection by flow cytometry

Dextramer analysis

For the staining of CD8 T cells with dextramers (Immudex), the manufacturer's instructions were followed with minor modifications. Blood was collected either by submandibular bleeding or by cardiac puncture. 120 µL of whole blood were incubated with 5 μl of $OVA_{257-264}$ (SIINFEKL) dextramer-PE for 10' at room temperature in a 12 x 75 mm polystyrene test tube. To block Fc receptors, 3 μl of α-CD16/CD32 was added and incubated for 15' at room temperature. Then, 5 μl of 7-AAD, 5 μl of α-CD19-PerCP, 5 μl of α-CD11b-PerCP, 3 μl of α-CD3-FITC and 5 μl α-CD8-APC antibodies were added and incubated for 20' at 4°C in the dark (all these antibodies were purchased from Beckton Dickinson (BD)). At this stage, red blood cells were lysed with 2 ml of EasyLyse^{TM} working solution (Dako) for 15' at room temperature. Cells were centrifuged for 5' at 300 x g and washed 2 times with 2 ml of PBS+%% FBS. Cells were finally resuspended in 350 μl of PBS and acquired using BD FACSCanto. For a better detection of antigen specific CD8 T lymphocytes, a strategy to exclude unwanted cell populations and reduce the background noise was adopted, with minor modifications as previously described[161,162]. Briefly, after gating lymphocytes from all events on the basis of SSC-A and FSC-A, a very strictly gating strategy was used. Single cells were selected on SSC-A and SSC-W, excluding both duplets and aggregates, which would have bound more and in a nonspecific manner respectively, the following antibodies. A "dump channel" was constructed in order to exclude dead cells (7-AAD positive), monocytes (CD11b positive) and B lymphocytes (CD19 positive): all these antibodies carried the same fluorochrome molecule (PerCP) and were used in the same fluorescent channel. The exclusion of these cells is very important because all of them can bind in a nonspecific manner to antibodies and

multimer molecules, affecting the final output of the staining. After the exclusion of all the above mentioned cells, T lymphocytes were selected for CD3 expression and the positive fraction inspected for CD8 to obtain the mean fluorescent values of the CD8 positive cells to set in the following plot. Dextramer positive T cells were finally visualised against CD8 expression, gating on the CD3 positive population.

In order to detect the residual level of nonspecific staining and background noise, a negative control dextramer, which carries an irrelevant peptide, was used with the same gating strategy.

The $OVA_{257-264}$ specific CD8 T cell population was calculated as percentage of dextramer and CD8 positive cells on the total of CD8 cells.

Intracellular cytokine staining on splenocytes

Mice were immunized twice intraperitoneally at days 0 and 7 with either 20 µg "Empty" OMVs, 20 µg "Empty" OMVs + 100 μg M30 peptide, 20 µg Nm-fHbp-M30-vIII-OMVs or 20 µg of ads-pentatope-OMVs (20 μg of "Empty" OMVs + 20 μg of each of M03, M20, M26, M27 and M68 peptides). On day 12, mice were sacrificed and spleens collected. Spleens were then homogenized and splenocytes filtered using a 70 µm cell Strainer (BD). After centrifugation at 400 x g for 7', splenocytes were resuspended in RPMI+10%FBS and PSG and aliquoted in a 96-well plate at a concentration of $1x10^6$ cells per well. Cells were stimulated with 2 mg/ml of M30 peptide (spleens from mice immunized with Nm-fHbp-M30-vIII-OMVs and "Empty" OMVs + 100 μg M30 peptide) or with 0.4 mg/ml of each of the 5 pentatope peptides (M03, M20, M26, M27 and M68; spleens from mice immunized with ads-pentatope OMVs). As positive and negative controls, cells were stimulated with phorbol 12-myristate 13-acetate (PMA, 0.5 mg/ml) and Ionomycin (1 mg/ml) or with 2 mg/ml of an unrelated peptide, respectively. After 2 hours of stimulation at 37°C, Brefeldin A (BD) was added to each well and cells incubated for 4 hours at 37°C. After two washes with PBS, LIVE/DEAD™ Fixable Near-IR Dead Cell Stain Kit (Thermo Fisher Scientific) was incubated with the splenocytes for 20' at RT in the dark. After two washes with PBS and permeabilization and fixing with Cytofix/Cytoperm (BD) following manufacturer's protocol, Fc receptors were blocked with 3 μl of α-CD16/CD32 for 15' at room temperature. Splenocytes were stained with the following fluorescent-labeled antibodies: α-CD3-APC (BioLegend), α-

CD4-BV510 (BioLegend), α-CD8-PECF594 (BD), and α-IFN-γ-BV785 (BioLegend). Samples were acquired on a BD FACSCanto II flow cytometer. Briefly, after gating lymphocytes from all events on the basis of SSC-A and FSC-A, single cells were selected on SSC-A and SSC-W, excluding both duplets and aggregates, which would have bound more and in a nonspecific manner, respectively, the antibodies. Live cells were selected as negative to LIVE/DEAD™ Fixable Near-IR Dead Cell Stain Kit (Thermo Fisher Scientific) and T lymphocytes were selected for CD3 expression. CD4 and CD8 lymphocytes were identified as positive for CD4 and CD8 molecules, respectively. IFN-γ positive T cells were finally visualized against CD4 or CD8 expression (depending on the epitope nature), gating on the CD3 positive population. The IFN-γ releasing CD4 and CD8 T cell populations were calculated as percentage of IFN-γ/CD4 and IFN-γ/CD8 double positive cells on the total of CD4 or CD8 cells, respectively.

Graphs and statistical analyses (unpaired, two-tailed Student's t-test) were performed with GraphPad Prism 5.03.

Analysis of TILs

Tumor-infiltrating lymphocytes were isolated from subcutaneous B16F10-EGFRvIII tumors taken from sacrificed mice. Two tumors per group were collected and minced into pieces of 1–2 mm of diameter using a sterile scalpel. Tumor samples were then transferred into 15 ml tubes containing 5 ml of collagenase solution (Collagenase Type 3,200 U/ml, Collagenase Type 4,200 U/ml (DBA Italia)) diluted in Hank's Balanced Salt Solution (HBSS, Gibco, Thermo Fisher Scientific) with 3 mM $CaCl_2$ and incubated under agitation for 2 hours at 37°C. The resulting cell suspensions were filtered through a 70 μm cell strainer 70 μm, washed twice with PBS and 1×10^6 cells were dispensed in a 96-well plate. Then, cells were incubated with LIVE/DEAD™ Fixable Near-IR Dead Cell Stain Kit (Thermo Fisher Scientific) 20' at RTin the dark. After two washes with PBS, Fc receptors were blocked with 3 μl of α-CD16/CD32 for 15' at room temperature. Samples were stained with the following mixture of fluorescent-labeled antibodies (all antibodies were purchased from BD): α-GR1 (BV605), α-CD11b-BV480, α-CD45-BV786, α-CD3-BV421, α-CD4-PE, α-CD8- PECF594 and α-CD25-APC. The samples were then incubated 1 hour at RT. After two washes with PBS, Cytofix/Cytoperm (BD)

was added to each well and incubated 20' on ice in the dark. After two washes with PBS, cells were stained with α-Foxp3-A488 (BD) antibodies diluted in Permwash 1x buffer for 20' at RT in the dark. Finally, samples were washed two times with 1% BSA in PBS and analyzed on a BD FACSCanto II. Briefly, after selecting live cells as the population negative for LIVE/DEAD™ Fixable Near-IR Dead Cell Stain Kit (Thermo Fisher Scientific), a homogeneous cell population was individuated from all events on the basis of SSC-A and FSC-A. Single cells were selected on SSC-A and SSC-W, excluding both duplets and aggregates, which would have bound more and in a nonspecific manner, respectively, antibodies. Leukocytes were selected as population positive to CD45 antibodies. Helper and cytotoxic TILs were identified as leukocytes positive for the CD4 and CD8 molecules, respectively. Tregs were individuated as CD4 subpopulation positive to FoxP3 marker. MDSCs were identified as leukocytes positive for both CD11b and Gr1 markers. CD4, CD8 and CD11b/Gr1 double positive cell populations were calculated as a percentage of the total leukocyte population. Tregs were calculated as percentage of FoxP3 positive cells of the CD4 population.

ELISA

To obtain serum, blood was collected from the submandibular vein, let stand for half an hour at RT and centrifuged for 10' at 2,000 x g. ELISA was performed using Nunc Immobilizer Amino plates (Thermo Fisher Scientific). Plate coating was performed by incubating plates o/n at 4°C with 100 µl of synthetic EGFRvIII peptide (5 µg/ml, Genscript). The day after, wells were washed 3 times with PBST (0.05% Tween 20 dissolved in PBS), saturated with 100 µl of 1% BSA dissolved in PBS for 1 hour at 37°C and washed again 3 times with PBST. An equal amount of serum from each mouse immunized with either Nm-fHbp-vIII OMVs or "Empty" OMVs as a control was pooled and 100-fold diluted in PBST and 0.1% BSA. This starting solution was threefold serially diluted in PBST and 0.1% BSA and 50 µl/well of each solution added to the EGFRvIII coated plate. After 3 washes with PBST, 100 µl of each serum dilution were dispensed in plate wells and incubated 2 hours at 37°C. Wells were subsequently washed 3 times with PBST and incubated for 1 hour at 37°C with alkaline phosphatase-conjugated goat α-mouse total IgG (Sigma-Aldrich), goat α-mouse IgG1 (SouthernBiotech) or goat α-mouse IgG2a (SouthernBiotech) at a final dilution of

1:2,000. After triple PBST wash, 100µl of Alkaline Phosphatase substrate (Sigma-Aldrich) were added to each well and plates were maintained at RT in the dark for 30'. Finally, absorbance was read at 405nm using Tecan Infinite M200Pro Plate reader.

Protocol for OMV engineering for the personalized cancer vaccine platform

pET-PSP was modified and BamHI and XhoI restriction enzyme sites were added before PSP stop codon (no details can be given for confidentiality reasons).

Forward and reverse single stranded oligonucleotides coding for each one of the five neoepitopes were chemically synthesized. After oligo phosphorylation with T4 Polynucleotide Kinase (New England Biolabs), forward and reverse strands were annealed creating a mini-gene encoding the neoepitope (e.g. M03F and M03R after annealing create M03 neoantigen minigene with BamHI and XhoI overhangs at the 5' and 3' ends of the gene, respectively; for full list of oligos used and for their nucleotide sequences, see Table 5). Annealing was performed at 95°C for 10' and then lowering the temperature by 0.5°C every 20'' until 65°C. After annealing, they were ligated to pET-PSP linearized with BamHI and XhoI using T4 DNA Ligase (New England Biolabs). After cloning, a glycine/serine spacer is created between PSP and the neoepitope. This mixture was used to transform BL21(DE3)Δ*ompA* strain and PSP-neoepitope fusions was sequence verified from selected recombinant clones. Clones with the correct pET-PSP-neoepitope sequence were finally used to purify OMVs as described above.

Neoantigen	Oligo name	Sequence
M03	M03F	5'-GATCCGACAAGCCCTTACGTCGCAATAACTCCTATACGAGCTATATTATGGCGATCTGCGGGATGCCACTTGATAGCTTTCGTGCCTAAC-3'
M03	M03R	5'-TCGAGTTAGGCACGAAAGCTATCAAGTGGCATCCCGCAGATCGCCATAATATAGCTCGTATAGGAGTTATTGCGACGTAAGGGCTTGTCG-3'
M20	M20F	5'-GATCCCCTCTTTTACCTTTTTATCCACCAGACGAGGCATTGGAAATCGGCCTTGAATTAAATTCTTCAGCGTTGCCACCCACAGAATAAC-3'
M20	M20R	5'-TCGAGTTATTCTGTGGGTGGCAACGCTGAAGAATTTAATTCAAGGCCGATTTCCAATGCCTCGTCTGGTGGATAAAAAGGTAAAAGAGGG-3'
M26	M26F	5'-GATCCGTAATTCTTCCCCAGGCCCCGAGCGGACCGTCCTACGCAACATACTTACAACCTGCCCAGGCGCAGATGTTAACACCTCCTTAAC-3'
M26	M26R	5'-TCGAGTTAAGGAGGTGTTAACATCTGCGCCTGGGCAGGTTGTAAGTATGTTGCGTAGGACGGTCCGCTCGGGGCCTGGGGAAGAATTACG-3'
M27	M27F	5'-GATCCGAGCATATTCATCGTGCTGGTGGACTTTTTGTGGCTGACGCAATTCAAGTAGGATTTGGACGCATCGGTAAGCATTTCTGGTAAC-3'
M27	M27R	5'-TCGAGTTACCAGAAATGCTTACCGATGCGTCCAAATCCTACTTGAATTGCGTCAGCCACAAAAAGTCCACCAGCACGATGAATATGCTCG-3'
M68	M68F	5'-GATCCGTAACAAGCATCCCATCCGTCTCTAATGCTCTGAATTGGAAAGAATTTTCGTTTATTCAGAGTACCTTGGGCTACGTGGCCTAAC-3'
M68	M68R	5'-TCGAGTTAGGCCACGTAGCCCAAGGTACTCTGAATAAACGAAAATTCTTTCCAATTCAGAGCATTAGAGACGGATGGGATGCTTGTTACG-3'

Table 5 | Oligonucleotides. *List of all oligonucleotides used to create minigenes coding for each one of the five CT26 neoepitopes used to engineer OMVs.*

References

1.	Torre, L. & Rebecca Siegel, A. J. Global Cancer Facts & Figures 3rd Edition. *Am. Cancer Soc.* 1–64 (2015). doi:10.1002/ijc.27711

2.	Jemal, A. *et al.* Global Cancer Statistics. *CA Cancer J Clin* **61,** 69–90 (2011).

3.	Lennerz, V. *et al.* The response of autologous T cells to a human melanoma is dominated by mutated neoantigens. **102,** 16013–18 (2005).

4.	Snyder, A. *et al.* Genetic Basis for Clinical Response to CTLA-4 Blockade in Melanoma. *N. Engl. J. Med.* **371,** 2189–2199 (2014).

5.	Rizvi, N. A. *et al.* Mutational landscape determines sensitivity to PD-1 blockade in non-small cell lung cancer. *Science (80-.).* **348,** 124–128 (2015).

6.	Zhou, J., Dudley, M. E., Rosenberg, S. A. & Robbins, P. F. Persistence of Multiple Tumor-Specific T-Cell Clones Is Associated with Complete Tumor Regression in a Melanoma Patient Receiving Adoptive Cell Transfer Therapy. *J. Immunother.* **28,** 53–62 (2005).

7.	Robbins, P. F. *et al.* Mining exomic sequencing data to identify mutated antigens recognized by adoptively transferred tumor-reactive T cells. *Nat. Med.* **19,** 747–752 (2013).

8.	Tran, E. *et al.* Cancer Immunotherapy Based on mutation-specific CD4+ T cells in a patient with epithelial cancer. *Science (80-.).* **9,** 641–645 (2014).

9.	Tran, E. *et al.* Immunogenicity of somatic mutations in human gastrointestinal cancers. *Science (80-.).* **350,** 1387–1391 (2015).

10.	Castle, J. C. *et al.* Exploiting the mutanome for tumor vaccination. *Cancer Res.* **72,** 1081–1091 (2012).

11.	Kreiter, S. *et al.* Mutant MHC class II epitopes drive therapeutic immune responses to cancer. *Nature* **520,** 692–696 (2015).

12.	Gubin, M. M. *et al.* Checkpoint blockade cancer immunotherapy targets tumour-specific mutant antigens. *Nature* **515,** 577–581 (2014).

13.	Yadav, M. *et al.* Predicting immunogenic tumour mutations by combining mass spectrometry and exome sequencing. *Nature* **515,** 572–576 (2014).

14.	Sahin, U. *et al.* Personalized RNA mutanome vaccines mobilize poly-specific

therapeutic immunity against cancer. *Nature* **547,** 222–226 (2017).

15. Ott, P. A. *et al.* An immunogenic personal neoantigen vaccine for patients with melanoma. *Nat. Publ. Gr.* **547,** 217–221 (2017).

16. Beveridge, T. J. Sructure of fram-negative cell walls and their derived mebrane vesicles. *J. Bacteriol.* **181,** 4725–4733 (1999).

17. D. Mayrand, D. G. Biological activities of outer membrane vesicles. *Can. J. Microbiol.* **6,** 607–13 (1989).

18. Campos, J. H. *et al.* Extracellular Vesicles: Role in Inflammatory Responses and Potential Uses in Vaccination in Cancer and Infectious Diseases. *J. Immunol. Res.* **2015,** (2015).

19. Ellis, T. N. & Kuehn, M. J. Virulence and Immunomodulatory Roles of Bacterial Outer Membrane Vesicles. *Microbiol. Mol. Biol. Rev.* **74,** 81–94 (2010).

20. Moshiri, A., Dashtbani-Roozbehani, A., Peerayeh, S. N. & Siadat, S. D. Outer membrane vesicle: A macromolecule with multifunctional activity. *Hum. Vaccines Immunother.* **8,** 953–955 (2012).

21. Ellis, T. N., Leiman, S. A. & Kuehn, M. J. Naturally produced outer membrane vesicles from Pseudomonas aeruginosa elicit a potent innate immune response via combined sensing of both lipopolysaccharide and protein components. *Infect. Immun.* **78,** 3822–3831 (2010).

22. Kaparakis, M. *et al.* Bacterial membrane vesicles deliver peptidoglycan to NOD1 in epithelial cells. *Cell. Microbiol.* **12,** 372–385 (2010).

23. Fantappiè, L. *et al.* Some Gram-negative Lipoproteins Keep Their Surface Topology When Transplanted from One Species to Another and Deliver Foreign Polypeptides to the Bacterial Surface. *Mol. Cell. Proteomics* **16,** 1348–1364 (2017).

24. Grandi, A. *et al.* Synergistic Protective Activity of Tumor-Specific Epitopes Engineered in Bacterial Outer Membrane Vesicles. *Front. Oncol.* **7,** 1–12 (2017).

25. American Cancer Society. Cancer Facts & Figures 2018. (2018). doi:10.1097/01.NNR.0000289503.22414.79

26. Byers, T. *et al.* The American Cancer Society challenge goal to reduce US cancer mortality by 50% between 1990 and 2015: Results and reflections. *CA.*

Cancer J. Clin. **0,** 1–11 (2016).

27. Siegel, R. L., Miller, K. D. & Jemal, A. Cancer statistics, 2018. *CA. Cancer J. Clin.* **68,** 7–30 (2018).

28. NIH-National Cancer Institute. Cancer Moonshot[SM] - National Cancer Institute. (2016). Available at: https://www.cancer.gov/research/key-initiatives/moonshot-cancer-initiative. (Accessed: 27th January 2018)

29. Finn, O. J. The dawn of vaccines for cancer prevention. *Nat. Rev. Immunol.* (2017). doi:10.1038/nri.2017.140

30. Huh, W. K. *et al.* Final efficacy, immunogenicity, and safety analyses of a nine-valent human papillomavirus vaccine in women aged 16–26 years: a randomised, double-blind trial. *Lancet* **390,** 2143–2159 (2017).

31. Gillison, M. Chapter 8. HPV vaccines and potential prevention of HPV-positive head and neck cancer. in *IARC HPV Working Group. Primary End-points for Prophylactic HPV Vaccine Trials.* 86–92 (International Agency for Research on Cancer; 2014. (IARC Working Group Reports, No. 7.), 2014).

32. Centers for Disease Control and Prevention. Epatocarcinoma prevention with HBV vaccines-Pinkbook | Hepatitis B | Epidemiology of Vaccine Preventable Diseases | CDC. (2018). Available at: https://www.cdc.gov/vaccines/pubs/pinkbook/hepb.html. (Accessed: 16th February 2018)

33. World Health Organization-WHO. Hepatitis B. (2018). Available at: http://www.who.int/mediacentre/factsheets/fs204/en/. (Accessed: 16th February 2018)

34. Kantoff, P. W. *et al.* Sipuleucel-T Immunotherapy for Castration-Resistant Prostate Cancer. *N. Engl. J. Med.* **363,** 411–422 (2010).

35. American Cancer Society. FDA approved immune checkpoint inhibitors to treat cancer. (2017). Available at: https://www.cancer.org/treatment/treatments-and-side-effects/treatment-types/immunotherapy/immune-checkpoint-inhibitors.html. (Accessed: 28th December 2017)

36. Farkona, S., Diamandis, E. P. & Blasutig, I. M. Cancer immunotherapy: the beginning of the end of cancer? *BMC Med.* **14,** 73 (2016).

37. Wolchok, J. D. *et al.* Nivolumab plus Ipilimumab in Advanced Melanoma. *N.*

Engl. J. Med. **369,** 122–133 (2013).

38.   U.S. Food and Drug Administration. Kymriah (tisagenlecleucel) - FDA approval brings first gene therapy to the United States. (2017). Available at: https://www.fda.gov/NewsEvents/Newsroom/PressAnnouncements/ucm57405 8.htm. (Accessed: 31st December 2017)

39.   Prasad, V. Immunotherapy: Tisagenlecleucel - the first approved CAR-T-cell therapy: implications for payers and policy makers. *Nat. Rev. Clin. Oncol.* (2017). doi:10.1038/nrclinonc.2017.156

40.   U.S. Food and Drug Administration. Kymriah overall remission rate. Press Announcements - FDA approval brings first gene therapy to the United States. (2017). Available at: https://www.fda.gov/NewsEvents/Newsroom/PressAnnouncements/ucm57405 8.htm. (Accessed: 25th January 2018)

41.   U.S. Food and Drug Administration. Kymriah overall remission rate and complete remission. Approved Drugs - FDA approves tisagenlecleucel for B-cell ALL and tocilizumab for cytokine release syndrome. (2017). Available at: https://www.fda.gov/drugs/informationondrugs/approveddrugs/ucm574154.htm. (Accessed: 25th January 2018)

42.   U.S. Food and Drug Administration. Yescarta (axicabtagene ciloleucel) - FDA approves CAR-T cell therapy to treat adults with certain types of large B-cell lymphoma. (2017). Available at: https://www.fda.gov/NewsEvents/Newsroom/PressAnnouncements/ucm58121 6.htm. (Accessed: 31st December 2017)

43.   U.S. Food and Drug Administration. Yescarta (axicabtagene ciloleucel) complete remission rate. Approved Drugs - FDA approves axicabtagene ciloleucel for large B-cell lymphoma. (2017). Available at: https://www.fda.gov/Drugs/InformationOnDrugs/ApprovedDrugs/ucm581296.ht m. (Accessed: 25th January 2018)

44.   Balkwill, F. & Mantovani, A. Inflammation and cancer: Back to Virchow? *Lancet* **357,** 539–545 (2001).

45.   Lizée, G. *et al.* Harnessing the Power of the Immune System to Target Cancer. *Annu. Rev. Med.* **64,** 71–90 (2013).

46. Sell, S. Cancer immunotherapy: Breakthrough or 'deja vu, all over again'? *Tumor Biol.* **39,** 101042831770776 (2017).

47. Ichim, C. V. Revisiting immunosurveillance and immunostimulation: Implications for cancer immunotherapy. *J. Transl. Med.* **3,** 8 (2005).

48. Burnet, M. Cancer: a Biological Approach III. Viruses Associated With Neoplastic Conditions. *Br. Med. J.* **1,** 841–847 (1957).

49. Rentsch, C. A. *et al.* Bacillus calmette-guérin strain differences have an impact on clinical outcome in bladder cancer immunotherapy. *Eur. Urol.* **66,** 677–688 (2014).

50. Kaplan, D. H. *et al.* Demonstration of an interferon γ-dependent tumor surveillance system in immunocompetent mice. *Immunology* **95,** 7556–7561 (1998).

51. Smyth, M. J. *et al.* Differential tumor surveillance by natural killer (NK) and NKT cells. *J. Exp. Med.* **191,** 661–668 (2000).

52. Street, S. E., Cretney, E. & Smyth, M. J. Perforin and interferon-gamma activities independently control tumor initiation, growth, and metastasis. *Blood* **97,** 192–197 (2001).

53. Rosenberg, S. A. IL-2: The First Effective Immunotherapy for Human Cancer. *J. Immunol.* **192,** 5451–5458 (2014).

54. Atkins, B. M. B. *et al.* High - Dose Recombinant Interleukin-2 Therapy for Patients With Meta static Melanoma : Analysis o f 270 Patients Treated Between 1985 and 1993. *J. Clin. Oncol.* **17,** 2105–2116 (1999).

55. Delves, P. J. & Roitt, I. M. The Immune System: Firts of Two Parts. *N. Engl. J. Med.* **343,** 37–49 (2000).

56. Murphy, K. & Weaver, C. *Janeway's Immunobiology. 9th Edition.* (Garland Science, 2016).

57. Delves, P. J. & Roitt, I. M. The Immune System: Second of Two Parts. *N. Engl. J. Med.* **343,** 782–786 (2000).

58. Groothuis, T. A. M. & Neefjes, J. The many roads to cross-presentation. *J. Exp. Med.* **202,** 1313–1318 (2005).

59. Coulie, P. G., Van Den Eynde, B. J., Van Der Bruggen, P. & Boon, T. Tumour antigens recognized by T lymphocytes: At the core of cancer immunotherapy.

Nat. Rev. Cancer **14,** 135–146 (2014).

60.   Ward, J. P., Gubin, M. M. & Schreiber, R. D. *The Role of Neoantigens in Naturally Occurring and Therapeutically Induced Immune Responses to Cancer. Advances in Immunology* **130,** (Elsevier Inc., 2016).

61.   Brichard, V. *et al.* The tyrosinase gene codes for an antigen recognized by autologous cytolytic T lymphocytes on HLA-A2 melanomas. *J. Exp. Med.* **178,** 489–495 (1993).

62.   Bakker, B. A. B. H. *et al.* Melanocyte lineage-specific antigen gp100 is recognized by melanoma-derived tumor-infiltrating lymphocytes. *J. Exp. Med.* **179,** 1005–1009 (1994).

63.   Kawakami, Y. *et al.* Cloning of the gene coding for a shared human melanoma antigen recognized by autologous T cells infiltrating into tumor. *Proc. Natl. Acad. Sci. U. S. A.* **91,** 3515–9 (1994).

64.   Ohminami, H., Yasukawa, M. & Fujita, S. HLA class I-restricted lysis of leukemia cells by a CD8(+) cytotoxic T-lymphocyte clone specific for WT1 peptide. *Blood* **95,** 286–93 (2000).

65.   Fisk, B. B., Blevins, T. L., Wharton, J. T. & Ioannides, C. G. Identification of an immunodominant peptide of HER-2/neu protooncogene recognized by ovarian tumor-specific cytotoxic T lymphocyte lines. *Peptides* **181,** (1995).

66.   Whitehurst, A. W. Cause and Consequence of Cancer/Testis Antigen Activation in Cancer. *Annu. Rev. Pharmacol. Toxicol.* **54,** 251–272 (2014).

67.   van der Bruggen, P. *et al.* A gene encoding an antigen recognized by cytolytic T lymphocytes on a human melanoma. *Science (80-.).* **254,** 1643–1647 (1991).

68.   Chen, Y.-T. *et al.* A testicular antigen aberrantly expressed in human cancers detected by autologous antibody screening. *Proc. Natl. Acad. Sci.* **94,** 1914–1918 (1997).

69.   Scanlan, M. J., Gure, A. O., Jungbluth, A. A., Old, L. J. & Chen, Y. T. Cancer/testis antigens: an expanding family of targets for cancer immunotherapy. *Immunol Rev* **188,** 22–32 (2002).

70.   Jungbluth, A. A. *et al.* Monoclonal antibody MA454 reveals a heterogeneous expression pattern of MAGE-1 antigen in formalin-fixed paraffin embedded

lung tumours. *Br. J. Cancer* **83,** 493–497 (2000).

71. Schulz, T. F. & Cordes, S. Is the Epstein-Barr virus EBNA-1 protein an oncogen? *Proc. Natl. Acad. Sci. U. S. A.* **106,** 2091–2092 (2009).

72. Marur, S. & Forastiere, A. A. Head and Neck Cancer: Changing Epidemiology, Diagnosis, and Treatment. *Mayo Clin. Proc.* **83,** 489–501 (2008).

73. Alexandrov, L. B. *et al.* Signatures of mutational processes in human cancer. *Nature* **500,** 415–21 (2013).

74. Bethune, M. T. & Joglekar, A. V. Personalized T cell-mediated cancer immunotherapy: progress and challenges. *Curr. Opin. Biotechnol.* **48,** 142–152 (2017).

75. Vormehr, M. *et al.* Mutanome directed cancer immunotherapy. *Curr. Opin. Immunol.* **39,** 14–22 (2016).

76. Zhang, X., Sharma, P. K., Peter Goedegebuure, S. & Gillanders, W. E. Personalized cancer vaccines: Targeting the cancer mutanome. *Vaccine* **35,** 1094–1100 (2017).

77. Vogelstein, B. *et al.* Cancer Genome Landscapes. *Science (80-.).* **339,** 1546–1558 (2013).

78. Greenman, C. *et al.* Patterns of somatic mutation in human cancer genomes. *Nature* **446,** 153–158 (2007).

79. Stratton, M. R. Exploring the Genomes of Cancer Cells: Progress and Promise. *Science (80-.).* **331,** 1553–1558 (2011).

80. Chen, D. S. & Mellman, I. Oncology meets immunology: The cancer-immunity cycle. *Immunity* **39,** 1–10 (2013).

81. Haabeth, O. A. W. *et al.* How do CD4+ T cells detect and eliminate tumor cells that either lack or express MHC class II molecules? *Front. Immunol.* **5,** 1–13 (2014).

82. Melero, I. *et al.* Therapeutic vaccines for cancer: An overview of clinical trials. *Nat. Rev. Clin. Oncol.* **11,** 509–524 (2014).

83. Dunn, G. P., Bruce, A. T., Ikeda, H., Old, L. J. & Schreiber, R. D. Cancer immunoediting: From immunosurveillance to tumor escape. *Nat. Immunol.* **3,** 991–998 (2002).

84. Schreiber, R. D., Old, L. J. & Smyth, M. J. Cancer Immunoediting: Integrating

Immunity's Roles in Cancer Suppression and Promotion. *Science (80-.).* **331,** 1565–1570 (2011).

85. MacKie, R. M., Reid, R. & Junor, B. Fatal Melanoma Transferred in a Donated Kidney 16 Years after Melanoma Surgery. *N. Engl. J. Med.* **348,** 567–568 (2003).

86. Bodmer, W. F. *et al.* Tumor Escape from Immune Response by Variation in HLA Expression and Other Mechanisms. *Ann. N. Y. Acad. Sci.* **690,** 42–49 (1993).

87. Garrido, F., Ruiz-Cabello, F. & Aptsiauri, N. Rejection versus escape: the tumor MHC dilemma. *Cancer Immunol. Immunother.* **66,** 259–271 (2017).

88. Drake, C. G., Jaffee, E. & Pardoll, D. M. Mechanisms of Immune Evasion by Tumors. *Adv. Immunol.* **90,** 51–81 (2006).

89. Seliger, B., Maeurer, M. J. & Ferrone, S. Antigen-processing machinery breakdown and tumor growth. *Immunol. Today* **21,** 455–464 (2000).

90. Landsberg, J. *et al.* Melanomas resist T-cell therapy through inflammation-induced reversible dedifferentiation. *Nature* **490,** 412–416 (2012).

91. Vyas, M., Müller, R. & von Strandmann, E. P. Antigen loss variants: Catching hold of escaping foes. *Front. Immunol.* **8,** 1–7 (2017).

92. Garcia-Diaz, A. *et al.* Interferon Receptor Signaling Pathways Regulating PD-L1 and PD-L2 Expression. *Cell Rep.* **19,** 1189–1201 (2017).

93. Spranger, S. *et al.* Up-Regulation of PD-L1, IDO, and Tregs in the Melanoma Tumor Microenvironment Is Driven by CD8+ T Cells. *Sci. Transl. Med.* **5,** 200ra116-200ra116 (2013).

94. Motz, G. & Coukos, G. Deciphering and Reversing Tumor Immune Suppression. *Immunity* **39,** 61–73 (2013).

95. Van Der Burg, S. H., Arens, R., Ossendorp, F., Van Hall, T. & Melief, C. J. M. Vaccines for established cancer: Overcoming the challenges posed by immune evasion. *Nat. Rev. Cancer* **16,** 219–233 (2016).

96. Sharma, P., Wagner, K., Wolchok, J. D. & Allison, J. P. Novel cancer immunotherapy agents with survival benefit: recent successes and next steps. *Nat. Rev. Cancer* **11,** 805–812 (2011).

97. Parker, B. S., Rautela, J. & Hertzog, P. J. Antitumour actions of interferons:

Implications for cancer therapy. *Nat. Rev. Cancer* **16,** 131–144 (2016).

98. Dranoff, G. Cytokines in cancer pathogenesis and cancer therapy. *Nat. Rev. Cancer* **4,** 11–22 (2004).

99. Scott, A. M., Wolchok, J. D. & Old, L. J. Antibody therapy of cancer. *Nat. Rev. Cancer* **12,** 278–287 (2012).

100. Pardoll, D. M. The blockade of immune checkpoints in cancer immunotherapy. *Nat. Rev. Cancer* **12,** 252–264 (2012).

101. Rosenberg, S. A. & Restifo, N. P. Adoptive cell transfer as personalized immunotherapy for human cancer. *Science (80-.).* **348,** 62–68 (2015).

102. Restifo, N., Dudley, M. & Rosenberg, S. A. Adoptive immunotherapy for cancer: harnessing the T cell response. *Nat. Rev. Immunol.* **12,** 269–281 (2012).

103. Guo, C. *et al. Therapeutic cancer vaccines. Past, present, and future. Advances in Cancer Research* **119,** (Elsevier Inc., 2013).

104. Melief, C. J. M., van Hall, T., Arens, R., Ossendorp, F. & van der Burg, S. H. Therapeutic Cancer Vaccines. *J. Clin. Invest.* **125,** 3401–12 (2015).

105. Galluzzi, L. *et al.* Classification of current anticancer immunotherapies. *Oncotarget* **5,** 12472–12508 (2014).

106. Schuster, M., Nechansky, A., Loibner, H. & Kircheis, R. Cancer immunotherapy. *Biotechnol. J.* **1,** 138–147 (2006).

107. Plotkin, S. A. Vaccines: Past, present and future. *Nat. Med.* **11,** S5 (2005).

108. Grandi, A., Tomasi, M. & Grandi, G. Vaccinology: The art of putting together the right ingredients. *Hum. Vaccines Immunother.* **12,** 1311–1317 (2016).

109. Yang, A., Farmer, E., Wu, T. C. & Hung, C. F. Perspectives for therapeutic HPV vaccine development. *J. Biomed. Sci.* **23,** 1–19 (2016).

110. Karaki, S., Pere, H., Badoual, C. & Tartour, E. Hope in the Long Road Toward the Development of a Therapeutic Human Papillomavirus Vaccine. *Clin. Cancer Res.* **22,** 2317–2319 (2016).

111. Lee, Y. Bin, Lee, J.-H., Kim, Y. J., Yoon, J.-H. & Lee, H.-S. The effect of therapeutic vaccination for the treatment of chronic hepatitis B virus infection. *J. Med. Virol.* **87,** 575–582 (2015).

112. Michel, M. L., Deng, Q. & Mancini-Bourgine, M. Therapeutic vaccines and

immune-based therapies for the treatment of chronic hepatitis B: Perspectives and challenges. *J. Hepatol.* **54,** 1286–1296 (2011).

113. Kirkwood, J. M. *et al.* Immunotherapy of cancer in 2012. *CA. Cancer J. Clin.* **62,** 309–335 (2012).

114. Wurz, G. T., Kao, C.-J. & DeGregorio, M. W. Novel cancer antigens for personalized immunotherapies: latest evidence and clinical potential. *Ther. Adv. Med. Oncol.* **8,** 4–31 (2016).

115. Kaiko, G. E., Horvat, J. C., Beagley, K. W. & Hansbro, P. M. Immunological decision-making: How does the immune system decide to mount a helper T-cell response? *Immunology* **123,** 326–338 (2008).

116. Mellman, I., Coukos, G. & Dranoff, G. Cancer immunotherapy comes of age. *Nature* **480,** 480–489 (2011).

117. Topalian, S. L., Weiner, G. J. & Pardoll, D. M. Cancer immunotherapy comes of age. *J. Clin. Oncol.* **29,** 4828–4836 (2011).

118. Klebanoff, C. A., Acquavella, N., Yu, Z. & Restifo, N. P. Therapeutic cancer vaccines: Are we there yet? *Immunol. Rev.* **239,** 27–44 (2011).

119. Bobisse, S., Foukas, P. G., Coukos, G. & Harari, A. Neoantigen-based cancer immunotherapy. *Ann. Transl. Med.* **4,** 262–262 (2016).

120. Martin, S. D., Coukos, G., Holt, R. A. & Nelson, B. H. Targeting the undruggable: Immunotherapy meets personalized oncology in the genomic era. *Ann. Oncol.* **26,** 2367–2374 (2015).

121. Yarchoan, M., Johnson, B. A., Lutz, E. R., Laheru, D. A. & Jaffee, E. M. Targeting neoantigens to augment antitumour immunity. *Nat. Rev. Cancer* **17,** 209–222 (2017).

122. Barber, D. L. *et al.* Restoring function in exhausted CD8 T cells during chronic viral infection. *Nature* **439,** 682–687 (2006).

123. Loke, P. & Allison, J. P. PD-L1 and PD-L2 are differentially regulated by Th1 and Th2 cells. *Proc. Natl. Acad. Sci.* **100,** 5336–5341 (2003).

124. Iwai, Y. *et al.* Involvement of PD-L1 on tumor cells in the escape from host immune system and tumor immunotherapy by PD-L1 blockade. *Proc. Natl. Acad. Sci.* **99,** 12293–12297 (2002).

125. Okazaki, T., Chikuma, S., Iwai, Y., Fagarasan, S. & Honjo, T. A rheostat for

immune responses: The unique properties of PD-1 and their advantages for clinical application. *Nat. Immunol.* **14,** 1212–1218 (2013).

126. Garon, E. B. *et al.* Pembrolizumab for the Treatment of Non–Small-Cell Lung Cancer. *N. Engl. J. Med.* **372,** 2018–2028 (2015).

127. Le, D. T. *et al.* PD-1 Blockade in Tumors with Mismatch-Repair Deficiency. *N. Engl. J. Med.* **372,** 2509–2520 (2015).

128. Germano, G. *et al.* Inactivation of DNA repair triggers neoantigen generation and impairs tumour growth. *Nature* (2017). doi:10.1038/nature24673

129. Duraiswamy, J., Kaluza, K. M., Freeman, G. J. & Coukos, G. Dual blockade of PD-1 and CTLA-4 combined with tumor vaccine effectively restores T-cell rejection function in tumors. *Cancer Res.* **73,** 3591–3603 (2013).

130. Curran, M. A., Montalvo, W., Yagita, H. & Allison, J. P. PD-1 and CTLA-4 combination blockade expands infiltrating T cells and reduces regulatory T and myeloid cells within B16 melanoma tumors. *Proc. Natl. Acad. Sci.* **107,** 4275–4280 (2010).

131. Larkin, J. *et al.* Combined Nivolumab and Ipilimumab or Monotherapy in Untreated Melanoma. *N. Engl. J. Med.* **373,** 23–34 (2015).

132. Rosenberg, S. A. & Restifo, N. P. Adoptive cell transfer as personalized immunotherapy for human cancer. *Science (80-.).* **348,** 62–68 (2015).

133. Dudley, M. E. Cancer Regression and Autoimmunity in Patients After Clonal Repopulation with Antitumor Lymphocytes. *Science (80-.).* **298,** 850–854 (2002).

134. Rosenberg, S. A., Restifo, N. P., Yang, J. C., Morgan, R. A. & Dudley, M. E. Adoptive cell transfer: A clinical path to effective cancer immunotherapy. *Nat. Rev. Cancer* **8,** 299–308 (2008).

135. Gubin, M. M., Artyomov, M. N., Mardis, E. R. & Schreiber, R. D. Tumor neoantigens: building a framework for personalized cancer immunotherapy. *J. Clin. Invest.* **125,** 3413–3421 (2015).

136. Aldous, A. R. & Dong, J. Z. Personalized neoantigen vaccines: A new approach to cancer immunotherapy. *Bioorganic Med. Chem.* (2017). doi:10.1016/j.bmc.2017.10.021

137. Matsushita, H. *et al.* Cancer exome analysis reveals a T-cell-dependent

mechanism of cancer immunoediting. *Nature* **482,** 400–404 (2012).

138. Kulp, A. & Kuehn, M. J. Biological Functions and Biogenesis of Secreted Bacterial Outer Membrane Vesicles. *Annu. Rev. Microbiol.* **64,** 163–184 (2010).

139. Kaparakis-Liaskos, M. & Ferrero, R. L. Immune modulation by bacterial outer membrane vesicles. *Nat. Rev. Immunol.* **15,** 375–387 (2015).

140. Schwechheimer, C. & Kuehn, M. J. Outer-membrane vesicles from Gram-negative bacteria: biogenesis and functions. *Nat. Rev. Microbiol.* **13,** 605–19 (2015).

141. Kim, O. Y. *et al.* Immunization with Escherichia coli outer membrane vesicles protects bacteria-induced lethality via Th1 and Th17 cell responses. *J. Immunol.* **190,** 4092–102 (2013).

142. Fantappiè, L. *et al.* Antibody-mediated immunity induced by engineered Escherichia coli OMVs carrying heterologous antigens in their lumen. *J. Extracell. vesicles* **3,** 1–14 (2014).

143. Rosenthal, J. A. *et al.* Mechanistic insight into the Th1-biased immune response to recombinant subunit vaccines delivered by probiotic bacteria-derived outer membrane vesicles. *PLoS One* **9,** 1–24 (2014).

144. Kuehn, N. C. K. and M. J. Incorporation of Heterologous Outer Membrane and Periplasmic Proteins into Escherichia coli Outer Membrane Vesicles. **279,** 2069–2076 (2012).

145. Chen, D. J. *et al.* Delivery of foreign antigens by engineered outer membrane vesicle vaccines. *Proc. Natl. Acad. Sci. U. S. A.* **107,** 3099–3104 (2010).

146. Gerritzen, M. J. H., Martens, D. E., Wijffels, R. H., van der Pol, L. & Stork, M. Bioengineering bacterial outer membrane vesicles as vaccine platform. *Biotechnol. Adv.* **35,** 565–574 (2017).

147. Alaniz, R. C., Deatherage, B. L., Lara, J. C. & Cookson, B. T. Membrane vesicles are immunogenic facsimiles of Salmonella typhimurium that potently activate dendritic cells, prime B and T cell responses, and stimulate protective immunity in vivo. *J. Immunol.* **179,** 7692–7701 (2007).

148. Laughlin, R. C., Mickum, M., Rowin, K., Adams, L. G. & Alaniz, R. C. Altered host immune responses to membrane vesicles from Salmonella and Gram-negative pathogens. *Vaccine* **33,** 5012–5019 (2015).

149. Giuliani, M. M. *et al.* A universal vaccine for serogroup B meningococcus. *Proc. Natl. Acad. Sci. USA* **103,** 10834–9 (2006).

150. Serruto, D., Bottomley, M. J., Ram, S., Giuliani, M. M. & Rappuoli, R. The new multicomponent vaccine against meningococcal serogroup B , 4CMenB : Immunological , functional and structural characterization of the antigens. *Vaccine* **30S,** B87–B97 (2012).

151. Deatherage, B. L. *et al.* Biogenesis of bacterial membrane vesicles. *Mol. Microbiol.* **72,** 1395–1407 (2009).

152. Bernadac, A. *et al.* Escherichia coli tol-pal Mutants Form Outer Membrane Vesicles Escherichia coli tol-pal Mutants Form Outer Membrane Vesicles. *J. Bacteriol.* **180,** 4872–4878 (1998).

153. Berlanda Scorza, F. *et al.* High yield production process for Shigella outer membrane particles. *PLoS One* **7,** (2012).

154. Bousso, P. T-cell activation by dendritic cells in the lymph node: Lessons from the movies. *Nat. Rev. Immunol.* **8,** 675–684 (2008).

155. Nikaido, H. Maltose transport system of Escherichia coli: an ABC-type transporter. *FEBS Lett.* **346,** 55–58 (1994).

156. Rueda, P., Morón, G., Sarraseca, J., Leclerc, C. & Casal, J. I. Influence of flanking sequences on presentation efficiency of a CD8+ cytotoxic T-cell epitope delivered by parvovirus-like a particles. *J. Gen. Virol.* **85,** 563–572 (2004).

157. Klock, H. E., Koesema, E. J., Knuth, M. W. & Lesley, S. A. Combining the polymerase incomplete primer extension method for cloning and mutagenesis with microscreening to accelerate structural genomics efforts. *Proteins Struct. Funct. Genet.* **71,** 982–994 (2008).

158. Bordier, C. Phase separation of integral membrane proteins in Triton X-114 solution. *J. Biol. Chem.* **256,** 1604–1607 (1981).

159. Immudex. IMMUDEX - Immudex makes Dextramers-next generation of MHC tetramer. Available at: http://www.immudex.com/. (Accessed: 31st January 2018)

160. Batard, P. *et al.* Dextramers: New generation of fluorescent MHC class I/peptide multimers for visualization of antigen-specific CD8+T cells. *J.*

Immunol. Methods **310,** 136–148 (2006).

161. Perfetto, S. P., Chattopadhyay, P. K. & Roederer, M. Seventeen-colour flow cytometry: unravelling the immune system. *Nat. Rev. Immunol.* **4,** 648–655 (2004).

162. Chattopadhyay, P. K. *et al.* Techniques to improve the direct ex vivo detection of low frequency antigen-specific CD8 [+] T cells with peptide-major histocompatibility complex class I tetramers. *Cytom. Part A* **73A,** 1001–1009 (2008).

163. Vecchio, D., Li, G. & Wong, A. J. Targeting EGF receptor variant III : tumor-specific peptide vaccination for malignant gliomas. *Expert Rev. Vaccines* **11,** 133–144 (2012).

164. Heimberger, A. B. *et al.* Epidermal growth factor receptor VIII peptide vaccination is efficacious against established intracerebral tumors. *Clin. Cancer Res.* **9,** 4247–4254 (2003).

165. Schuster, J. *et al.* A phase II, multicenter trial of rindopepimut (CDX-110) in newly diagnosed glioblastoma: The ACT III study. *Neuro. Oncol.* **17,** 854–861 (2015).

166. Weller, M. *et al.* Rindopepimut with temozolomide for patients with newly diagnosed, EGFRvIII-expressing glioblastoma (ACT IV): a randomised, double-blind, international phase 3 trial. *Lancet Oncol.* **18,** 1373–1385 (2017).

167. Tanenbaum, M. E. *et al.* A complex of Kif18b and MCAK promotes microtubule depolymerization and is negatively regulated by aurora kinases. *Curr. Biol.* **21,** 1356–1365 (2011).

168. Snapper, C. M. & Paul, W. E. Interferon-gamma and B cell stimulatory factor-1 reciprocally regulate Ig isotype production. *Science (80-.).* **236,** 944–947 (1987).

169. Maisonneuve, C., Bertholet, S., Philpott, D. J. & De Gregorio, E. Unleashing the potential of NOD- and Toll-like agonists as vaccine adjuvants. *Proc. Natl. Acad. Sci.* **111,** 12294–12299 (2014).

170. Medzhitov, R. Toll-like receptors and innate immunity. *Nat. Rev. Immunol.* **1,** 135–145 (2001).

171. Akira, S. & Takeda, K. Toll-like receptor signalling. *Nat. Rev. Immunol.* **4,** 499–

511 (2004).

172. Honda, K. & Taniguchi, T. IRFs: Master regulators of signalling by Toll-like receptors and cytosolic pattern-recognition receptors. *Nat. Rev. Immunol.* **6,** 644–658 (2006).

173. Strober, W., Murray, P. J., Kitani, A. & Watanabe, T. Signalling pathways and molecular interactions of NOD1 and NOD2. *Nat. Rev. Immunol.* **6,** 9–20 (2006).

174. Duque, G. A. & Descoteaux, A. Macrophage cytokines: Involvement in immunity and infectious diseases. *Front. Immunol.* **5,** 1–12 (2014).

175. Guo, H., Callaway, J. B. & Ting, J. P. Y. Inflammasomes: Mechanism of action, role in disease, and therapeutics. *Nat. Med.* **21,** 677–687 (2015).

176. Jo, E.-K., Kim, J. K., Shin, D.-M. & Sasakawa, C. Molecular mechanisms regulating NLRP3 inflammasome activation. *Cell. Mol. Immunol.* **13,** 148–159 (2016).

177. He, Y., Hara, H. & Núñez, G. Mechanism and Regulation of NLRP3 Inflammasome Activation. *Trends Biochem. Sci.* **41,** 1012–1021 (2016).

178. Liu, T., Zhang, L., Joo, D. & Sun, S.-C. NF-κB signaling in inflammation. *Signal Transduct. Target. Ther.* **2,** 17023 (2017).

179. Martinon, F., Agostini, L., Meyland, E. & Tschopp, J. Identification of Bacterial Muramyl Dipeptide as Activator of the NALP3/Cryopyrin Inflammasome. *Curr. Biol.* **14,** 1929–1934 (2004).

180. Finethy, R. *et al.* Inflammasome activation by bacterial outer membrane vesicles requires guanylate binding proteins. *MBio* **8,** 1–11 (2017).

181. Lee, D. H. *et al.* Adjuvant effect of bacterial outer membrane vesicles with penta-acylated lipopolysaccharide on antigen-specific T cell priming. *Vaccine* **29,** 8293–8301 (2011).

182. Luckheeram, R. V., Zhou, R., Verma, A. D. & Xia, B. CD4 +T cells: Differentiation and functions. *Clin. Dev. Immunol.* **2012,** (2012).

183. Lazarevic, V., Glimcher, L. H. & Lord, G. M. T-bet: a bridge between innate and adaptive immunity. *Nat. Rev. Immunol.* **13,** 777–789 (2013).

184. Trinchieri, G. Interleukin-12 and the regulation of innate resistance and adaptive immunity. *Nat. Rev. Immunol.* **3,** 133–146 (2003).

185. Lohoff, M. & Mak, T. W. Roles of interferon-regulatory factors in T-helper-cell

differentiation. *Nat. Rev. Immunol.* **5,** 125–135 (2005).

186. Ho, I. C., Tai, T. S. & Pai, S. Y. GATA3 and the T-cell lineage: Essential functions before and after T-helper-2-cell differentiation. *Nat. Rev. Immunol.* **9,** 125–135 (2009).

187. Ley, K., Laudanna, C., Cybulsky, M. I. & Nourshargh, S. Getting to the site of inflammation : the leukocyte adhesion cascade updated. *Nat. Rev. Immunol.* **7,** 678–689 (2007).

188. Liu, M., Guo, S. & Stiles, J. K. The emerging role of CXCL10 in cancer. *Oncol. Lett.* **2,** 583–589 (2011).

189. Groom, J. R. & Luster, A. D. CXCR3 ligands: Redundant, collaborative and antagonistic functions. *Immunol. Cell Biol.* **89,** 207–215 (2011).

190. Guel, N. & Van Egmond, M. Antibody-dependent phagocytosis of tumor cells by Macrophages: A Potent effector mechanism of monoclonal antibody therapy of cancer. *Cancer Res.* **75,** 5008–5013 (2015).

191. Fantappiè, L. *et al.* Antibody-mediated immunity induced by engineered Escherichia coli OMVs carrying heterologous antigens in their lumen. *J. Extracell. Vesicles* **3,** (2014).
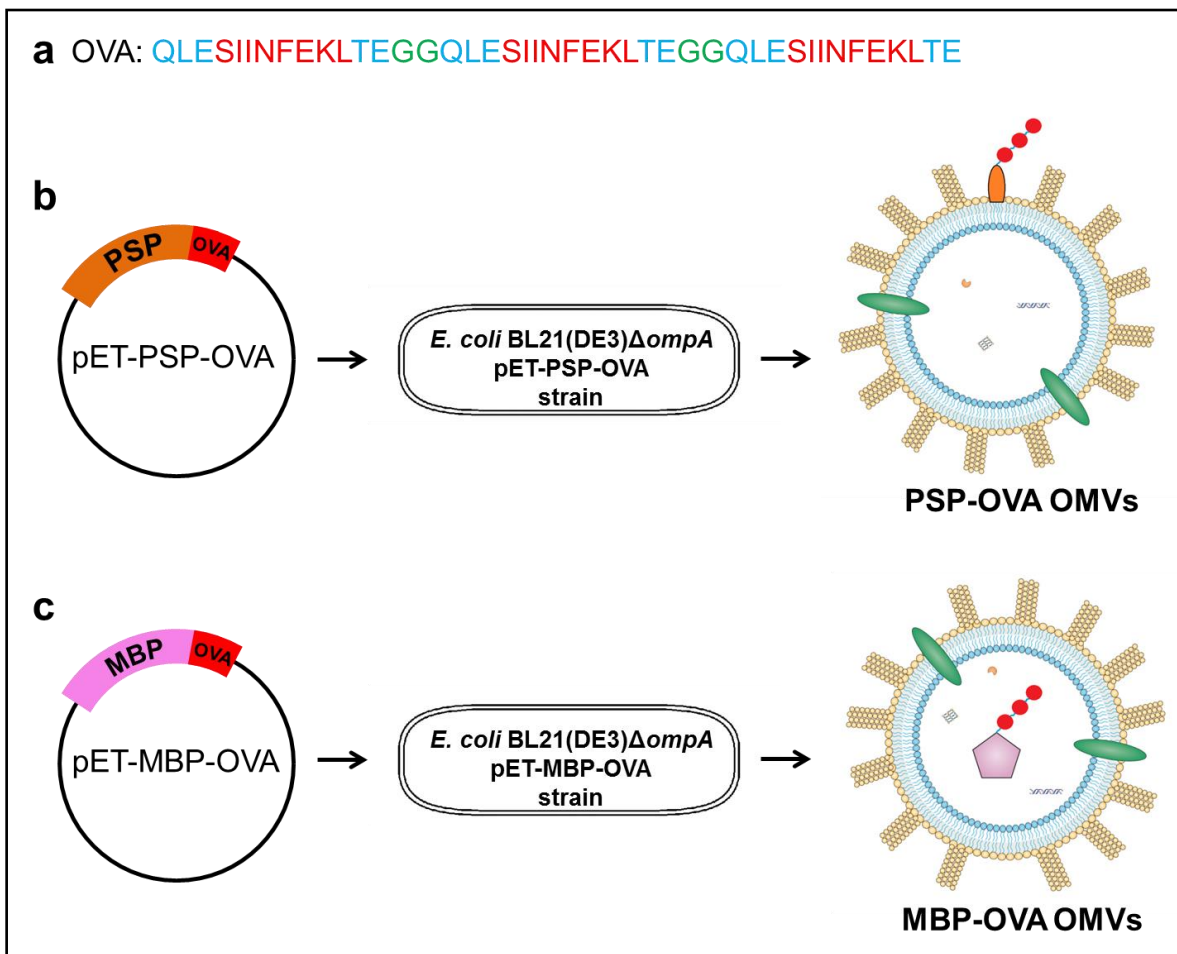
Appendix

Figure 18 | Scheme of the constructs used to engineer OMVs with the OVA antigen. a, *Amino acid sequence of the OVA antigen, composed of three copies of the OVA$_{257-264}$ epitope (red) with its natural flanking sequences (blue) separated by a glycine-glycine spacer (green). b, Schematic representation of pET-PSP-OVA construct used to generate PSP-OVA OMVs. c, Schematic representation of pET-MBP-OVA construct used to generate MBP-OVA OMVs. OMV drawing modified from Kaparakis-Liaskos and Ferrero, 2015[139].*

Publications

Grandi, A., **Tomasi, M.** & Grandi, G. Vaccinology: The art of putting together the right ingredients. *Hum. Vaccines Immunother.* **12,** 1311–1317 (2016)

Fantappiè, L., Irene, C., De Santis, M., Armini, A., Gagliardi, A., **Tomasi, M.**, Parri, M., Cafardi, V., Bonomi, S., Ganfini, L., Zerbini, F., Zanella, I., Carnemolla, C., Bini, L., Grandi, A. and Grandi, G. Some Gram-negative Lipoproteins Keep Their Surface Topology When Transplanted from One Species to Another and Deliver Foreign Polypeptides to the Bacterial Surface. *Mol. Cell. Proteomics* **16,** 1348–1364 (2017).

Zerbini, F., Zanella, I., Fraccascia, D., König, E., Irene, C., Frattini, LF., **Tomasi, M.**, Fantappiè, L., Ganfini, L., Caproni, E., Parri, M., Grandi, A. and Grandi, G. Large scale validation of an efficient CRISPR/Cas-based multi gene editing protocol in Escherichia coli. *Microb. Cell Fact*. 16, 1–18 (2017).

Grandi, A., **Tomasi, M.**, Zanella, I., Ganfini, L., Caproni, E., Fantappiè, L., Irene, C., Frattini, L., Isaac, S. J., Koenig, E., Zerbini, F., Tavarini, S., Sammicheli, C., Giusti, F., Ferlenghi, I., Parri, M. and Grandi, G. Synergistic Protective Activity of Tumor-Specific Epitopes Engineered in Bacterial Outer Membrane Vesicles. *Front. Oncol*. 7, 1–12 (2017)

Declaration of authorship

I, Michele Tomasi, confirm that this is my own work or work I have done together with other members of our group and the use of all material from other sources has been properly and fully acknowledged.

Michele Tomasi

Acknowledgments

I would like to thank Professor Guido Grandi for the opportunity he gave me to spend my PhD in his laboratory. His guidance during this period contributed to my scientific and intellectual growth.

Thanks also to all the people who were part of our laboratory during those years, colleagues and friends who I had useful discussions and shared many ideas with.

A special mention to all my family, for the constant support and for believing in me all the time.

Thanks to all my friends, inside and outside science, for the wonderful moments spent together.